uOttawa

L'Université canadienne
Canada's university

FACULTÉ DES ÉTUDES SUPÉRIEURES ET POSTOCTORALES

uOttawa

L'Université canadienne
Canada's university

FACULTY OF GRADUATE AND POSDOCTORAL STUDIES

Valérie Charbonneau
AUTEUR DE LA THÈSE / AUTHOR OF THESIS

M.Sc. (Chemistry)
GRADE / DEGREE

Department of Chemistry
FACULTÉ, ÉCOLE, DÉPARTEMENT / FACULTY, SCHOOL, DEPARTMENT

Study of the Presence and Impact of C-H---X Hydrogen Bonds in Phase-Transfer Catalysis

TITRE DE LA THÈSE / TITLE OF THESIS

Dr. K. Fagnou
DIRECTEUR (DIRECTRICE) DE LA THÈSE / THESIS SUPERVISOR

CO-DIRECTEUR (CO-DIRECTRICE) DE LA THÈSE / THESIS CO-SUPERVISOR

EXAMINATEURS (EXAMINATRICES) DE LA THÈSE / THESIS EXAMINERS

Dr. L. Barriault

Dr. R. Ben

Gary W. Slater
Le Doyen de la Faculté des études supérieures et postdoctorales / Dean of the Faculty of Graduate and Postdoctoral Studies

A STUDY OF THE PRESENCE AND IMPACT OF C-H···X⁻ HYDROGEN BONDS IN PHASE-TRANSFER CATALYSIS

Valérie Charbonneau

Thesis submitted to the
Faculty of Graduate & Postdoctoral Studies
University of Ottawa
in partial fulfillment of the requirements for the
M.Sc. degree in the

Ottawa-Carleton Chemistry Institute

Thèse soumise à la
Faculté des études supérieures et postdoctorales
Université d'Ottawa
en vue de l'obtention de la maîtrise ès sciences à

L'Institut de chimie d'Ottawa-Carleton

Your file Votre référence
ISBN: 978-0-494-25751-7
Our file Notre référence
ISBN: 978-0-494-25751-7

Acknowledgements

First and foremost, I would like to thank Keith, whose precious advice I will remember all my life. Even though we often disagreed, I have a tremendous amount of respect for you. Above all, I really enjoyed our philosophical discussions.

Secondly (and although I know in most theses this should be placed at the end of the acknowledgements), I want to thank my better half who supported me through the ups and downs of the past two years. I couldn't have done this without you, hun.

Now I really owe a great big thanks to the lab for listening to my seminar a gazillion times. I don't even want to imagine what it would have been like without your feedback. LC, Marc and Megan deserve a special mention for trying to teach me to play poker even though I'm a bit of a lost cause ☺. Melissa (and Keith), thanks a whole bunch for always making sure there was a vegetarian option for me to eat – it never went unnoticed. And Mathieu, well, what can I say? You're the cuddliest little guy I know. J.P., Megan and Dave, you guys are a godsend – and I'm an atheist, so that's saying a lot! It was always really nice to have you guys around. Sophie, you're one of the brightest and kindest young ladies I've met. I wish you all the best!

There are a handful of people that were there for me through good times and bad times and that deserve a special hug. Nicole, I absolutely adore you, dear. Our regular coffee outings and our chitchats are some of the most precious memories I'll keep from this lab. (P.S. Next time I'll check the ring finger before I try to set up a friend with anyone)

Praew, you're sunshine personified *Hugs*! Irina, I'm a better person for having met you.

Despite the many challenges we faced, I hope you'll all fondly remember the good times we had as a lab: the car auctions, the autographs from famous profs. I know I will.

To everyone, I wish all the happiness and success you can handle!

Cheers!

List of Tables

List of Figures

List of Schemes

List of Abbreviations

AIBN	azaisobisbutyronitrile
Ar	aryl
Ac	acetyl
BINOL	1,1'-bi(2-naphthol)
n-Bu	*normal*-butyl
sec-Bu	*secondary*-butyl
t-Bu	*tertiary*-butyl
Bn	benzyl
DCM	dichloromethane
DIPEA	diisopropylethyl amine
DMF	dimethylformamide
DMSO	dimethyl sulfoxide
dppb	1,4-bis(diphenylphosphino)butane
dppe	1,2-bis(diphenylphosphino)ethane
dppp	1,3-bis(diphenylphosphino)propane
Et	ethyl
eq.	equivalent
FT	fourier transform
GC	gas chromatography
NBS	N-bromosuccinimide
NMR	nuclear magnetic resonance spectroscopy
Me	methyl

MOM	methoxymethyl
Oct	octyl
Ph	phenyl
PMB	4-methoxybenzyl
i-Pr	iso-propyl
py	pyridine
rac	racemic
rxn	reaction
s.m.	starting material
SN_2	second order nucleophilic substitution
$\%T$	percentage transmission
Tf	trifluoromethanesulfonic ester
THF	tetrahydrofuran
TLC	thin layer chromatography
TMEDA	tetramethylethylenediamine

Abstract

In the first section are described our attempts at synthesizing a novel two centre phase-transfer catalyst. The various synthetic routes we undertook are illustrated as well as the problems that arose in each.

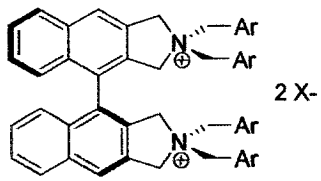

32

The second section summarizes our efforts towards demonstrating the existence of C-H hydrogen bonds in phase-transfer catalysts dissolved in organic solvents. These bonds had been shown to exist in the solid phase but no data regarding their presence under conditions resembling those encountered in phase-transfer catalyzed reactions had yet been gathered.

In the third section, we attempted to study the potential effects of C-H hydrogen bonding in the phase-transfer catalyzed allylbenzene isomerization reaction. We compared the rate of reaction using both hydrogenated and deuterated phase-transfer catalysts.

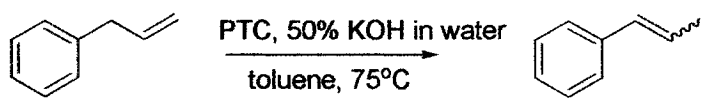

68 69

Table of Contents

1 General Introduction

1.1 Phase-transfer catalysis

The importance of phase-transfer catalysis (PTC) in modern-day chemistry can hardly be overstated. It has been estimated that PTC has been used in the manufacture of more than 10 billion USD worth of chemicals per annum.[1] It is the most widely used method for solving the insolubility problem of inorganic salts in organic solvents and is well recognized as an environmentally benign alternative to some traditional organic reactions such as SN_2 substitutions, alkylations and carbene reactions. Phase-transfer catalyzed reactions are done with lipophobic alkali bases in low polarity solvents (toluene, hexanes, etc.). The more polar solvents necessary for homogeneous reactions (DMSO, DMF) are often more expensive, difficult to dry and hard to remove after the reaction is complete. In addition, the lipophilic bases used in most "conventional" organic reactions are usually flammable and moisture-sensitive.

Another advantage to phase-transfer catalyzed reactions is the enhanced reactivity. When inorganic anions are transferred to the organic phase, they are usually less hydrated, less solubilized and thus their reactivity is enhanced, sometimes by a few orders of magnitude.

The term "phase-transfer catalysis" was first coined by Starks[2] who, along with Makosza[3] and Brändström[4], pioneered the method in the 1960s. There are three generally recognized types of phase-transfer catalysis: liquid/liquid, liquid/solid and gas/liquid.

The latter, being of little interest to organic chemists, will not be discussed here. In liquid/liquid systems, the reaction is usually carried out at higher temperatures (above -10°C) with an organic solvent and an aqueous, often alkaline solution. In most processes, the base of choice is sodium or potassium hydroxide 50 wt% in water since it also serves as a desiccant. Solid/liquid reactions are used when the mixture needs to be cooled beyond the freezing point of the aqueous component (in which case cesium hydroxide monohydrate or rubidium hydroxide hydrate is typically used as base) or for reactions performed with potassium fluoride. The latter reagent is normally used in phase-transfer catalyzed reactions because its basicity is significantly increased in anhydrous organic environments, and the use of aqueous potassium fluoride would negatively impact the desired reactivity.

As for the catalysts themselves, a variety of quaternary ammonium, phosphonium and arsonium salts[5] have been used but tetraalkylammonium salts are the most frequently encountered ones because of their availability, stability and low cost. The phosphonium and arsonium catalysts will not be discussed in this document.

Mechanistic studies of the phase-transfer process were carried out forty years ago and there seems to have been little published since. The originally proposed mechanism[2a] involved the extraction of the ion pair Q^+Y^- from the aqueous into the organic phase as shown below. The Y^- anion is now available to react with reagent RX in the organic phase. After the reaction, Q^+X^- returns to the aqueous phase, where the anion can be exchanged and the cycle restarted.

Figure 1: The First Proposed Phase-Transfer Mechanism

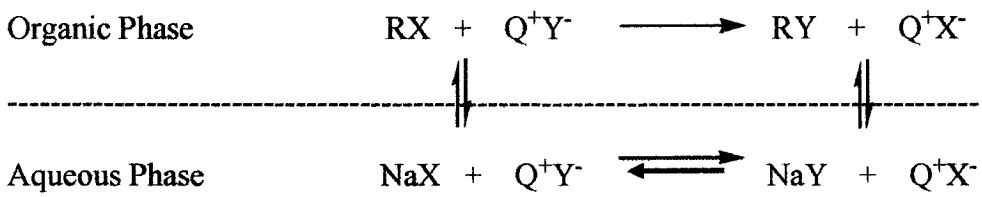

Further studies revealed that for most reactions (with the exception of alkylations), lipophilic catalysts, that were present almost exclusively in the organic phase, were considerably more active than their very polar counterparts. It was thus suggested that migration of the catalyst in the aqueous phase was not necessary to achieve anion exchange. Rather, the exchange is now thought to occur at the interface[6,7,8] as shown in Figure 2.

Figure 2: Interface Mechanism of Phase-Transfer Catalysis

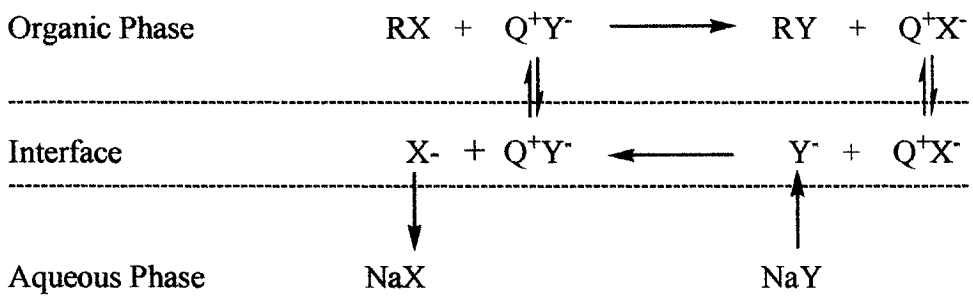

The effect of the catalyst and the reagent anion on the speed and feasibility of the reaction and on the extraction of the ion pair into low-polarity solvent has been thoroughly analyzed.[9,6] For any phase-transfer reaction, competitive extraction of two ion pairs (Q^+X^- and Q^+Y^-) occurs, and formation of the desired product depends on their relative

probability of extraction into the "interface". These values have been quantified and they depend on the solvent used as well as the size and nature of the catalyst and anion. As a general rule, in order to be effective, a phase-transfer reaction must be carried out with a relatively lipophilic catalyst and hydrophilic anion.[5]

Despite its prominence in almost all chemical industries, little is known and understood about the nature of the substrate-catalyst interactions driving phase-transfer catalysis. Those who specialize in advising companies on PTC process development and optimization still use very abstract notions such as catalyst "size" and simple personal experience to determine reaction conditions rather than relying on a sound, broad scientific knowledge. We thought that some of the new ideas and principles discovered in recent years may be useful in providing such a solid scientifically based understanding.

1.2 C-H···X Hydrogen Bonds

Although the definition of a hydrogen bond is ever-changing, it is generally accepted by most organic chemists that it consists of a donor atom (**D**), a hydrogen atom (**H**) that is bound covalently to the donor atom and an acceptor atom (**A**) that comes in close contact with the hydrogen atom at an angle of usually $120^{\circ} - 180^{\circ}$.[10,11] The interaction of the acceptor atom **A** with the hydrogen atom **H** is usually represented by a dotted line as such: **D-H···A.** This is quite a broad description but normally, when most chemists think of a hydrogen bond, the donor atoms are limited to nitrogen or oxygen and the acceptor atoms are usually very electronegative atoms such as halogens, oxygen, etc. Increasingly however, new types of interactions are emerging to predict or explain more complex

systems such as protein folding and crystal packing and, simultaneously, the common vision of the hydrogen bond is being extended to include hydrogen-π and C-H$^{\cdots}$X^{-} bonding. The latter is the object of our interest.

Figure 3: Different Types of Hydrogen Bonds

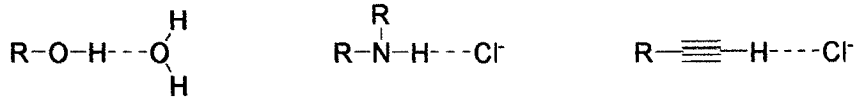

The existence of C-H$^{\cdots}$X hydrogen bonds has been a subject of debate since the first half of the 20th century. The first systematic survey of the crystallographic databases in search of compounds that exhibited potential C-H hydrogen bonds was carried out by Sutor in 1963.[12] This study suggested that the short C-H$^{\cdots}$O distances observed could indeed be considered hydrogen bonds but this research was based on X-ray crystals, and therefore the hydrogen atoms were not present, their position had to be inferred and because of this flaw, many contested the author's interpretation of the results.[13] For two decades, the debate continued with mounting evidence from spectroscopic studies[14,15,16] and quantum mechanical potential energy calculations[17,18,19,20] pointing towards the presence of these bonds in various systems. However, extensive and conclusive experimental proof of any direct interaction of hydrogen bond acceptors with properly aligned methyl, methylene or methyne groups remained to be found until 1982. Taylor and Kennard[21], after a thorough review of neutron diffraction crystal structures from the Cambridge Structural Database[22] demonstrated that hydrogen atoms bonded to carbon often appeared in intermolecular contact with oxygen, nitrogen or chlorine atoms. These interactions were considered attractive and described as hydrogen bonds.

Figure 4: The Shortest C-H···X Contacts from the Kennard Survey

C-H···O Contacts

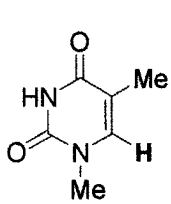

1

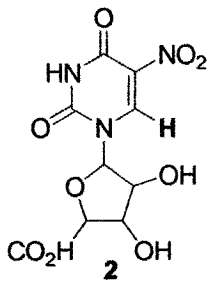

2

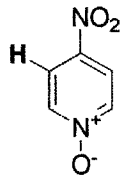

3

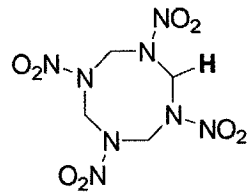

4

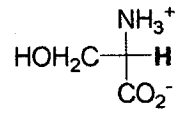

5

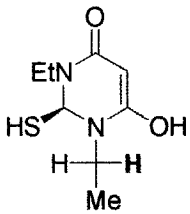

6

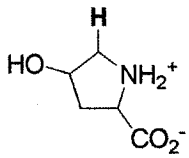

7

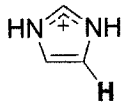

8

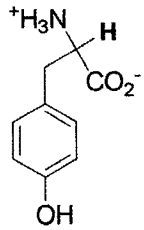

9

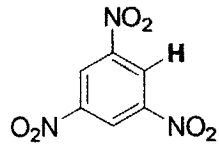

10

C-H···S Contacts

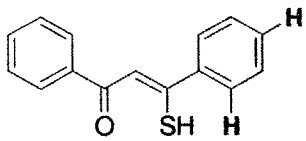

11

C-H···N Contacts

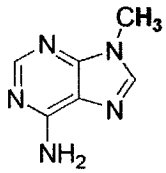

12

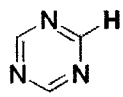

13

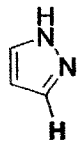

14

C-H···Cl Contacts

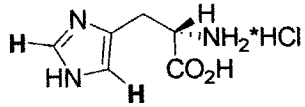

15

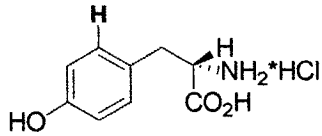

16

17

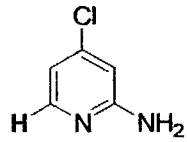

18

Nowadays, the presence of C-H···X hydrogen bonds is widely accepted in numerous systems and thought to play an important role in protein folding[23,24,25,26], protein-DNA interactions[27] and protein-ligand interactions.[28,23] But despite these advances and although it is widely recognized that the ammonium group is one of the most activating for C-H hydrogen bonds, few mentions have been made of their presence in phase-transfer catalysts. We will now look briefly at the various methods used to study the presence and strength of these bonds in the alpha hydrogen atoms of quaternary ammonium centres.

Figure 5: C-H hydrogen Bonds in Quaternary Ammonium Compounds

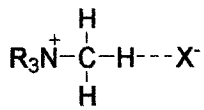

1.2.1 Crystallography

As mentioned previously, the first compelling evidence of the presence of C-H hydrogen bonds was obtained from neutron diffraction crystallography since it allows the scientist to know with relative certainty the position of hydrogen atoms. It was thus established that these hydrogen bonds had the same geometrical characteristics as their better known O-H···X or N-H···X counterparts. They also preferred to be almost linear, most being within 30° of the donor-hydrogen plane. It was also suggested that close contacts

between oxygen or nitrogen atoms and C-H groups occurred often enough to have a significant role in crystal packing.[21]

It was apparent through this research that positively charged nitrogen atoms had a particularly strong activating effect on the adjacent hydrogen atoms. In fact, within the database studied, 64 molecules possessed hydrogen atoms alpha to a positively charged nitrogen and 56 of these formed at least one contact to a hydrogen-bond acceptor (O, N or Cl). By contrast, in the remainder of the database (597 compounds), only half (293 compounds) formed C-H hydrogen bonds.[21] Despite the clear importance of this data to elucidate interactions in phase-transfer catalysts, it took several years before a crystallographic study of quaternary ammonium salts appeared.

In an attempt to generate "naked" carbanions for polymerization, Reetz and coworkers prepared various tetrabutylammonium enolates[29] and analyzed them by X-ray crystallography. To their surprise, the anions were dimeric in the solid state and bound to the counterion by H-bonding to the α–methylenes as shown in Figure 5. Moreover, freezing point depression studies showed that in benzene, this dimeric structure was retained. It was concluded that tetraalkylammonium salts could not be considered "naked" enolates. Although the authors point out the relevance of this research to asymmetric PTC design, it seems that this publication remained unnoticed by most organic chemists in the PTC field.[30]

Figure 6: Dimeric Structure of Tetrabutylammonium Malonate Highlighting the C-H···O⁻ Bonds as Ascribed by Reetz.

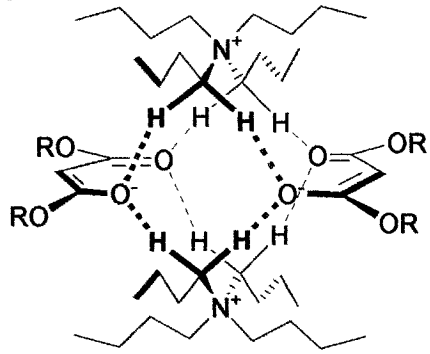

19

Several other classes of tetraalkylammonium salts were studied by Reetz[31] such as tetrabutylammonium sulfonates[31g] and nitroalkyl.[31j] It appeared that malonate-type anions had the tendency to form dimers whereas most other species preferred to form extended aggregates in the solid state and monomers in solution.[31g] Interestingly, a recent study[31i] attempted to look at tetrabutylammonium phenolates by deprotonation of phenol with tetrabutylammonium hydroxide and subsequent dehydration. The desired compound could not be formed, however, only a phenol-phenolate dimer shown in Figure 7 was obtained but it revealed some interesting features about phase-transfer catalysts. The anionic dimer, although already stabilized via the hydrogen bond holding it together, was still involved in C-H hydrogen bonding with the cation, indicating that even in protic solvent, there is a chance that weak H-bonding to the phase-transfer catalyst may be present. Secondly, only one hydrogen bond appeared to be holding the counterion to the tetrabutylammonium, which may be the result of either or both geometry constraints and a lessened need for stabilization.

Figure 7: Structure of the Tetrabutylammonium Phenol – Phenolate Crystal Highlighting the Hydrogen Bonds as Ascribed by Reetz.

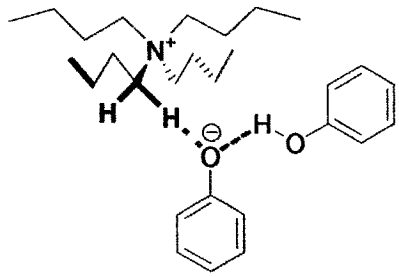

20

Other groups have also discovered crystallographic evidence of H-bonding to α–methylenes of different types of tetraalkylammonium salts. Tetrabutylammonium has been found to form C-H···C$^-$ bonds to cyclopentadienyl anion[32] and N$^+$-C-H···Br$^-$ bonding was suggested to explain the very short distance between trioctylbenzylammonium and its counterion. The sum of van der Waals radii for bromide and hydrogen is 3.13 Å and the benzylic hydrogen atoms of the catalyst were found to be 2.79 Å from the centre of the halogen, a strong indication of H-bonding.

Figure 8: Illustration of the Suggested Hydrogen Bonding In Trioctylbenzylammonium Bromide

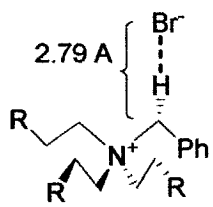

21

It is worth mentioning that extensive crystallographic studies of zwitterionic and positively charged amino acids have been carried out and clearly show C-H hydrogen bonding at the C_α-H position. Thorough statistical reviews of the Cambridge Structural Database[22] even showed a clear link between the proximity of the oxygen anion and the lengthening of the carbon-hydrogen bond.[33]

1.2.2 Computational Modelling

Quantum chemistry provided some of the earliest support for the existence of C-H···X hydrogen bonds and, to this day, most studies are complemented by computer modelling to support the sometimes unusual experimental observations. At the heart of the debate on the nature of the C-H···X interaction, computational modelling played a crucial role. Although different studies supported varying opinions on the relative importance of electrostatic and H-bonding, most experiments clearly revealed that N^+-C-H···X^- interactions had all the characteristic traits of hydrogen bonds: a slight lengthening of the C-H bond, increase of the positive charge on the hydrogen atom as the anion approaches and directionality of the bond relative to the lone pair electrons of the acceptor.[34]

It has been calculated that upon approach of a good hydrogen bond acceptor, the C-H bonds of tetramethylammonium are lengthened by 0.010 Å to 0.013 Å[34], which is too small to be detected by neutron diffraction crystallography. The hydrogen atoms closest to the acceptor presented the most pronounced C-H elongation and the largest increase in positive charge.[34, 35] Furthermore, the charge distribution on phase-transfer catalysts was often found to be considerably more complex than originally thought. The positive

charge on the ammonium is not concentrated at the nitrogen atom but rather it is spread out to a radius of as much as 6 Å around the nitrogen centre. At a shorter range, it encircles the α-methyls or methylenes.[34] Some have even calculated that the central nitrogen may have a slight negative charge.[36]

Like their O-H or N-H counterparts, C-H hydrogen bonds also have strong directionality. The hydrogen bond acceptor lone pairs have been found, through modelling of various conformations, to be preferentially aligned within 120° to 180° of the C-H bond.[35] When the ammonium has four equivalent alkyl chains with methyls or methylenes, structure optimization experiments revealed that the counterion[34,35,37,38] or uncharged hydrogen bond acceptor[34,39] preferentially binds to phase-transfer catalysts via three hydrogen atoms: one from each of three alkyl branches, as shown in Figure 9. Infrared studies have confirmed experimentally that not all hydrogen atoms in tetramethylammonium were equivalent.[16]

Figure 9: Optimized Geometry of Tetramethylammonium Salts.

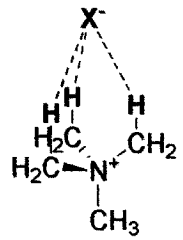

22

The distance between the counterion and hydrogen atoms is usually measured at around 2 Å[40] although there are slight differences arising from the quality of the calculation program or basis set used. In order to be considered a hydrogen bond, the distance

between the hydrogen and the acceptor must be smaller than the sum of their van der Waals radii. Most anions and even uncharged species normally appear to satisfy this criterion. As a general rule, just like with O···H and N···H hydrogen bonds, the shorter the bond, the stronger the interaction. The computed X···H distances for several tetraalkylammonium salts have been compiled in Table 1. Comparisons between different catalysts should be used only qualitatively since the structure of the alkyl chains will impact the length of the bonds.

Table 1: Calculated Distances in Optimized Geometries of Phase Transfer Catalysts and Counterions

Cation	Anion	C-H···X⁻ distance (Å)	C···X⁻ distance (Å)
Me_4N^+	OH^-	1.898[40]	
	F^-	1.859[40]	
	Cl^-	2.374[40]	3.61[16]
	Br^-		3.75[16]
	I^-		3.96[16]
	ClO^-		3.2[16]
	SiF_6^-		3.16[16]
	Formate	2.953[34]	
	Dimethylphosphate	2.974[34]	
	Methyl Acetate Enolate	2.02[35]	
Et_4N^+	OH^-	1.889[40]	
	F^-	1.842[40]	
	Cl^-	2.365[40]	

Despite these small differences, the trend that emerges from this data is that the more electronegative acceptors tend to bind more closely to the ammonium. Simultaneously, shorter distances between the acceptor and cation are indicative of stronger binding. The precise strength of N^+-C-H···X^- hydrogen bonds is not known with certainty but some of

the calculated values are included in Table 2 below. There is a wide discrepancy between the values obtained using different computational methods. These variations highlight the need for experimentally measured C-H hydrogen bond strengths that can be used as benchmarks but unfortunately such measurements are quite difficult to obtain.

Table 2: Calculated Strength of a Single Hydrogen Bond from Phase-Transfer Catalysts to Various Anions.

Cation	Anion	Hydrogen Bond Strength (kJ/mol)
Me_4N^+	F^- [37]	-48.1
	F^- [40,a]	-157.3
	Methyl Acetate Enolate[35]	-18
	OH^- [40,a]	-161
	Cl^- [40,a]	-126.9
	Cl^- [38]	-6.5
	BH_4^- [37]	-5.7
Et_4N^+	OH^- [40a]	-158.6
	F^- [40a]	-155.0
	Cl^- [40a]	-125.5

[a] *Note that these results were obtained with MP_2, which tends to overestimate the strength of hydrogen bonds. All the energy values included in this table are for complexes in the gas phase.*

Since the repartition of the positive charge on tetraalkylammonium compounds is still not precisely known, the contribution of Coulombic interactions to the overall stabilization of the cation cannot be estimated with any certainty. As a result, some authors have speculated that quaternary ammonium ions bind through C-H hydrogen bonds strengthened by ion pairing[40], others that the interactions are predominantly ionic in nature.[35] Practically, however, under standard reaction conditions, the extent of each contribution will vary immensely with the solvent. In water, we can expect hydrogen bonding between the anion and catalyst to be minimal but it may play an important role

in solvents with low dielectric constants such as toluene and benzene. In fact, this has been demonstrated with calculations[35] but never studied experimentally. The association energy of tetramethylammonium and methyl acetate enolate in various organic solvents as modelled by Houk[35] is summarized in Table 3.

Table 3: The Interaction Energy of Tetramethylammonium and Methyl Acetate Enolate in Various Solvents.

Solvent	Interaction Energy (kcal/mol)
Gas Phase	-95.1
Toluene	-40.9
Chloroform	-22.2
THF	-15.2
Methanol	+0.7
Water	+2.3

We can see that the strength of association between the phase-transfer catalyst and enolate is reduced as the solvent becomes more polar, becoming destabilizing in methanol and water. It is possible that a solvent-separated ion pair is formed upon dissolution in water that would be more stable than the closed-shell ion pair optimal in organic solvents.

In some cases, computational modelling was used to estimate the infrared spectrum of tetraalkylammonium salts and obtain an approximation of the band shift upon formation of the hydrogen bonds (see Table 4). Although quite different from the experimental results discussed in the next section, these calculations revealed a significant red-shifting of the C-H stretching frequency upon addition of hydroxide, chloride and fluoride

counterions.[40] The reasons for the observed shift and its directionality will be discussed in greater detail in Section 1.2.3.

Table 4: Calculated C-H Stretching Frequency for Quaternary Ammonium Cations Complexed with Different Anions.

Cation	Anion	C-H Stretching Frequency (cm^{-1})	Δ Stretching Frequency with Gas Phase (cm^{-1})
Me_4N^+	Gas Phase	3154	N/A
	OH^-	3032	-122
	F^-	3055	-99
	Cl^-	3092	-62
Et_4N^+	Gas Phase	3157	N/A
	OH^-	3034	-123
	F^-	3057	-100
	Cl^-	3093	-64

Computational chemistry provides insightful and indeed now indispensable information regarding the nature of chemical interactions but it remains nevertheless theoretical insight until it is supported by solid experimental data. The existence and nature of C-H···X hydrogen bonds could hardly be studied solely from calculations, because benchmark values are needed to validate any computational results. The next sections will describe experimental proofs accumulated supporting the existence of such interactions.

1.2.3 Infrared Spectroscopy

To organic chemists, one of the most important indicators of hydrogen bonding is the lowering of the donor bond stretching frequency (called red-shifting) in infrared (IR) spectroscopy. With O-H or N-H hydrogen bonding, this shift is quite significant and can

be directly linked to the strength of the hydrogen bond via various correlations.[41,42] For C-H hydrogen bonds, the shift in stretching frequency is much more complex and only recently have formulae been developed to translate it into an indicator of bond strength.[43] Almost all IR spectroscopy studies have focussed on the tetramethylammonium (TMA) cation because of its relative simplicity and because it offers a clear resolution of the C-H stretching region.

The Harmon research group has, over the past three decades, accumulated a wealth of data supporting and demonstrating the presence of C-H···X hydrogen bonds in a wide variety of TMA salts.[16] Harmon postulates that the presence of hydrogen bonding is revealed by a wide band around 2950 cm^{-1} that is more or less intense depending on the strength of the hydrogen bond. In complexes that are very weakly bound such as TMA hexafluorosilicate, a clear, sharp, intense peak at 3045 cm^{-1} is seen for C-H stretch and a very small, almost insignificant band can be seen around 2960 cm^{-1}. As hydrogen bonding becomes more pronounced (for example with TMA chloride) the intensity of the 3050 cm^{-1} peak is diminished and a band becomes very noticeable at 2920 cm^{-1}. In fluoride salts, the sharp peak is completely obscured by the presence of an unusually large band of over 700 cm^{-1} in width. This was interpreted as particularly strong hydrogen bonding. Table 5 summarizes the frequencies obtained for each salt and Figure 10 provides spectra of the region of interest for some of these salts

Table 5: Infrared Spectra of Tetramethylammonium Ion Salts[a] from Harmon[16]

Anion	ν_sC-H (cm^{-1} [b])	
F^-	3200 – 2500 (bs)	
Cl^-	3050 (s)	2920 (bm)
Br^-	3020 (s)	2940 (bm)
I^-	3010 (s)	2930 (bm)
ClO_4^-	3048 (s)	2975 (bm)
BH_4^-	3030 (s)	2960 (bm)
$CdCl_3$-	3035 (s)	2970 (m)
SiF_6^{2-}	3045 (s)	[c]
$SnCl_6^{2-}$	3038 (s)	2970 (vw)
$SnBr_6^{2-}$	3038 (s)	2965 (vw)
Ph_4B^-	3060 (s)	-
SbF_6^-	3060 (s)	[d]

[a] Symbols used: (vw) very weak, (w) weak, (m) medium, (s) strong, (vs) very strong, (bw) broad weak, (bm) broad medium, (bs) broad strong, (sh) shoulder. [b] Fluorolube mulls. [c] Complex set of six weak bands also present. [d] Region not well defined.

Figure 10: Infrared Spectra of the C-H Stretching Mode of Tetramethylammonium Ion Salts[a, b]

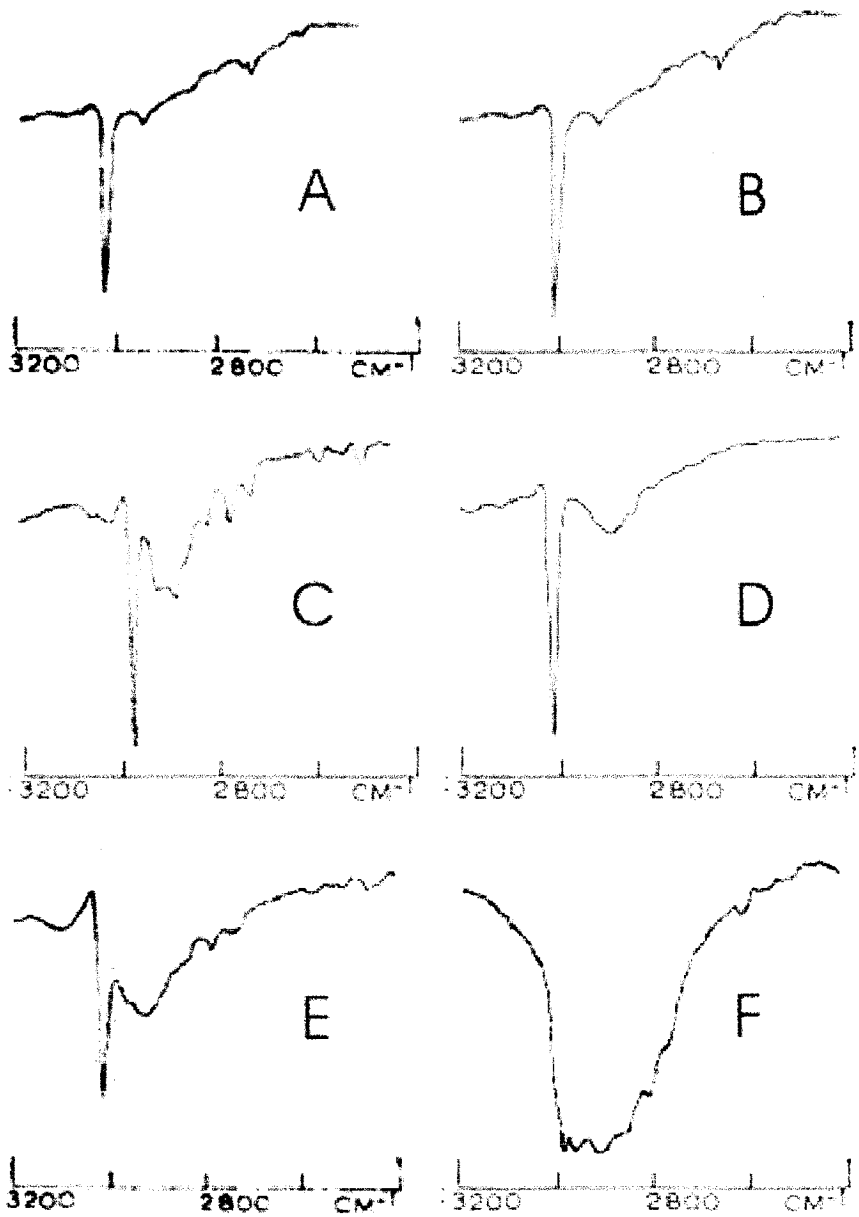

*[a] Salts: **A** hexabromostannate[37,16]; **B** hexafluorosilicate[38]; **C** bromide[16]; **D** borohydride[38]; **E** chloride[37,16]; **F** fluoride[37,16]. [b] Fluorolube mull on CsI plates. Units are in cm^{-1} (wavenumbers) and %T.*

We will see shortly that other groups have also studied these and similar systems, and their conclusions regarding these observations vary greatly. In particular, it became obvious that these hydrogen bonds did not behave as expected in the torsional and methyl deformation[44] regions of the infrared. Normal hydrogen bonds cause a red-shifting and intensity decrease of these bands too but with C-H···X hydrogen bonds, those effects were not observed. Using inelastic neutron scattering spectroscopy to study the vibrational dynamics of TMA borohydride, TMA borohydride-d_4 and TMA-d_{12} borohydride between 100 cm^{-1} and 2000 cm^{-1}, no conclusive information regarding the existence of "H···H" hydrogen bonds[45] could be gathered. The torsional bands of TMA were not shifted to lower frequencies with better hydrogen bond acceptors, like halides, relative to the borohydride and tetrafluoroborate salts. Although Eckert agreed that there may be some level of N^+-C-H···H-BH_3^- "dihydrogen" bonding in TMA borohydride, they proposed that "nonbonded interactions" were predominant.

Koller on the other hand agreed with Harmon with regards to the presence of hydrogen bonds in TMA salts. The experiments performed in his group, using infrared spectra and ab initio calculations, provided support to Harmon's observations of the red shifting of antisymmetric methyl stretching vibrations and the elongation of the C-H bond in complexes of TMA with oxyanions.[34] Their results are shown in Table 6 and the regions of interest in the infrared spectra are shown in Figure 11. If we assume that boron tetrafluoride is a weak hydrogen bond acceptor and bromide or hydroxide are reasonably good, it appears that the C-H stretching frequency is increasingly red-shifted as the anion becomes a better hydrogen bond acceptor.

Table 6: Infrared Spectra of Tetramethylammonium Ion Salts from Koller[34]

Anion	ν_sC-H (cm^{-1} [a])
Br^-	3012.5, 3018.6
Dihexadecylphosphate (anhydrous)	3028.7
Dihexadecylphosphate*$2H_2O$	3031.0
OH^-*$5H_2O$	3029.8
AcO^-	3035.7
NO_3^-	3035.2
ClO_4^-	3042.2
BF_4^-	3025.3

[a] Hexachlorobutadiene mulls, [b] 60 mM solution in chloroform

Figure 11: Infrared Spectra of the C-H Stretching Mode of Tetramethylammonium Ion Salts[a, b] from the Koller Group.

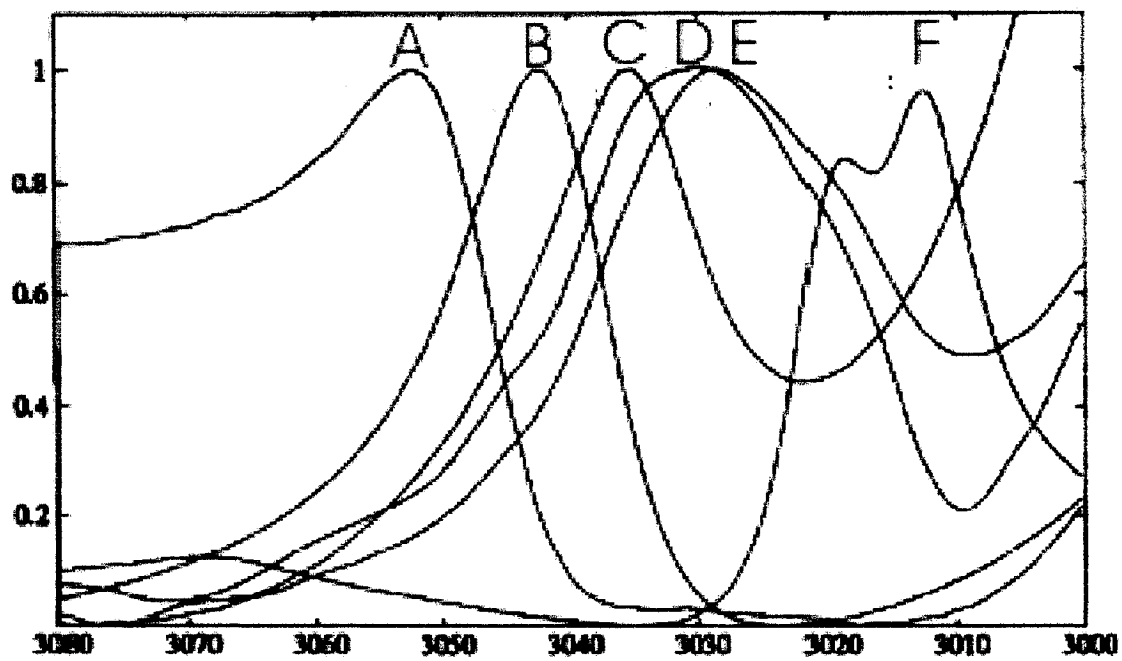

[a] *Salts: **A** tetrafluoroborate; **B** perchlorate; **C** nitrate; **D** dihexadecylphosphate * $2H_2O$; **E** dihexadecylphosphate (anhydrous); **F** bromide.* [b] ***A**, **B**, **C** and **F** are hexachlorobutadiene mulls; **D** and **E** are 60 mM solutions in $CHCl_3$. Units are in cm^{-1} (wavenumbers) and optical density.*

Only a few quaternary ammoniums outside of TMA were the object of IR studies searching for C-H hydrogen bonds. Of these, acetylcholine[46,47] and related molecules as well as various amino acids[48] were probably the compounds most often studied. Some believe that C-H hydrogen bonding may play an important role in the activity of acetylcholine[49] and in many biologically important processes.[23 - 28] A detailed review of the results of these studies will not be included here but we will rapidly cover some the more striking data. Infrared spectra of the anhydrous bromide, iodide and chloride salts of choline were gathered and compared[49] in the same manner as the TMA salts seen earlier. In the bromide spectrum, sharp peaks could be seen at 3010 cm^{-1} and 2980 cm^{-1} as well as a weak band at 2960 cm^{-1} that was assigned to hydrogen bonding. For iodide, the hydrogen bonding peak appeared to be stronger than in bromide. This may rather surprising but both are still considered weak hydrogen bonds and a significant change is only observed with the chloride where the C-H stretching region is completely dominated by a strong, wide band at 2920 cm^{-1} attributed to hydrogen bonding (see Figure 13). The very strong absorption at higher frequency in these spectra is the choline hydroxyl stretch. Note that for the fluoride this absorption is at much lower frequency and is not shown.

Figure 12: Representation of Selected C-H$^{\cdots}$Br^{-} Hydrogen Bonds on Acetylcholine Bromide and Choline Bromide

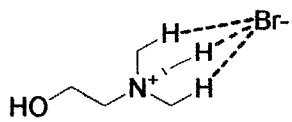

23

Choline bromide

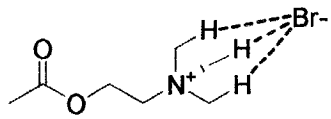

24

Acetylcholine bromide

Figure 13: The Infrared Spectra of Acetylcholine Salts[a,b].

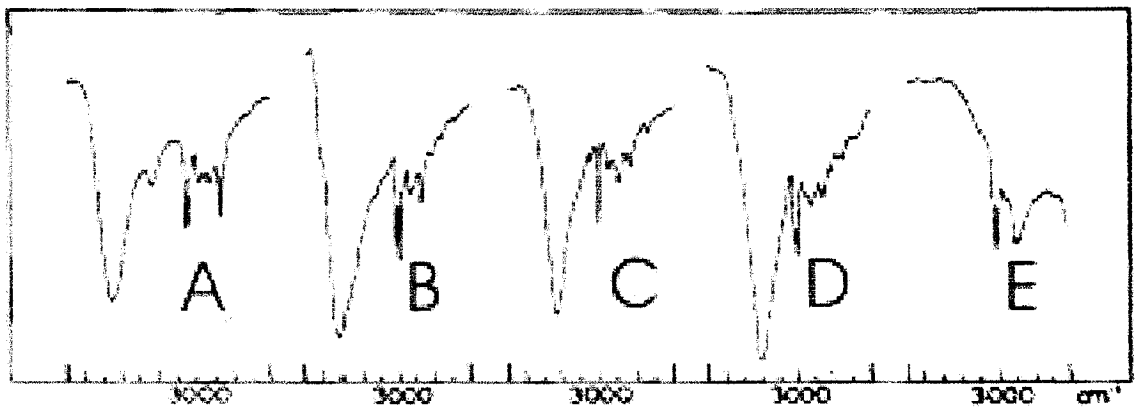

[a] ***A*** *hexafluorosilicate;* ***B*** *Iodide;* ***C*** *Bromide;* ***D*** *Chloride;* ***E*** *Fluoride.* [b] *Fluorolube mulls on NaCl plates. Units are in* cm^{-1} *(wavenumbers) and %T.*

An interesting result that was obtained from IR studies is that addition of one molecule of heavy water affects the infrared spectrum to the extent that it appears to almost destroy hydrogen bonding. At the very least, it seems that the nature of the interaction is dramatically altered.[50] In anhydrous TMA fluoride, the presence of hydrogen bonds is clear from the massive band that covers the 2800 – 3000 cm^{-1} region. When the sample is hydrated with one equivalent of deuterium oxide (which, unlike water, leaves the C-H stretching region clear), this band disappears and leaves only the sharp antisymmetric stretching peak around 3000 cm^{-1} and a small, weak and wide band caused by hydrogen bonding at about 2900 cm^{-1} as we can see in Figure 14. Even more pronounced is the effect on the spectrum of TMA (hydroxide monohydrate)-d_3 where only a very weak band is observed in the hydrogen bonding region, leaving us to believe that the hydroxide monohydrate may only bind as strongly as some of the weaker hydrogen bond acceptors such as chloride or perchlorate. Note that the large, wide band in the low-energy part of the last two spectra is the O-D stretching band. It has been reported that these C-H hydrogen bonds were very greatly reduced in water[35] and it is believed that the

interaction of quaternary ammonium cations with water itself is mostly apolar in nature.[51] Whether this affects merely the nature of the bond, or its very existence, is still not understood.

Figure 14: Infrared Spectra of Anhydrous and Hydrated Salts of Tetramethylammonium Ion[50a,b]

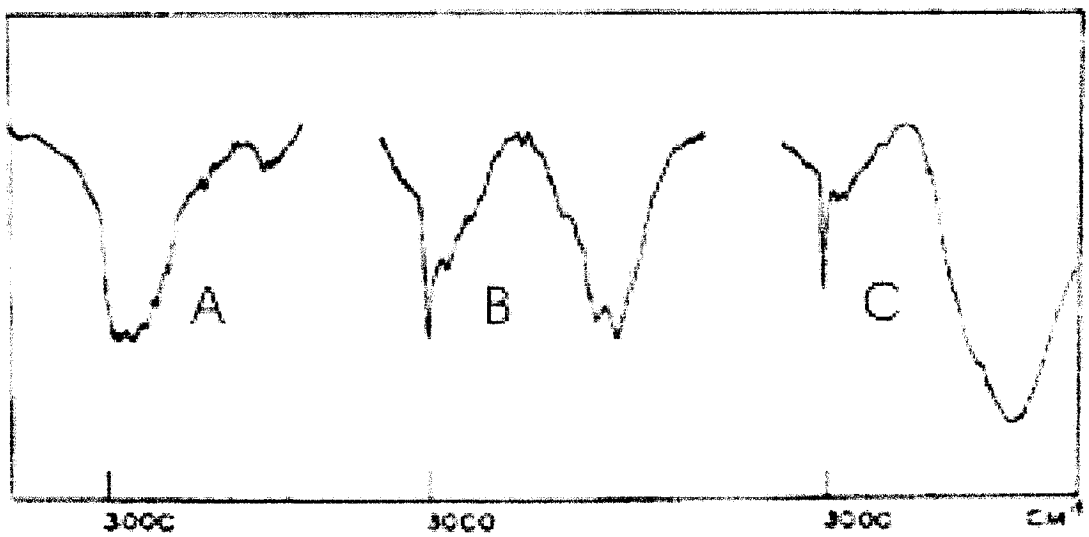

[a] *A anhydrous TMA fluoride; **B** TMA fluoride (monohydrate)-d_2; **C** TMA (hydroxide monohydrate)-d_3.* [b] *Fluorolube mulls on sodium chloride or potassium bromide plates. Units are in cm^{-1} (wavenumbers) and %T.*

The explanation given by Harmon and Koller for their observations was the subject of some controversy. Many believed that the lower-frequency band observed is the product of Fermi resonance[44,52,53] or combination and overtone bands of methyl deformation modes[54] not hydrogen bonding. It has actually been calculated[52] that there was indeed some Fermi resonance in the C-H stretch region but only for TMA iodide in dilute aqueous solution. To the best of our knowledge, other counterions and solid samples were not studied. Interestingly, while studying the Fermi resonance of TMA iodide, the authors observed that there were non-equivalent C-H stretching modes in the solution but

they attributed this to different electrostatic environments. However, the changes observed in infrared spectra with the various anions could not be satisfyingly explained by electrostatics.

After studying the formation of C-H hydrogen bonds in TMA and choline salts, the Harmon research group undertook a study of more complex anions, attempting to study their hydrogen bond acceptor ability of these exotic species. It was thus discovered that anions like $H_2F_3^-$ also formed detectable hydrogen bonds to TMA at both 10K and 300K.[55] The degree of hydrogen bonding sometimes appears to be almost a subjective measurement and some argue about the hydrogen bonding propensity of weak acceptors like SiF_6^- and $SbCl_6^-$. It has been suggested that, at room temperature, hexafluorosilicate actually forms very weak hydrogen bonds with TMA whereas hexachloroantimonate showed no evidence of H-bonding at all. Meanwhile hexafluoroantimonate was the subject of controversy, with some stating that it did for very weak hydrogen bonds to TMA[56] and others opposing this view.[57] To the best of our knowledge, this debate has not yet been satisfyingly settled. Although these results are of little importance to phase-transfer catalysis, they have very concrete applications in materials science and solid state chemistry.

Inorganic chemistry has uncovered an interesting and initially puzzling aspect of the physical properties of phase-transfer catalysts. Many TMA salts have been reported to undergo phase transition upon cooling. When a certain, very low temperature is reached, the crystals change appearance and the geometry and infrared spectra of the crystals are

significantly altered. This is generally understood as a reorganization of the cation and freezing out of the methyl group rotation. The methyl hydrogen atoms have been known to point in the direction of the counterion from neutron diffraction spectroscopy and their IR spectra show the presence of hydrogen bonds as ascribed by Harmon. Even very poor hydrogen bond acceptors like hexachlorostannate, -tellurate or -platinate that have been shown to form no H-bonds to TMA at room temperature undergo phase transition at very low temperature.[58,59,60] Quaternary ammonium halides[61,62,63,64,65,66] also undergo several (the exact number seems to depend on the technique used) phase transitions as the crystals are cooled. Some authors have explained the observed phase-transitions by sterics and symmetry[54] or by the tumbling motion governed by the free space in the crystal lattice where the differences between counterions is caused by their varying size.[67] However, tumbling, symmetry and sterics cannot fully explain why deuterated TMA undergoes phase transition at a different temperature than its hydrogenated counterpart. It is known that deuteration of the methyl groups of TMA can either strengthen or weaken the hydrogen bonds to the acceptor anion[68] though the precise reasons for this odd behaviour is not yet well understood. As a result however, $(CD_3)_4N^+$ undergoes phase transition at a temperature either lower or higher than $(CH_3)_4N^+$, providing support for the hydrogen bond formation at low temperature.[58,59,60]

1.2.4 Mass Spectroscopy

Mass spectroscopy is a useful method to study phase-transfer catalysts but unfortunately, it has not been used to its full potential. It is actually the only experimental technique that can measure the association energy between a quaternary ammonium cation and a hydrogen bond acceptor. Its only downside is that the molecules have to be studied in the gas phase. Unfortunately, since this technique has not been used by organic chemists at all, no studies have been performed on anions. The attraction for physical chemists is mostly to be able to study the association energy between tetraalkylammonium ions and uncharged solvent molecules. The experimental data is then complemented with calculations to elucidate the probable structure of the complex.

The Meot-ner group has been particularly interested in the study of tetraalkylammonium complexes.[69,46] Their results are summarized in Table 7 and compared to "normal" hydrogen bonded complexes, represented here by the trimethylammonium ion. Some of the measurements looking at the addition of a second protic solvent molecule (water, methanol) were not included here since it was demonstrated that the second molecule binds to the first solvent molecule, not the ammonium. In the case of acetone however, it is hard to imagine a situation where it could form a hydrogen bond with a second acetone molecule thus it is assumed that the second and third molecules do bind to the cation.[70]

Table 7: Thermochemistry of the Dissociation of Quaternary Ammonium Complexes and of Trimethylammonium (as a Reference) with Solvent Molecules.

Cation	Ligand	ΔH°_{D} (kcal/mol)	ΔS°_{D} (cal/mol)
Me_4N^+	H_2O	9.0	21.5
	MeOH	9.8	23.2
	Me_2CO	14.6	24.7
	Me_2CO (2)	13.0	29.2
	Me_2CO (3)	11.7	-
	$MeO(CH_2CH_2)_2OMe$	20.6	28.7
	$MeO(CH_2CH_2)_3OMe$	24.2	33.8
	$(n\text{-}C_4H_9)_2O$	12.9	25
	C_6H_6	9.4	20
	Toluene	9.5	20.3
	$MeCONMe_2$	18.0	21.6
	$MeNH_2$	8.7	17.0
	Me_3N	9.9	20.6
Me_3NH^+	H_2O	15.5	-
	MeOH	18	-
	Me_2CO	22	-
	$MeO(CH_2CH_2)_2OMe$	32.8	-
	$MeO(CH_2CH_2)_3OMe$	34.6	-
	$(n\text{-}C_4H_9)_2O$	23	-
	C_6H_6	15.9	-
	$MeCONMe_2$	27.2	-
	$MeNH_2$	20	-
	Me_3N	22.6	-
Et_4N^+	H_2O	7.0	-
	Me_2CO	12.4	26.7
$Me_3N(CH_2)_2NMe_3^{2+}$	H_2O	12.7	19.3
$Me_3N(CH_2)_3NMe_3^{2+}$	H_2O	11.0	16.5
Acetylcholine	H_2O	8.0	22.0
	Me_2CO	13.2	21.7
	Toluene	8.1	15.5

It becomes apparent, when comparing the trimethylammonium and tetramethylammonium complexation energy, that C-H···B hydrogen bonds are considerably weaker than conventional hydrogen bonds. The energy difference between the two is about 7-10 kcal/mol for monofunctional oxygen ligands and 11-13 kcal/mol for nitrogen ligands. It is also apparent that quaternary ammonium ions bind much more strongly to acetone and DMA, molecules that have large dipole moments (2.9 and 3.8 D respectively), than to ligands such as water (1.2 D) or methanol (1.8 D). The authors explained this difference[69a] as a sign that C-H hydrogen bonds were mostly electrostatic in nature.

Tetraethylammonium cation binds to solvents a bit less strongly (by about 2 kcal/mol) than TMA. Since the tetraethyl cation is larger, it is expected that the positive charge on the nitrogen centre may be dampened by induction from the alkyl chains, thus reducing the positive charge on each proton. A similar trend would be expected from the ion pairing model where an increased cation size would increase the distance between the two charges and thus reduce the binding energy. Also, not unexpectedly, doubly charged cations bind water more strongly (11-13 kcal/mol)[71] than monocationic species (9 kcal/mol).

Finally, in the case of acetylcholine, the binding energies are very similar to TMA although systematically weaker by about 1 kcal/mol. This may be caused by partial internal bonding in acetylcholine. However, it does demonstrate that TMA can be used as a reliable model for acetylcholine in experimental or theoretical studies.

2 Catalyst Design and Synthesis

2.1 Design, chiral pocket

The structural diversity among the most efficient and selective phase-transfer catalysts is remarkable. The classical cinchona alkaloids[72] have a [2.2.2] bicyclic backbone whereas the Maruoka catalyst[73] was designed from a 1,1'-binaphthyl core and the Shibasaki catalyst[74] from a diethyl tartrate precursor. And yet despite such striking dissimilarities in their core structure, all of these catalysts promote the same reactions in high yields and excellent enantioselectivity.

Scheme 1: Common Chiral Phase-Transfer Catalysts.

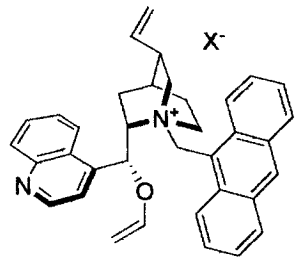

25

Cinchona Alkaloid Catalyst

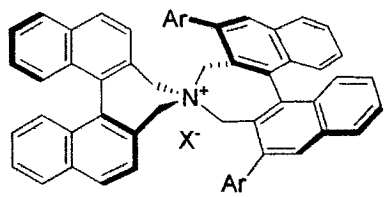

26

Maruoka Catalyst

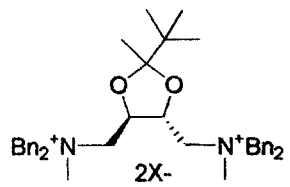

27

Shibasaki Catalyst

To explain the chirality transfer from various phase-transfer catalysts (PTC) to substrates and provide a logical, systematic approach to catalyst design, Corey[75] proposed a model inspired from the cinchona alkaloids that inspired numerous novel PTC structures.[72c,d, 76] According to this system, the nitrogen is placed in the centre of a tetrahedron and three of the four faces of this tetrahedron must be sterically blocked to prevent close approach of

the counterion. The fourth must allow for close contact between the substrate counterion and the positively charged nitrogen. Next to the open face there should also be a binding surface for attractive π-interactions. Cinchona alkaloids fit this model particularly well since the bicyclic ring system completely blocks one face of the tetrahedron as seen in Figure 15.

It was originally believed that all counterions were bound to cinchona alkaloid catalysts by the face indicated in Figure 15. Crystal structures of the bromide and p-nitrophenoxide salts of *O*-allyl-*N*-(9-anthracenylmethyl)-cinchonidinium provided support to this assumption although a crystal structure of actual reaction intermediates such as the catalyst bound to an enolate could not be obtained. The interaction of the *t*-butyl glycinate-benzophenone Schiff base with the (9-anthracenylmethyl)cichonidinium catalyst was later modeled by Houk.[35] He proposed a completely different model for these interactions where the enolate sits "under" the catalyst, with π–interactions between the benzophenone imine and the anthracenyl moiety of the catalyst. Instead of placing the plane of the enolate perpendicular to the N^+-C-H hydrogens as it is in the Corey model, they are now periplanar so that the O^-, CH_2^- and N of the substrate can simultaneously interact with the alpha hydrogens as shown in Figure 16.

The best known phase-transfer catalyst, developed by Maruoka[73] in 1999 also fits this general description quite well although it is slightly more difficult to visualize. The large, variable aryl groups on the binaphthyl component block two of the faces of the tetrahedron while the binaphthyl moiety itself serves as a van der Waals binding surface.

The two faces of the tetrahedron left can both be used by the counterion since the catalyst is C_2 symmetric. One of these faces is highlighted in Figure 15. In this catalyst, as well as with the cinchona-based catalysts, the enantioselectivity arises from steric hindrance in the catalyst that only allows the anion to bind in the desired chiral pockets.

Figure 15: Illustrative Representation of the Cinchoninium and Maruoka PTC According to the Corey Rationale.

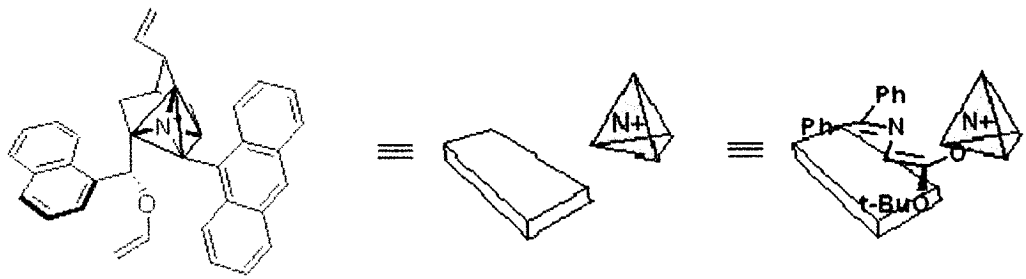

28

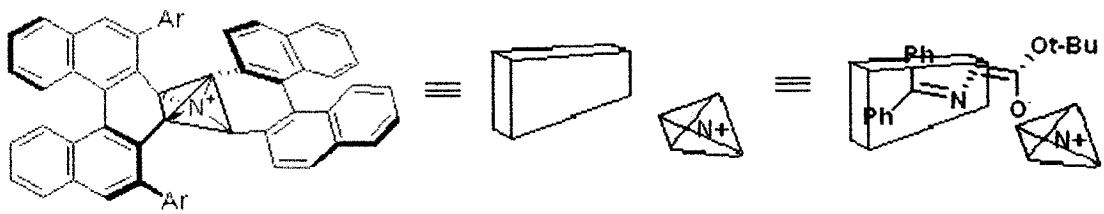

29

Figure 16: Model Proposed by Houk to Rationalize the Enantioselective Alkylation of tert-Butyl Glycinate Benzophenone Imine Catalyzed by Cinchonidinium Salts.

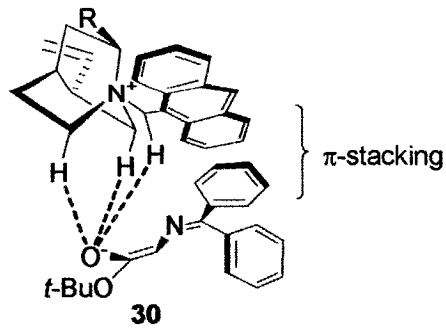

30

On the other hand, in the catalyst designed by Shibasaki, the anion approach is not blocked as efficiently by sterics. In fact, the anion could bind to several of the faces of the nitrogen-centered tetrahedron. How then does this catalyst transfer chirality to the substrates? Shibasaki rationalized the enantiomeric excess (80-93% ee in the alkylation of the Schiff base of *t*-butyl glycinate) obtained with this catalyst by inferring that the enolate did not bind as an ion pair to the positively charged nitrogen but rather via hydrogen bonding to the α-methylene and methyne groups[30] as shown in Figure 17. It was also suggested that the enolate preferred to sit between the two nitrogen groups since the reaction was not only much faster but also considerably more selective when both nitrogen centres (as opposed to only one of the two) were quaternized.[74] These suppositions were supported by computational modeling.[74, 30]

Figure 17: Interaction of the Shibasaki PTC with an enolate according to optimized molecular modeling calculations

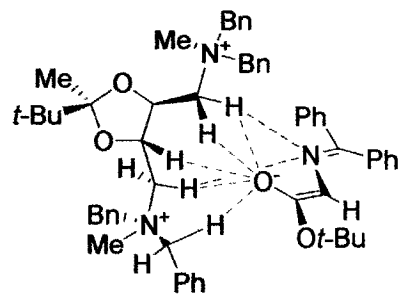

31

Based on this approach, we envisioned a new PTC with a binaphthyl backbone that would function in a way that resembled Shibasaki's catalyst. Here too, the chirality would be transferred to the substrate not via steric hindrance but by preferential binding of the enolate to the chiral pocket that provided the most C-H hydrogen bond stabilization. We therefore imagined that the enolate would here too prefer to bind in the

middle of the two nitrogen centres, where seven hydrogen atoms are available rather than on the outside face, where it would only be stabilized by three C-H bonds. The naphthalene rings should provide rigid surfaces for π-interactions with the substrate, hopefully flattening it against the catalyst. The enolate would thus expose only one face to electrophilic attack. Furthermore, the C_2 symmetry of our catalyst should reduce the number of substrate binding modes and facilitate chiral induction.

Figure 18: Our Proposed Two-Centred Catalyst

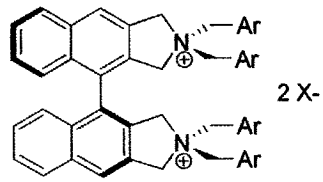

32

Figure 19: Three-Dimensional View of Our Two-Centred Catalyst Illustrating the Chiral Pocket.

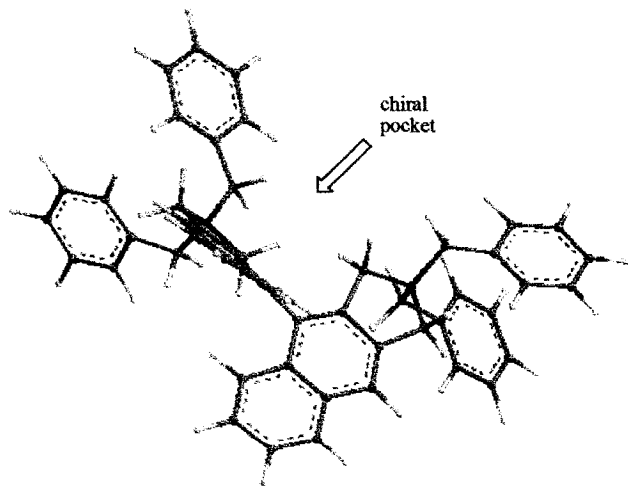

2.2 Attempted Synthesis of a Bifunctional Phase-Transfer Catalyst

2.2.1 First Synthetic Route

2.2.1.1 Overview

Our first attempt at the synthesis of this two-centre phase-transfer catalyst was made by Dr. Irina Denissova. The original synthetic route used chirally pure BINOL as a starting material since it was relatively inexpensive and eradicated the need for chiral resolution. Following this route, we expected to obtain the catalyst in eight steps, which was comparable to the eight steps necessary to make the Maruoka catalyst.[73b]

Scheme 2: First Synthetic Route for Our Two-Centred Phase-Transfer Catalyst.

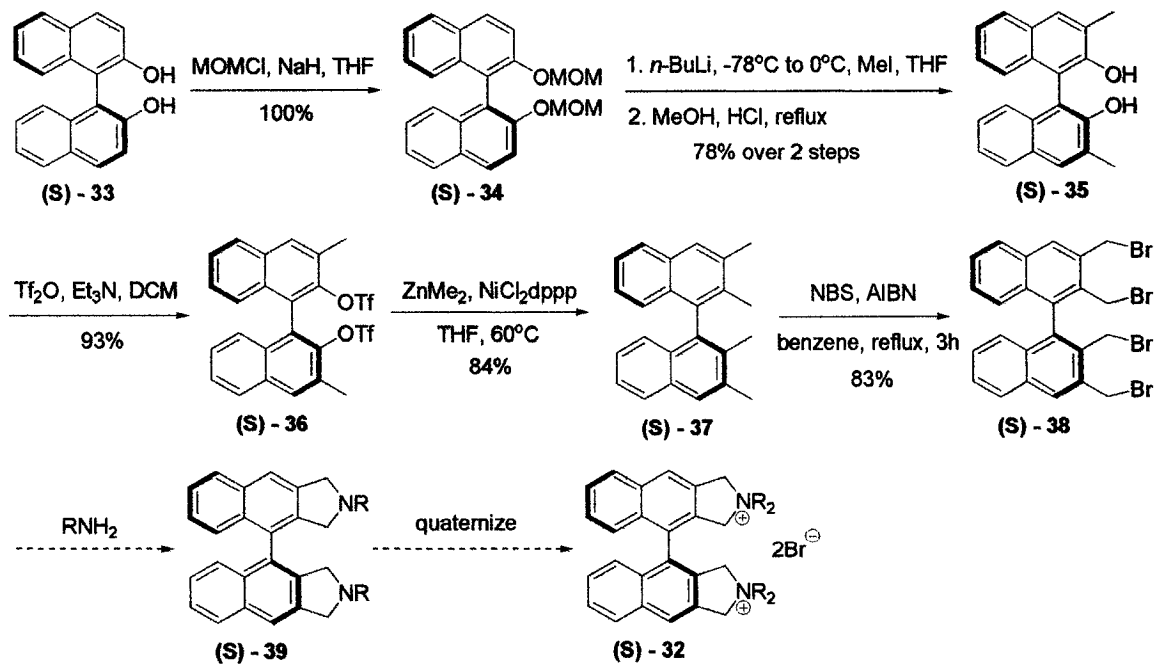

Pure (*S*)-BINOL was first protected with MOM, giving (*S*)-MOM_2BINOL in 100% yield. Subsequent ortholitiation of the MOM-protected alcohol using *n*-BuLi at -78°C proceeded smoothly and the carbanion was successfully quenched with MeI at 0°C, providing the desired dimethylated product which was deprotected in refluxing MeOH with conc. HCl to give the corresponding diol (*S*)-**35** in good yield.

The ditriflate was then obtained by treating diol **35** with freshly distilled triflic anhydride in the presence of triethylamine in DCM. Two more methyl groups were then installed via Kumada coupling. Initial efforts to carry out the coupling reaction with methylmagnesium bromide were not successful. The reaction necessitated prolonged reflux and gave a mixture of products including mono-coupling product and products of hydrolysis of the triflate group. However, when methylmagnesium bromide was replaced with dimethylzinc, the coupling reaction proceeded smoothly to give the desired (*S*)-**37** in 84 % yield. Bromination of (*S*)-2,2',3,3'-tetramethyl -1,1'-binaphthalene under radical conditions afforded tetrabromide **38** in 83% yield as a stable white solid.

For the next reaction, it was expected, based on Baldwin's rules that treating the tetrabromide **38** with a primary amine would result in the preferential formation of two five-membered rings. Surprisingly, when the tetrabromide was treated with an excess of benzylamine or 4-methoxybenzylamine in benzene[77], the product appeared to be much more polar than expected by TLC. This product was isolated by flash chromatography on silica gel and careful examination of ^{1}H, ^{13}C and NOSY NMR revealed that, contrary to all expectations, we had obtained triamine **40**.

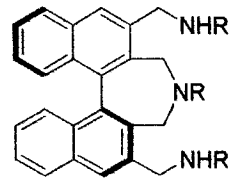

(S) - 40

Preferential formation of seven-membered ring over five-membered cycle could be explained if intermolecular addition of a second amine molecule occurred faster than the intramolecular five-membered ring formation. However, prior to the intramolecular cyclization, the deprotonation of **36** would have to take place. It was speculated that a hydrogen bond formed before the deprotonation might assist in the nucleophilic displacement of the second bromide by RNH_2 through a pseudo-intramolecular fashion resulting in protonated disubstitution product. Once product **42** is formed, it is impossible to generate the desired diamine **39**.

Scheme 3: Suggested Mechanism for the Formation of the Observed Triamine

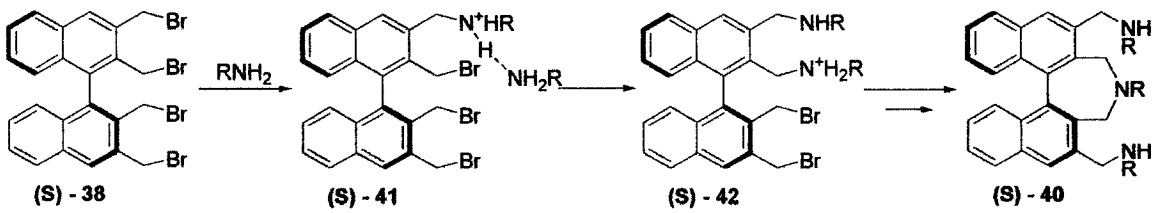

(S) - 38 (S) - 41 (S) - 42 (S) - 40

Furthermore, from the suggested geometry of tetrabromide (*S*)-**38** shown in Figure 20 we can infer that once **41** is formed, the molecule would have to twist and displace the "internal" bromide from its optimal position and dramatically increase the steric strain in order to allow attack from the oncoming nitrogen. Conversely, the molecule seems

perfectly positioned for the nucleophilic attack forming the seven membered ring observed.

Figure 20: Nucleophilic Attack on the Tetrabromide Reagent.

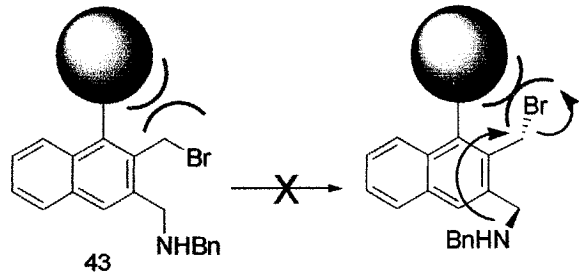

2.2.1.2 Investigation of the Conditions for Dicarbonylation

Faced with this obstacle, Dr. Denissova investigated if it was possible to alter the reactivity by decreasing the number of amine equivalents, by adding drop wise a dilute amine solution or by using a hindered base which could not participate in the substitution as a proton scavenger. It is clear from the results seen in Table 8 that even when an almost stoichiometric amount of the amine and a hindered base were used, the reaction still proceeds to give triamine **40**. It also appeared that the concentration of base was extremely important; the rate of the reaction was increased in the presence of a large excess of base. The reaction was also accelerated more efficiently by DIPEA than by Et_3N and seemed to also occur more rapidly in more polar solvents such as THF than in benzene, which is consistent with the S_N2 mechanism of the reaction.

Table 8: Screening of Reaction Conditions for the Attempted Formation of Diamine 39.

Entry	Equivalents of $PMBNH_2$	Base	Solvent	Results
1	2	DIPEA, 4 eq.	Benzene 0.025 M	s.m. and decomposition
2	2	DIPEA, 4 eq.	MeCN, 0.025 M	s.m.
3	2.5	DIPEA, 4 eq.	Benzene 0.1M	s.m. and decomposition
4	2.5 + 2.5	DIPEA, 4 eq.	THF, 0.1 M	s.m. and decomposition
5	2.5 + 2.5 (after 2.5 hours)	DIPEA, 4 eq.	THF, 0.1 M	**40**
6	2.5	Et_3N, 20 eq.	THF, 0.1 M	**40**
7	2.5	K_2CO_3, 20 eq.	THF, 0.1 M	Decomposition
8	2.5	DIPEA, 20 eq.	THF, 0.1 M	**40**

Since it was postulated that hydrogen bonding during the deprotonation step may have been the source of the problem, deprotonation of the 4-methoxybenzylamine with *n*-BuLi at -78°C *prior* to its addition to the tetrabromide solution was also attempted. Unfortunately, no reaction was observed.

Scheme 4: Attempted Nucleophilic Attack by 4-Methoxybenzylamine Anion

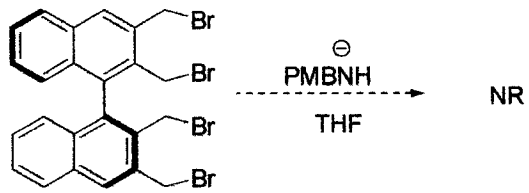

(S) - 38

2.2.2 Modified Synthetic Route

2.2.2.1 Introduction

As it became apparent that our first approach to the synthesis of catalyst **27** had hit a roadblock, a new route based on the recently published Maruoka catalyst[78] synthesis was attempted. The authors have developed a strategy to introduce groups *ortho* to isopropoxycarbonyl functionalities in diester **44** via direct *ortho* magnesation using magnesium bis(2,2,6,6-tetramethylpiperamide) ($MgTMP_2$) followed by reaction with an electrophile, in our case benzyl isocyanate. This was done in collaboration with Dr. Irina Denissova. My work began with the achiral synthesis.

Scheme 5: *ortho*-Magnesiation Developed by Maruoka

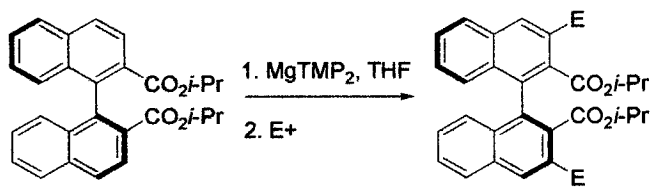

(S) - 44 (S) - 45

We imagined that it would be possible for us to use an approach similar to the one shown above in the synthesis of our catalyst. Our efforts towards the synthesis of the two-centred catalyst **32** are summarized below.

2.2.2.2 New Approach to the Synthesis of Our Two-Centre Catalyst

Initially, this new synthetic route also utilized chirally pure (*S*)-BINOL as a convenient starting material. From (*S*)-BINOL, we produced the ditriflate (*S*)-**46** using standard procedure.[73b] The next step in our synthesis, however, turned out to be quite problematic.

Scheme 6: First Attempted Synthesis of 1,1'-Binaphthyl-2,2'-Diisopropylester.

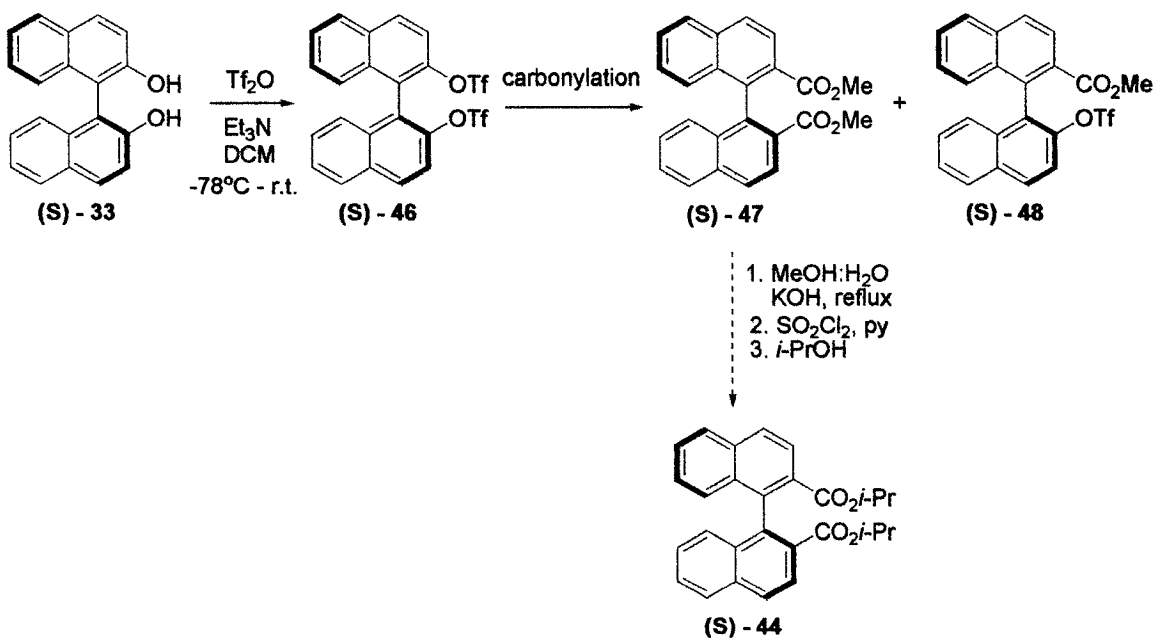

It had been shown in the literature that dimethylester **47** could be obtained from the corresponding ditriflate **46** via Pd(II) catalyzed carbonylation in up to 80 % yield.[79] Unfortunately we were unable to reproduce these results. Screening of the reaction

conditions (see Table 9) enabled us to get at best 27% of the desired diester along with 29% of the mono-carbonylated product. Being yet again faced with a difficult synthetic problem, we changed our strategy once more.

Table 9: Investigation of the Conditions for the Dicarbonylation of 1,1'-Binaphthyl-2,2'-Ditriflate.

Entry	Mass of Starting Material (mg)	Catalyst (%mol)	Ligand (%mol)	CO Pressure (atm)	Solvent (T, °C)	Time (h)	Results
1	450	$Pd(OAc)_2$ (15)	dppp (15)	1	80	72	32% **48** + s.m
2	40	$Pd(OAc)_2$ (20)	dppe (20)	1	95	24	No rxn
3	40	$Pd(OAc)_2$ (20)	dppb (20)	1	100	24	No rxn
4	40	$Pd(OAc)_2$ (20)	dppp (20)	5	120	72	Traces **48**
5	20	$PdCl_2(PPh_3)_2$ (20)	-	1	96	16	BINOL
7	411	$Pd(OAc)_2$ (15)	dppp (15)	100 psi	80	72	29% **47** 27% **48**

With the carbonylation being unsuccessful, we decided to focus our energy on a whole new approach starting from affordable, achiral materials. We felt that the catalyst could probably be resolved into pure enantiomers either at the diacid stage with chiral amines or at the diamine stage with tartrates. However, since we expected to again encounter difficulties with this synthesis, we chose to proceed with achiral version at first.

Scheme 7: New, Achiral Approach for the Synthesis of 1,1'-Binaphthyl-2,2'-Diisopropylester.

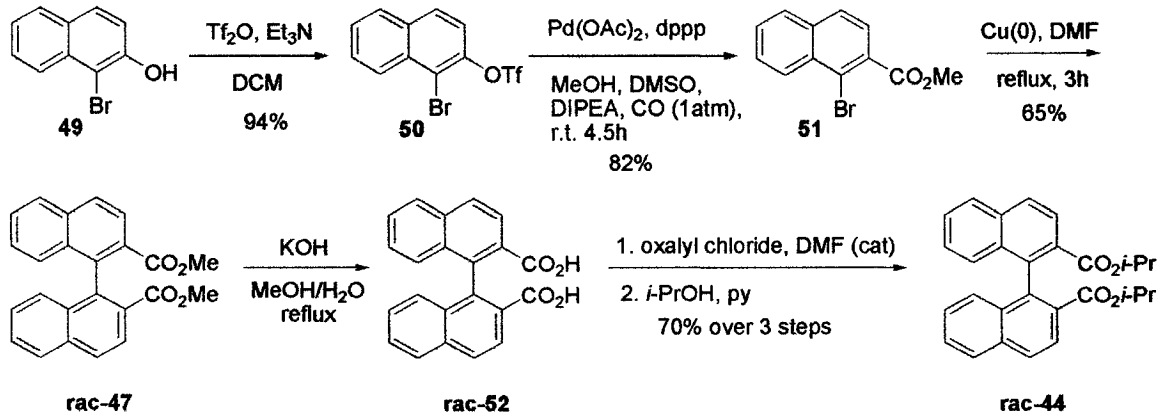

Triflate **50** was obtained in excellent yield from the reaction of 1-bromo-2-naphthol with freshly distilled triflic anhydride and triethylamine in dichloromethane at 0°C. The triflate was then subjected to carbonylation, which proceeded to give methylester **51** in 82% yield. The reaction was done in a round-bottom flask, at room temperature with a balloon filled with carbon monoxide. It had to be very closely monitored because as the starting material was consumed, we began to observe carbonylation at both the triflate and bromide positions. Reducing the catalyst loading from 10 % to 2.5 %mol and lowering the temperature from reflux to 25°C improved the yields from 58% to 82% and reduced the amount of dicarbonylated side-product formed.

The racemic diester **47** was produced by copper catalyzed homocoupling of **51** in refluxing DMF for 3 h. Activation of the copper bronze before the reaction had no impact on the yield. The scale of the reaction however largely affected the yield, with 65% being obtained only when the reaction was carried out 3.3 g of starting material.

Diester **47** was then hydrolyzed with KOH in a refluxing methanol: water mixture and the diacid **52** was used crude. It was treated with oxalyl chloride in DCM with catalytic DMF at 0°C. The acid chloride obtained after evaporation of the solvent was immediately redissolved in isopropanol with freshly distilled pyridine and the mixture was refluxed for 2 h, giving us the desired diisopropylester **44** in 70% yield over three steps.

The next stage in the synthesis was the *ortho*-magnesiation reported by Maruoka and presented earlier. In their case, the electrophile used to quench the carbanion was usually bromide. We proposed using a benzyl isocyanate, which would give us an amide and save us the extra organometallic coupling step.

Scheme 8: The Final Steps in our Proposed Synthesis of the Two-Centred Catalyst.

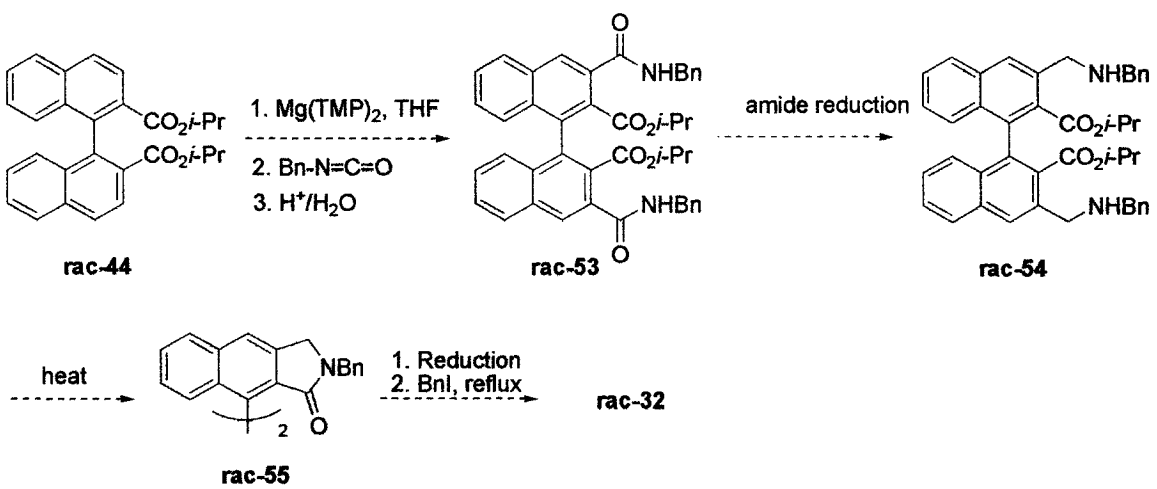

Although similar reactions had been reported in the literature as shown in the next section, we were unfortunately not able to isolate the benzyl amide. In the next section we present an overview of our efforts towards the preparation of diamide **53**.

2.2.2.3 Investigation of the Conditions for the *ortho*-Alkylation of 1,1'-Binaphthyl-2,2'-Diisopropylester.

Our first idea was to try to quench the anion formed by reaction of diisopropylester **38** with DMF. We could thus have isolated the aldehyde, which could be used, after reductive amination, to access the corresponding secondary amine. This amine might have then formed the five-membered ring we needed by nucleophilic attack on the carbonyl next to it followed by ejection of isopropanol. Reduction and quaternization would then have given us our catalyst.

Scheme 9: *ortho*-Magnesiation of 1,1'-Binaphthyl-2,2'-Diisopropyl Ester Followed by Quenching with DMF.

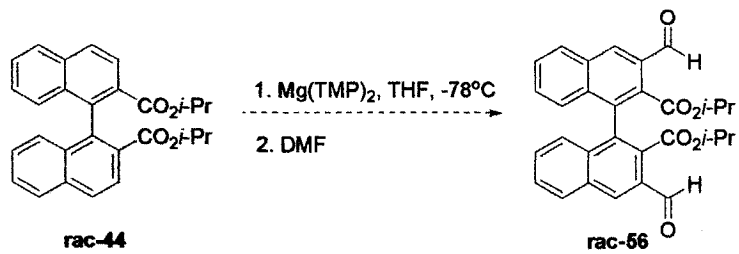

rac-44 rac-56

When this reaction was performed however, the starting material was consumed but none of the desired product was obtained. Crude ^{1}H NMR showed that there was almost no isopropyl left and from the TLC we could see that a very large number of products were formed. The following sequence was proposed to explain our results and the DMF route was thus abandoned. Instead, we decided to use isocyanates as electrophiles.

Scheme 10: Proposed Mechanism for the Reaction of the 1,1'-Binaphthyl-2,2'-Diisopropylester Dianion with DMF.

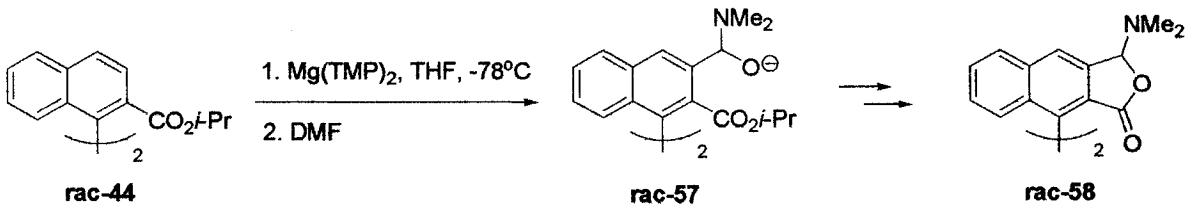

The reported conditions for *ortho*-magnesiation and electrophilic quenching of **38** did not work with benzyl isocyanate as an electrophile. We were able to quench the reaction with heavy water and observed significant conversion (about 80% from the crude ^{1}H NMR). This led us to think that benzyl isocyanate was probably just not a good enough electrophile to efficiently react with the "carbanion".

We did see an improvement when the $Mg(TMP)_2$ solution was made on small reaction scale and used immediately instead of preparing a large stock solution. Note that in this case, improvement means that we actually saw one major product as opposed to purely starting material or a streak of compounds. Unfortunately, this bright blue spot we saw after quenching the reaction seemed to decompose on silica gel. Crude ^{1}H NMR did not allow us to clearly identify the product and any attempt to purify it led to decomposition.

The reaction was performed numerous times, varying the base and temperature, and in all occasions, either there was no reaction, or a multitude of products were formed. Although both steps shown in Scheme 10 had already been reported in the literature, we were unable to reproduce these results.[80,81] Our attempts are summarized in Table 10.

Scheme 11: Previously Reported *ortho*-Lithiation and Cyclization

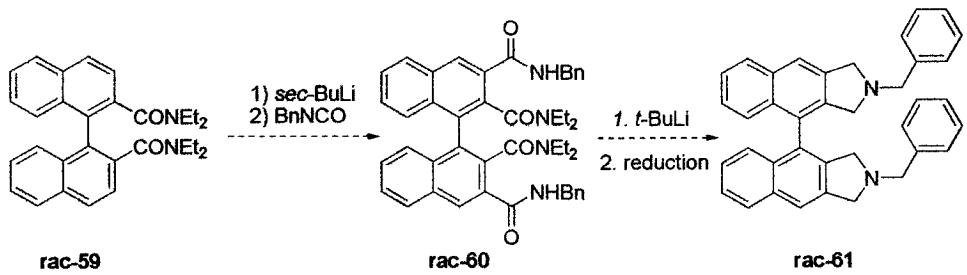

rac-59 rac-60 rac-61

Table 10: Summary of our Attempts at *ortho*-Alkylations

Starting Material	Base	T_{dep}[a] (°C)	t_{dep}[a] (h)	Electrophile	T_{elect}[a] (°C)	t_{elect}[a] (h)	Results
	TMPLi	-78	0.5	BnNCO	0.3	r.t.	sm, blue[b]
	TMPLi	0 – r.t	2	BnNCO	1	0	Sm
Diester 38	TMPLi	0	1	BnNCO	1	0	blue[b], tr. Sm
	TMPLi	-78 – 0	2	BnNCO	1	r.t	Sm
	TMP_2Mg	r.t.	16	BnNCO	1	0	sm, blue[b]
	TMP_2Mg	0	3	BnNCO	1	0	sm, blue[b]
	TMP_2Mg	-78	2	CO_2	1	0	Sm
	TMP_2Mg	-78 – r.t	16	CO_2	1	-78 – -50	Sm
Diacid 46	*t*-BuLi	-78	1.5	BnNCO	0.5	-78 – 0	Sm
Diamide 53	*sec*-BuLi, TMEDA	-78	0.58	BnNCO	1	-78 – r.t	Sm

Note: [a]T_{dep} refers to the temperature at which the deprotonation was carried out; t_{dep} is the time allowed for deprotonation; T_{elect} is the temperature at which the electrophile was added and reacted; t_{elect} is the time for which the electrophile was allowed to react before workup. [b]"Blue" refers to the unidentified blue product discussed below.

With the catalyst synthesis being so fraught with difficulties, and not knowing if this catalyst would compete with the very efficient phase-transfer catalyst designed by Maruoka[73b] now in the market, the project was abandoned.

2.3 Experimental

General Experimental

The following general experimental details apply to all reactions described herein unless otherwise specified.

Reactions were performed in round-bottom flasks equipped with a magnetic stirbar and rubber septum under N_2 atmosphere unless otherwise noted. All flasks were either flame-dried under vacuum or oven dried and cooled before use. Solvents and solutions were transferred with syringes or cannulae using standard inert atmosphere techniques.

^{1}H NMR spectra were recorded using either a Bruker Avance 300 MHz NMR spectrometer or a Bruker Avance 500 MHz Wide Bore spectrometer with $CDCl_3$ (δ = 7.26 ppm) or acetone-d_6 (δ = 2.05 ppm) as reference standard. Spectral features are tabulated in the following order: chemical shift (δ, ppm); number of protons; multiplicity (s-singlet, d-doublet, t-triplet, q-quartet, m-complex, br-broad); coupling constants (J, Hz). ^{13}C NMR spectra were recorded at 300 or 500 MHz with $CDCl_3$ (δ = 77.0 ppm) or acetone-d_6 (δ = 30.83 - sept) as reference standard or some other suitable solvent.

IR spectra were obtained using a Bomem Michaelson 100 FTIR spectrometer as a thin film on KBr plates. High resolution mass spectra (HRMS) were obtained from a Kratos IIH instrument using EI ionization and ESI mass spectra were obtained from a VG Platform Electrospray-Quadrupole instrument. Melting points were taken on an Electrothermal Meltemp® apparatus and are uncorrected.

Gas chromatography was performed on an Agilent 6890N gas chromatograph with an Agilent 190915-433 Hp-SMS 0.25 mm x 30 m x 0.25 μm column. Reactions were monitored by analytical TLC using EMD Chemicals Inc. silica gel 60 F_{254} precoated 250 μm thick glass plates. Column chromatography was performed as "Flash Chromatography" as reported by Still[82] using (230-400 mesh) Merck grade silica gel.

Acetonitrile was distilled from calcium hydride immediately before use. THF, ether, benzene, toluene and dichloromethane were obtained from an mBraun Auto-SPS solvent purification system. All other reagents were obtained from Aldrich. Strem or Lancaster and used as received unless otherwise stated.

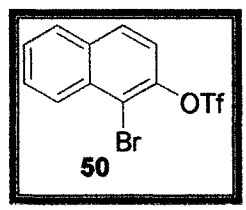

50

1-Bromo-2-trifluoromethylsulfonyloxynaphthyl.

To a solution of bromonaphtol (1.0 g, 4.5 mmol) in DCM (22.4 mL) was added Et_3N (1.3 mL, 9.0 mmol, freshly distilled from CaH_2) followed by addition of Tf_2O (0.83 mL, 5.0

mmol) at -78°C. The dry ice bath was then replaced by an ice bath. The mixture was stirred at 0°C for 10 min, quenched with a diluted aqueous solution of $NaHCO_3$, and extracted with DCM x 3. Purification by flash chromatography (15% EtOAc/hexanes) on silica gel afforded the bromotriflate (1.5 g, 94%) as a viscous oil, which solidifies after storing overnight in the freezer. ^1H NMR (300 MHz, $CDCl_3$): δ_{ppm} 8.28 (d, J = 14.4, 1H), 7.87 (d, J = 8.7 Hz, 2H), 7.63 (dddd, J = 24.3, 8.4, 6.9, 1.2, 2H), 7.42 (d, J = 9.0 Hz, 1H); ^{13}C NMR (300 MHz, $CDCl_3$): δ_{ppm} 145.0 (C_4), 133.0 (C_4), 132.6 (C_4), 129.7 (CH), 128.8 (CH), 128.3 (CH), 127.8 (CH), 127.7 (CH), 119.9 (CH), 116.6 (C_4), 116.2 (C_4). The spectroscopic data was in accord with that reported in the literature.[83]

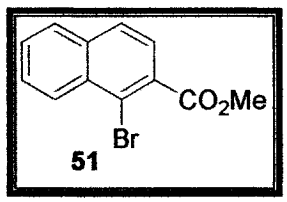

51

Methyl 1-Bromo-2-naphthoate

A solution of bromotriflate (20.54 g, 57.8 mmol), DIPEA (46.3 mL, 0.266 mol) freshly distilled over CaH_2 and MeOH (117 mL, 0.289 mol) in DMSO (300 mL) in a round-bottom flask was degassed with CO (using a balloon) for at least 1 h. To the solution were quickly added $Pd(OAc)_2$ (0.6520, 2.89 mmol) and dppp (1.198 g, 2.89 mmol). CO was bubbled through the mixture for 3.5 h. Leaving the reaction longer leads to over-carbonylation. The reaction mixture was diluted with a saturated aqueous solution of NaCl and extracted with EtOAc x 3. The combined organic fractions were dried over $MgSO_4$, concentrated and purified by flash chromatography (10% EtOAc/hexanes) to give the methylester (9.54 g, 82%) as a white solid. ^1H NMR (300 MHz, $CDCl_3$): δ_{ppm}

8.43 (d, J = 8.4 Hz, 1H), 7.80 (d, J = 8,7 Hz, 2H), 7.67 – 7.54 (m, 3H), 3.99 (s, 3H); ^{13}C NMR (75 MHz, $CDCl_3$) δ_{ppm} 167.7 (C_4), 135.0 (C_4), 132.1 (C_4), 131.0 (C_4), 128.4 (CH), 128.0 (CH) x 3, 127.7 (CH), 125.6 (CH), 122.5 (C_4), 52.6 (CH_3). The data is in accordance with the literature.[84]

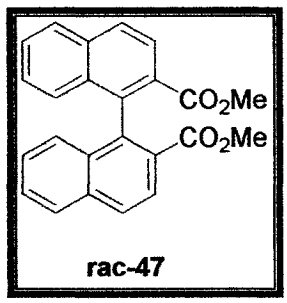

rac-47

1.1'-Binaphthyl-2,2'-dimethyl ester

To a solution of bromomethylester (3.13 g, 0,012 mol) in DMF (4.5 mL) was added Cu-bronze (1.3 g, 0.02 mol). The flask was equipped with the air-cooled condenser and the mixture was heated at 120°C (oil bath) for 4 h. It was left stirring overnight at r.t. The mixture was filtered through a pad of celite, which was then rinsed with DMF (5 mL) and EtOAc (20 mL). The obtained filtrate was partially concentrated on the rotovapor. The remaining DMF was removed using a distillation apparatus under vacuum. Purification by flash chromatography on silica gel (20 % EtOAc/hexanes) gave a coupling product (1.45 g, 65%) as a white solid. ^{1}H NMR (300 MHz, $CDCl_3$): δ_{ppm} 8.20 (d, J = 8.7 Hz, 2H), 8.02 (d, J = 8.7 Hz, 2H), 7.94 (d, J = 8.1 Hz, 2H), 7.53 – 7.48 (m, 2H), 7.26 – 7.20 (m, 2H), 7.09 (d, J = 8.4 Hz, 2H), 3.50 (s, 6H); ^{13}C NMR (75 MHz, $CDCl_3$) δ_{ppm} 167.1 (C_4), 140.3 (C_4), 134.8 (C_4), 132.9 (C_4), 127.9 (CH), 127.8 (CH), 127.7 (CH), 127.2 (CH), 127.1 (C_4), 126.7 (CH), 125.9 (CH), 51.9 (CH_3). The spectroscopic data is in accordance with the literature.[84]

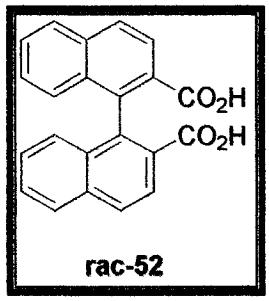

rac-52

1.1'-Binaphthyl-2,2'-dicarboxylic acid

To a solution of the diester (610 mg, 1.65 mmol) in MeOH (HPLC grade, 4.6 mL) was added H_2O (0.9 mL) followed by addition of KOH pellets (351 mg, 6.27 mmol). The reaction mixture was refluxed for 2 h, cooled to r.t. and concentrated under reduced pressure. The residue was dried to dryness on the vacuum pump. The resulting solvent was redissolved in H_2O and acidified using concentrated HCl until pH 1. Formation of a white precipitate was observed. The precipitate was then partially dissolved by adding EtOAc and some H_2O. The mixture was transferred to the separatory funnel and shaken vigorously t make sure everything is dissolved. The aqueous phase was extracted with EtOAc x 4. The combined organic fractions were dried and concentrated on the rotovapor to give the desired diacid as a white solid. It was used in the next step without further purification.

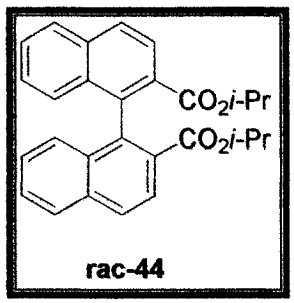

rac-44

The diacid (crude, 1.65 mmol) was transferred to the reaction flask as a solution in EtOAc (it is not soluble in DCM). The solvent was evaporated and the residue was dried using a vacuum pump. To the flask was added DCM (12 mL), followed by addition of 10% mol DMF and oxalyl chloride (0.6 mL, 6.60 mmol). After stirring for 5 min the clear yellow solution was obtained. The reaction mixture was stirred for 4.5 h at r.t., concentrated on the rotovapor and dried on the vacuum pump. The solid was redissolved in isopropanol (HPLC grade, 1.7 mL) and pyridine freshly distilled over CaH_2. The mixture was refluxed for 2 h, cooled to r.t., concentrated, diluted with H_2O and extracted with EtOAc x 4. Purification by flash chromatography on silica gel (15% EtOAc/hexanes) afforded diisopropyl ester (494 mg, 70% yield over 3 steps) as a white solid.

^1H NMR (300 MHz, $CDCl_3$): δ_{ppm} 8.01 (t, J = 4.2 Hz, 2H), 7.93 (d, J = 8.1 Hz, 2H), 7.50 (t, J = 7.2 Hz, 2H), 7.24 (t, J = 7.5 Hz, 2H), 7.13 (d, J = 8.7 Hz, 2H), 4.76 (sept., J = 6.3 Hz, 2H), 0.76 (d, J = 6.0 Hz, 6H), 0.44 (d, J = 6.3 Hz, 6H); ^{13}C NMR (300 MHz, $CDCl_3$): δ_{ppm} 166.8 (C_4), 139.6 (C_4), 134.7 (C_4), 133.2 (C_4), 128.3 (CH), 127.7 (CH), 127.6 (C_4), 127.5 (CH), 126.5 (CH), 126.1 (CH), 67.7 (CH), 21.1 (CH_3), 20.7 (CH_3). The spectroscopic data was in accord the literature[78].

3 IR Study of C-H Hydrogen Bonds in Ammonium Ions

3.1 Introduction

We have seen earlier that although infrared spectroscopy is a tool of considerable importance for the study of hydrogen bonds, its use in investigations of C-H hydrogen bonding had been limited to very simple, highly symmetrical systems such as TMA. Since C-H hydrogen bonds are fairly weak, they would not produce a vibrational stretching shift great enough to move the new band in an empty window of the spectrum. Instead, the hydrogen bonded vibration would be hidden under the non-bonded C-H stretching region preventing any clear measurement of the frequency shift. To get around this problem and be able to selectively look at the C-H vibrations of a particular region of a more complex compound without interference from the rest of the molecule, Mendelsohn and Koch[85] labeled specific components of phospholipids with deuterium. Such an approach had been used before for the carbonyl stretching shift with various isotopic substitutions.[86]

We know that the small vibrations in chemical bonds produced by exposure to infrared radiations behave like a harmonic oscillator. Therefore changing one of the two atoms in a bond for a heavier one reduces the frequency of the vibration by approximately the ratio of the reduced masses of both atoms in a bond. For a C-H versus C-D bond, the effect is quite pronounced since deuterium is twice the mass of hydrogen. The calculation to approximate the region where the C-D stretch should appear is shown below.

$$\mu^{a} = \frac{m_1 m_2^{\,b}}{m_1 + m_2} \qquad (1)$$

$$\mu_H = \frac{13 \times 1}{13 + 1} = 0.93 \text{ a.u.}$$

$$\mu_D = \frac{13 \times 2}{13 + 2} = 1.73 \text{ a.u.}$$

$$\omega_2^{\,c} = \omega_1 (\mu_2/\mu_1)^{1/2} \qquad (2)$$

$$\omega_D = \omega_H (\mu_H/\mu_D)^{1/2}$$

$$\omega_{D\,s}{}^{d} = 2926 \text{ cm}^{-1} (0.93/1.73)^{1/2} = 2151 \text{ cm}^{-1}$$

$$\omega_{D\,as} = 2853 \text{ cm}^{-1} (0.93/1.73)^{1/2} = 2097 \text{ cm}^{-1}$$

Note: [a] μ is the reduced mass of bond; [b] m_1 and m_2 are the atomic mass of each of the two atoms in said bond; [c] ω is the frequency of the bond stretch in wavenumbers; [d] 2926 cm^{-1} and 2853 cm^{-1} are the commonly accepted frequencies for general C-H antiymmetric and symmetric stretch.[87]

We thus expected to observe the C-D stretching band(s) around 2100 cm^{-1}, well detached from the C-H stretching region. Furthermore, this area is generally an open window in infrared, with the exception of the nitrile stretch. We could therefore expect to observe modest shifts quite clearly and without disruption from other functionalities. This technique was used in biological sciences to study amino proteins[88], nucleosides[89], etc. However, the difference between most of these studies and the one we were undertaking is that they used isotopic labeling to isolate the C-D band and monitor its *position* or its properties (such as infrared circular dichroism). We wanted to monitor the *shift* in frequency upon modification of the counterion. That had only, to the best of our knowledge, been done in the Arkin study discussed below.

The Arkin group has recently used the shift in C-D frequency to investigate postulated C-H hydrogen bonding in the hydrophobic region of lipid bilayers.[90] This shift in C-D stretching frequency was then mathematically extrapolated into the corresponding C-H frequency shift by multiplying it by $\mu_D/\mu_H = 1.36$. The calculated "C-H" frequency shift was then used to calculate the strength of the hydrogen bond thought to have caused the shift using the Rozenberg method.[43] It is common to perform this arithmetic on "normal", strong O-H or N-H hydrogen bonds but we have not seen other occasions where this approach was applied to C-H hydrogen bonds. Therefore it does not seem that the use of this mathematical approximation was ever solidly proven to be applicable to these weak hydrogen bonds. Nonetheless, the Arkin calculations have been quoted in some of the world's top journals.[91] We therefore decided to try their technique to study similar C-H hydrogen bonds in phase-transfer catalysts.

We proposed that by labeling selected carbons alpha the central nitrogen atom with deuterium and changing the salt counterion from poor to good hydrogen bond acceptors we should be able to notice a red shifting of the C-D stretching frequency in infrared. We could also compare the stretching frequency and the shifts between different families of compounds, some electron donating and some electron withdrawing and see the effect that this has on the hydrogen bonding ability of the alpha hydrogen (deuterium) atoms. This was interesting to us because typically, 4-methoxybenzyl groups afford significantly improved stereoselectivity over 4-fluorobenzyl groups in chiral phase-transfer catalysts.[75, 92] We felt that the methodology described above could be used to investigate the cause of this phenomenon.

Since, according to Arkin,[90] the C-D red shift could be used to calculate the hydrogen bond strength, we thought we may be able to provide the first experimental, solid phase measurement of this bond strength in complex phase-transfer catalysts. Moreover, we proposed that by taking our infrared spectra in an organic solvent transparent to infrared, we may be have been able to provide the first experimental measurement of C-H hydrogen bonding in solvated phase-transfer catalysts.

3.2 Study of Hydrogen Bonding in Phase-Transfer Catalysts

3.2.1 Hydrogen Bonding in the Solid State

For this study, we wanted to look at molecules that were commonly used as phase-transfer catalysts. We chose catalysts that allowed for facile deuterium labelling of the carbons *alpha* to the positively charged nitrogen atom either via reaction of an amine with iodomethane-d_3 or by reduction of the benzyl precursor with lithium aluminium deuteride.

Quaternization of tertiary amines was done in acetonitrile at room temperature. When primary or secondary amines were used, potassium carbonate was added to the vigorously stirred mixture.

Hydrogenated versions of these catalysts were found in the literature and all had an empty window in the C-D stretching region. In order to be quite sure, we made and

performed ion exchanges on non-labelled versions of the catalysts in Table 11 and, as we expected, their infrared spectra were empty between 2000 cm^{-1} and 2300 cm^{-1}.

The ion exchanges were done with DOWEX Cl^- anionic resin using standard procedure.[93] Our salts were usually eluted through the resin at least twice to ensure full ion exchange. The samples were then dried for about two days over phosphorus pentoxide under vacuum. To take our spectra, we dissolved a small amount of sample in dry dichloromethane, deposited it onto the salt plate and evaporated the solvent under a flow of nitrogen.

When we were finally able to get mass spectra for these salts, we noticed that for quite a few of them a peak appeared for the $2M^+X^-$ cation therefore we could see if the ion exchange had worked properly. It was then that we discovered that some of our attempts had failed to produce the desired salt and/or that there was some iodide left over contaminating the sample. Most of the acetate salts, the cyanide salts and several of the chloride salts contained some iodide. These results were discarded, leaving us with only about half of the samples that we had originally prepared. Until then, we had not realized just how difficult it was for quaternary ammonium iodides to actually change their ion.

Table 11: Measured Frequency of the C-D Stretching Band in Various Selectively Deuterated Phase-Transfer Catalysts (Thin Film)

Cation	Anion			
	I^- (cm^{-1})	OH^- (cm^{-1})	Cl^- (cm^{-1})	AcO^- (cm^{-1})
$Bu_3NCD_3^+$ **62**	2250[a]	2271	2269	2272
$Bu_3NCD_2Ph^+$ **63**	2237	2249	-	-
$Oct_3NCD_3^+$ **64**	2261	2275	2271	2276
$Oct_2N(CD_3)_2^+$ **65**	2258	2271	-	-
$Bn_2N(CD_3)_2^+$ **66**	2263	2274	-	-
$BnN(CD_3)_3^+$ **67**	2250 2258 (shoulder)	2263 2281 (shoulder)	-	-

[a]*There was a small shoulder on the peak at approximately 2258 cm^{-1}.*

Upon examination of this data, it can be observed that changing the counterion from a poor hydrogen bond acceptor like iodide to a good hydrogen acceptor such as hydroxide induced a *blue* shift in the C-D stretching frequency of about 10 cm^{-1}. In fact, as the acceptor becomes increasingly better ($OH^- \approx OAc^- > Cl^- > I^-$), the C-D bond becomes more and more blue-shifted. This result took us rather by surprise since Arkin observed a red shift which indicates a bond weakening in the donor upon formation of the hydrogen bond.

Previous infrared studies of phase-transfer catalysts had been almost completely limited to tetramethylammonium salts (see Section 1.2.3 Infrared Spectroscopy). In those cases, a red shift was observed with stronger acceptor ions. We wondered if the hydrogen atoms in our systems were also red shifted or if they behaved like the deuterated parts of the same molecules. Most of the catalysts that we made had far too many aliphatic C-H stretches to be able to discern a small shift specifically in those α to the central nitrogen atom. There were two however that did allow us to clearly see particular N^+C—H stretching frequencies: the di(methyl-d_3) dibenzylammonium and tri(methyl-d_3) benzylammonium ions. In those two molecules, the only aliphatic C-H stretch is the one in the benzylic position which comes out as a narrow, strong band around 2970 cm-^{1} that is quite distinct from the aryl C-H stretch at 3030 cm^{-1}. The benzylic C-H frequencies measured are summarized in Table 12.

Table 12: Measured Frequency of the Benzylic C-H Stretching Band in $BnN^+(CD_3)_3$ and $BnN^+(CD_3)_2$ Salts (Thin Film).

Cation	Anion	
	I^- (cm^{-1})	OH^- (cm^{-1})
$Bn_2N(CD_3)_2^+$ **66**	2946	2988
$BnN(CD_3)_3^+$ **67**	2969	2989

Upon changing the anion from the weakly hydrogen bonding iodide to the strongly hydrogen bonding hydroxide, we observed a significant blue shift in the benzylic C-H stretching frequency of these two compounds. In $BnN(CD_3)_3^+$ this shift is 20 cm^{-1} and in

$Bn_2N(CD_3)_2^+$ it is 42 cm^{-1}. This was quite interesting because, to the best of our knowledge, it was the first time that a blue shift was observed for this family of molecules. It also validated the blue shift we measured with the deuterated parts of our catalysts.

3.2.2 Hydrogen Bonding in Solvated Phase-Transfer Catalysts

Our first choice solvent for these experiments was dichloromethane since it solubilizes most phase-transfer catalysts. However, in large concentrations, the IR absorptions of the solvent completely masked the solute absorption bands. We attempted to subtract the solvent spectrum from the overall spectrum but the results, although they did give us an idea of where the C-D stretch came out, they were far from clean and we did not consider them reliable (see Figure 21).

In order to be able to clearly observe infrared bands in solution, we needed to find a solvent that was invisible in the IR window of interest. Carbon tetrachloride was our solvent of choice since it does not absorb infrared radiation in these important areas. The downside to this solvent (other than its well know carcinogenicity) is that it is not very polar and poorly solubilizes salts. The tributylammonium series was not at all soluble, forming at best a mull. We therefore had to increase the catalyst lipophilicity by substituting long, greasy alkyl chains in place of "short" butyl chains. One of the more commonly used phase-transfer catalysts of considerable lipophilicity is trioctylmethylammonium iodide. A labeled version of this catalyst could easily be

prepared using iodomethane-d_3 and was reasonably soluble in CCl_4. The spectra we obtained (shown in Figure 22) were much more reliable since no subtraction was performed and the spectra remained unaltered.

Table 13: Measured Frequency of the C-D Stretching Band in Various Selectively Deuterated Phase-Transfer Catalysts in Solution.

Cation (Solvent)	Anion			
	I^- (cm^{-1})	OH^- (cm^{-1})	Cl^- (cm^{-1})	AcO^- (cm^{-1})
$Bu_3NCD_3^+$ **62** (DCM)	2266	2276	2270	2273
$Bu_3NCD_3^+$ **62** (DCM)*	2268	2270	2268	2278
$Oct_3NCD_3^+$ **63** (CCl_4)	2264	2272	2270	2270

Figure 21: Infrared Spectra of Different $Bu_3NCD_3^+$ Salts in Dichloromethane.

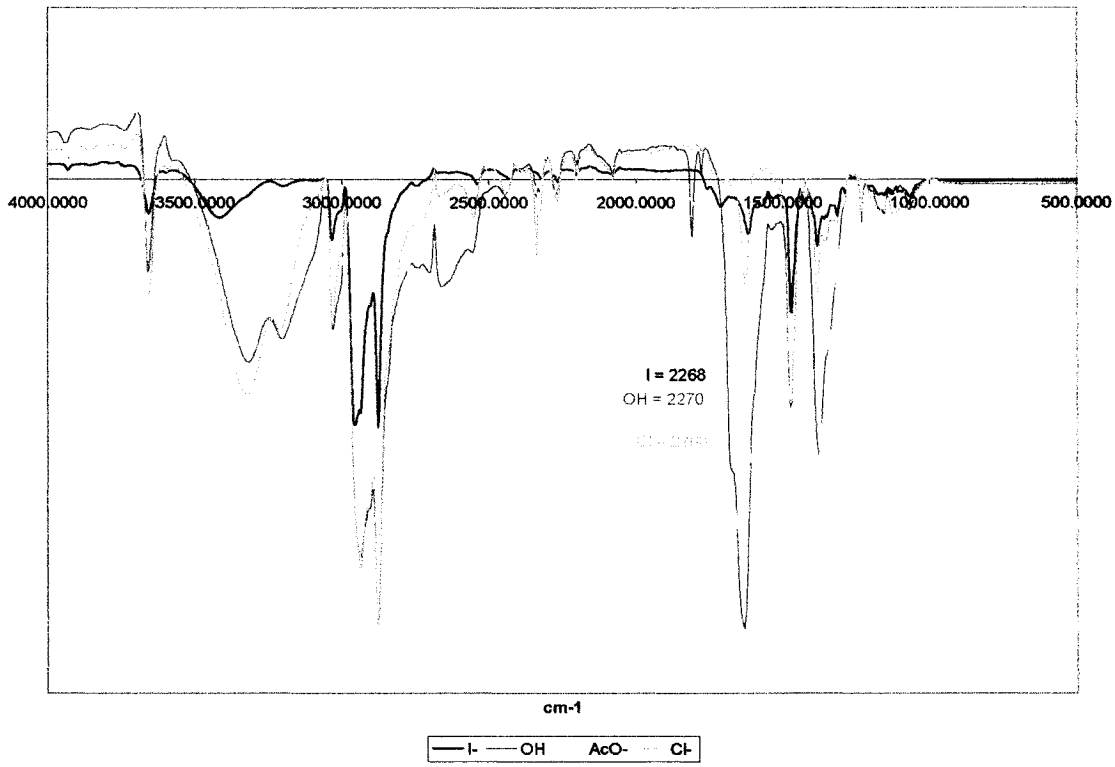

Figure 22: Infrared Spectra of Different $Oct_3NCD_3^+$ Salts in Carbon Tetrachloride.

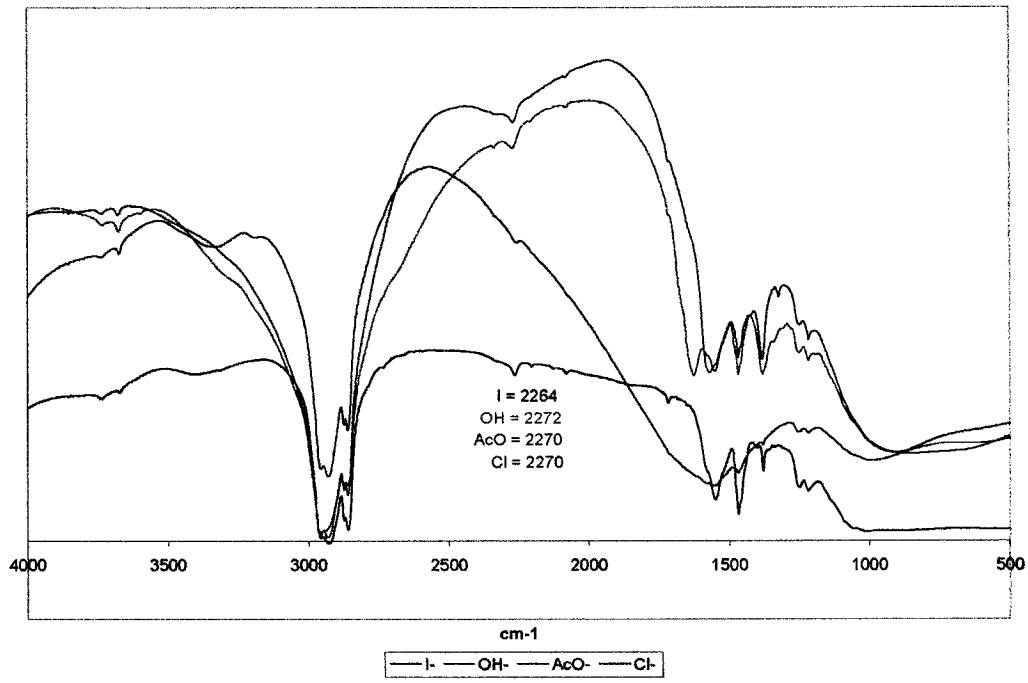

As we can see from Figure 22, the trend that we first observed in the solid state was repeated here: upon increasing the hydrogen bonding ability of the counterion, the carbon-deuterium stretching frequency was blue-shifted. The causes of the blue shift are still being hotly debated. We will review the main theories on the nature of the blue-shifted hydrogen bond in the next section and then attempt to explain our results based on these theories. What is possibly the most interesting aspect of our research is that it seems to be the first time that the same functionality gives a standard, red-shifting hydrogen bond with short alkyl chains (methyl[16]) and a blue-shifting hydrogen bond when these chains are elongated and the size increased – according to our measurements.

3.3 Blue-Shifted Hydrogen Bonds

3.3.1 Literature Overview of the Debate on the Nature of the Blue-Shifted Hydrogen Bond.

The first mention of a blue shift upon presumed formation of a hydrogen bond came in 1989 [94] though it remained unexplained and largely unnoticed. The second claim of a blue-shifted hydrogen bond was published in 1997 by Bodeskul.[95] In both cases, the shift was measured on chloroform upon mixing with various compounds that acted as hydrogen bond acceptors. The 1997 paper attempted to explain the blue shift by a strengthening of the C-H bond due to an increase in s character induced by intermolecular forces. They were not able to support their theory with calculations.

Soon after, the interest in this odd phenomenon rose when Hobza[96, 97] published a thorough computational analysis of the interaction of benzene with various C-H proton donors. In all cases, approach of the benzene molecule induced a strengthening and contraction of the carbon-hydrogen bond which led to the observed blue shifting of its stretching frequency. At the time, these were called anti-hydrogen bonds but the term was later replaced with improper, blue-shifted hydrogen bonds. Numerous studies were carried out since and it is still an active area of research. The reader is referred to a most instructive review written by Hobza[98] for more information on the history, the experiments that were carried out and the debates than ensued. A brief summary of the current theories on the nature of the blue-shifted hydrogen bond will be discussed herein.

We have already mentioned that the interaction of some mildly activated carbon-hydrogen bonds with moderate hydrogen bond acceptors produced a contraction of 0.008 Å to 0.01 Å in the C-H bond length. The strength of the carbon-hydrogen bond is heightened by this, the force constant of the bond is increased and, since the bond is stronger, its stretching frequency is raised by anywhere from less than 10 cm^{-1} to as much as 100 cm^{-1}. It was also noticed, first from computations[99] then experimentally[100] that the other bonds on the carbon centre involved in the hydrogen bond are elongated, and electronic density is increased on the three other atoms bound to this carbon. This, it turns out, is also true for normal, red-shifted hydrogen bonds.[101]

There were originally two schools of thought debating the origin of the blue-shift: those who argued that it was fundamentally the same as normal, red shifted hydrogen bonds[102,103,104,105] and those who thought that the two had different origins.[96,97,98] Both sides had their partisans and their opponents but as more experimental data was gathered, it appeared that neither was fully right. Nowadays, most believe that the difference between a blue-shifting and a red-shifting hydrogen bond comes down to a subtle balance between the bond characteristics and the forces in action, although the precise nature of these forces is still a subject of debate.

Hobza[98,106] has always believed that the blue shift was a result of electronic structural reorganization of the donor molecule upon hydrogen bond formation. This reorganization may come as a rehybridization of the donor or as a redistribution of the electron density in a remote part of the molecule. Unlike red-shifted hydrogen bonds, the

bulk of the electronic density is not transferred to the σ^*_{C-H} orbital. There have been studies supporting this view, particularly in the case of $H_3N\cdots HCF_nH_{3-n}$. In this series of compounds, it was found that for fluoroform, the complex was red shifted, with the electronic density situated mainly in the C-H antibonding orbital. The $H_3N\cdots HCH_2F$ complex on the other hand gives rise to a blue shift of the C-H stretching frequency and computational modelling suggests that the electronic density is directed mostly to the σ^*_{C-F} orbital.[107] It is assumed in line with these interpretations that the blue-shifted hydrogen bond is different in nature since it depends on the intrinsic properties of the donor molecule. Recently however, some interesting blue-shifted hydrogen bonds in diatomic molecules (HCl) have been observed that cannot be explained by charge transfer to a remote part of the molecule.[108]

Scheiner,[101,102] after studying numerous $F_nH_{3-n}C\text{-}H\cdots O$ compounds, has found that these dimers are similar to "normal" O-H and N-H red-shifted hydrogen bonds in terms of electron density shifts, geometric behaviour and energy components. According to this model, for all hydrogen bonds there are five parameters that vary in each system. Their equilibrium determines whether the hydrogen bond will be red or blue-shifted. Charge transfer, polarization, electrostatics and dispersion energy pull the hydrogen atom away from the donor while the exchange overlap pushes it away from acceptor. If the exchange is large compared to the other contributions, a blue shift is observed and vice versa in the case of red-shifted complexes. Here, there is no fundamental difference between the two types of hydrogen bonds.

A third category of explanations for the bond contraction is based on electrostatics. Some believe that a purely point charge analysis fully explains the phenomenon since calculations have shown that polarization of C-H bonds by small localized electric fields can lead to a bond contraction[109,110] while others suggest that at equilibrium distance, the electrostatic attraction and dispersion interaction causing the C-H bond elongation may be balanced out by sterics (Pauli repulsion) and when the latter is large enough, a bond contraction occurs.[111] The most complete explanation in this category however certainly comes from Hermansson.[112] He argues that for blue-shifting hydrogen bonds, it is necessary but not sufficient to have a negative derivative of the dipole moment with respect to the stretching coordinate. There have been exceptions to this "rule"[108] but the idea is still worthy of note. In order to actually observe the blue shift, Hermansson states that the exchange overlap must be quite large and a continuum of behaviour is observed where weakly interacting bases give blue shifts and stronger bases lead to red shifts.

Although these models are very useful for computational and theoretical chemists, all of them lack the ability to translate well into an explanation that would appeal to organic chemists. An attempt at providing such a description was made by Alabugin.[113] Admitting that it was merely an approximation, he used Bent's rule, to explain the blue shift observed with certain molecules. Bent's rule states that the formation of any hydrogen bond leads to an increase in s character for X-H bond of the donor molecule. Alabugin hypothesized that in cases where both the charge transfer from the acceptor and hyperconjugation (in this case referring to the donation of electron density from the acceptor lone pairs to the $\sigma^*_{C\text{-}H}$ orbital) were mild, they may be too weak to overcome the

bond strengthening caused by an increase in s character. For strong hydrogen bonds, the same forces would come into play but their relative magnitude would counterbalance the slight strengthening and lead to a red shift. The concept is somewhat similar to Hobza's two step process of charge transfer and reorganization[98] but this time it would be applicable to all hydrogen bonds. Since this is mostly an "organic" explanation, there are some very exotic molecules that disprove it. Blue shifts have been observed in complexes where rehybridization was impossible.[114] Nonetheless, for most cases and keeping in mind that it is merely an approximation, Alabugin provided us with a more palatable and esthetically pleasing explanation than the previous computationally-based analyses.

3.3.2 Analysis of Our Results

An attempt at rationalization of our results based on each of the theories described above will now be presented. Many cannot explain why TMA salts would give a clear, pronounced red shift whereas tributyl(methyl-d_3)ammonium or benzyltri(methyl-d_3)ammonium give blue shifts on both their deuterated and (in the benzyl salts) hydrogenated sections. Our data therefore seems to lend support to one particular model.

According to the Hobza explanation, after donation of electronic density into the C-H or C-D bond, there should be electronic reorganization that leads to a blue shift rather than a red shift. This reorganization is the result of the intrinsic properties of the hydrogen bond donor. But there is no obvious reason why the compounds that we have studied would be capable of such reorganization but not TMA. Similarly, following the Abagulin model,

in TMA the rehybridization upon hydrogen bond formation would be minimal whereas in all of our molecules, it would have to be significant. This simply does not seem to explain such a huge variation in frequency shifts. If rehybridization does indeed occur, in a compound such as benzyltri(methyl-$_{d3}$)ammonium hydroxide, we should observe contraction of some bonds and elongation of others as the p character in the three bonds not participating in the hydrogen bond is increased. Therefore one of either the C-H or C-D stretch should be shifted to the red and, as we saw, this does not occur.

Since the electrostatic contribution of hydroxide or chloride remains the same regardless of whether it is binding to TMA or our partially deuterated salts, pure electrostatic point charges can probably not alone explain the blue-shifting. The equilibrium geometry will be different and the strength of an electric field diminishes very rapidly (α $1/r^2$) which may be an important factor. Calculations or crystal structures would be necessary to clarify this point. An important piece of information that we have gathered from this study however is that a negative dipole moment derivative along the direction of the stretch is not necessary for all compounds. This is a rule that was developed for fluoroform and similar molecules and that simply does not apply here. When stretching any of our C-H or C-D bonds, the positive charge on the hydrogen/deuterium will increase not decrease as is the case for fluoroform. Yet we still observe a blue shifting hydrogen bond. The Hermansson model is thus not sufficient to rationalize our findings.

In fact, the most useful theory in our case is the one proposed by Scheiner. The direction of the frequency shift is the result of a subtle balance between polarization, electrostatics,

charge transfer, dispersion energy (or van der Waals interactions) and the exchange overlap (repulsion of electron clouds). Though a thorough computational analysis would be necessary to dissect the contribution of each component, we can already approximate that with our large catalysts, the exchange overlap would most likely be much larger than in small TMA salts. It is also known that deuterium is not polarized as easily as hydrogen and, with its smaller volume, the C-D dispersion energy would most likely be lower. On the other hand, the presence of aliphatic or aromatic side-chains would increase the dispersion energy but maybe not enough to counteract the unfavourable electronic repulsion.

3.4 Experimental

Ion Exchange Procedure

First, a slurry was made with the Dowex 1x2, Cl^--form strongly basic ion exchange resin in distilled water. The column (approx. 1cm diameter) was loaded with the resin (8-10 cm in height) and rinsed with distilled water. To change the counter-ion in the column, a 1M solution of the desired salt was prepared (e.g. NaOH, NaI, NaOAc, HCl) and approximately five times the resin volume was passed through slowly (~1 drop/second). Distilled water was then eluted through the column until it came out neutral. The resin was then rinsed with methanol several times to remove the aqueous environment and finally the sample, dissolved in methanol, was slowly eluted (max. 1 drop/second) through the column.

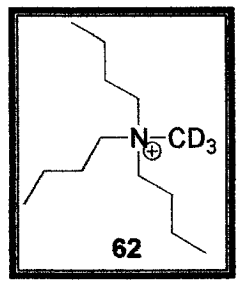

62

Tributyl(methyl-d_3)ammonium iodide

Tributylamine (200 μL, 0.84 mmol, 1 eq.), freshly distilled over CaH_2, was transferred to a round-bottom flask equipped with a magnetic stirbar. Methyl-d_3 iodide (0.10 mL, 1.6 mmol, 2 eq.) was added to the neat amine and the mixture was stirred at room temperature for 2h. The crude mixture was then recrystallized from dichloromethane (1 mL) with ether (4 mL) and hexanes (0.5 mL), filtered and dried under vacuum to give a pale yellow powder (0.2567 g, 93 %). ^{1}H NMR (300 MHz, $CDCl_3$): δ_{ppm} 3.50 – 5.44 (m, 6H), 1.70 (m, 6H), 1.47 (sext., J = 7.5 Hz, 6H), 1.02 (t, J = 7.2 Hz, 9H); ^{13}C NMR (300 MHz, $CDCl_3$): δ_{ppm} 61.6 (CH_2), 24.4 (CH_2), 19.7 (CH_2), 13.8 (CH_3); IR (cm^{-1}, neat) 2961, 2874, 2250, 1462, 1386, 1270, 1163, 1124, 1067, 734 cm^{-1}; ESI-MS *m/z* 203.4 (M^+); mp = 136 - 139 °C

Tributyl(methyl-d_3)ammonium hydroxide

^{1}H NMR (500 MHz, Acetone-d_6): δ_{ppm} 3.57 – 3.54 (m, 6H), 1.88 – 1.81 (m, 6H), 1.43 (sext., J = 7.5 Hz, 6H), 0.98 (t, J = 7.5 Hz, 9Hz); IR (cm^{-1}, neat) 3393 (b), 2961, 2874, 2733, 2270, 2080, 1630, 1469, 1381, 1155, 1067, 923, 835, 739; ESI-MS *m/z* 203.4 (M^+); mp = 135 - 142 °C

Tributyl(methyl-d_3)ammonium chloride

^{1}H NMR (300 MHz, $CDCl_3$): δ_{ppm} 3.48 (m, 6H), 1.74 – 1.63 (m, 6H), 1.44 (sext., J = 7.5 Hz, 6H), 1.00 (t, J = 7.2 Hz, 9H); IR (cm^{-1}, neat): 3397 (b), 2963, 2876, 2275, 1664, 1471, 1381, 1154, 1067, 920, 825; ESI-MS m/z 203.4 (M^+), m.p. = 134.3 – 136.6.

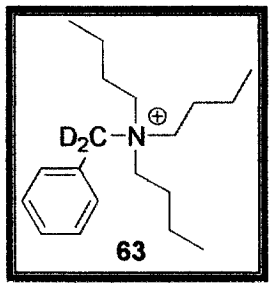

63

(Benzyl-(d_2))tributylammonium iodide

Sodium iodide (1.0043g, 6.7 mmol, 2 eq.) was dissolved in acetone (30 mL) in a round-bottom flask under nitrogen atmosphere. Benzyl-d_2 chloride (0.4219g, 3.3 mmol, 1 eq.) was added and the reaction was vigorously stirred at room temperature for 2h. It was then diluted with dichloromethane (30 mL) and filtered. The resulting benzyl-d_2 iodide was concentrated under reduced pressure and used immediately without purification for reasons of unstability.

Tributylamine (0.30 mL, 1.2 mmol, 1 eq.) was distilled over calcium hydride then added to an oven-dried round-bottom flask under nitrogen and diluted with acetonitrile (10 mL). Benzyl-d_2 iodide was canulated into the amine solution and the mixture was stirred at room temperature overnight. When the reaction appeared complete by TLC, the mixture was rotovaped, pumped and recrystallized from chloroform (1 mL) with ether (7 mL) and hexanes (0.5 mL).

^{1}H NMR (300 MHz, $CDCl_3$): δ_{ppm} 7.54 – 7.44 (m, 5H), 3.31 (m, 6H), 1.81 (m, 6H), 1.42 (sext, J = 7.5 Hz, 6H), 1.00 (t, J = 7.2 Hz); ^{13}C NMR (300 MHz, $CDCl_3$): δ_{ppm} 132.5 (C_4), 130.7 (CH), 129.4 (CH), 127.5 (CH), 58.5 (CH_2), 24.5 (CH_2), 19.8 (CH_2), 13.7 (CH_3); IR (cm^{-1}, neat): 2959, 2872, 2237, 1472, 1450, 1379, 1157, 1062, 719; ESI-MS *m/z* 278.5 (M^+); mp = 142 - 145 °C.

(Benzyl-(d_2))tributylammonium hydroxide – ^{1}H NMR (300 MHz, $CDCl_3$): δ_{ppm} 7.56 – 7.44 (m, 5H), 3.33 (m, 6H), 1.78 (m, 6H), 1.41 (sext., J = 7.2 Hz, 6H), 1.00 (t, J = 7.2 Hz, 9H); IR (cm^{-1}, neat) 3405 (b), 2962, 2875, 2635, 2249, 2179, 1632, 1475, 1381, 1060, 722; ESI-MS *m/z* 278.5 (M^+); mp = 161.7 – 163.2 °C

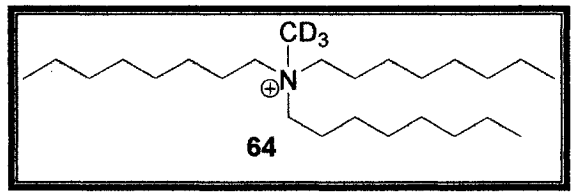

64

Trioctyl(methyl-d_3)ammonium iodide

Freshly distilled trioctylamine (50 μL, 0.11 mmol, 1 eq.) was placed in a round-bottom flask under nitrogen atmosphere. Methyl-d_3 iodide (15 L, 0.23 mmol, 2 eq.) was added to the neat amine and the mixture was stirred at room temperature 3 h. The residual methyl iodide was removed under reduced pressure, affording the product (0.0569 g, 99.7%) as yellow solid. The chloride, hydroxide and acetate equivalents were all yellow oils.

^{1}H NMR (300 MHz, $CDCl_3$): δ_{ppm} 3.45 (m, 6H), 1.71 (m, 6H), 1.37 – 1.27 (m, 30 H), 0.88 (t, J = 6.9 Hz, 9H); ^{13}C NMR (300 MHz, $CDCl_3$): δ_{ppm} 61.3 (CH_2), 31.6 (CH_2), 29.1 (CH_2), 29.0 (CH_2), 26.2 (CH_2), 22.5 (CH_2), 22.3 (CH_2), 14.0 (CH_3); IR (cm^{-1}, neat): 3497

(b), 2925, 2855, 2261, 1467, 1378, 1056, 765; ESI-MS *m/z* 371.7 (M^+), m.p = 59.3 – 61.2.

Trioctyl(methyl-d_3)ammonium hydroxide

^{1}H NMR (300 MHz, $CDCl_3$): δ_{ppm} 3.53 (s, 1H), 3.40 (m, 6H), 1.65 (m, 6H), 1.35 – 1.27 (m, 30 H), 0.88 (t, J = 6.0 Hz, 9H); IR (cm^{-1}, neat): 3397 (b), 2926, 2856, 2667, 2276, 1625, 1467, 1380, 1061, 996, 836; ESI-MS *m/z* 371.7 (M^+).

Trioctyl(methyl-d_3)ammonium chloride

^{1}H NMR (300 MHz, $CDCl_3$): δ_{ppm} 3.46 – 3.41 (m, 6H), 1.67 (m, 6H), 1.36 – 1.27 (m, 30 H), 0.87 (t, J = 6.3 Hz, 9); IR (cm^{-1}, neat): 3407 (b), 2924, 2856, 2271, 2082, 1634, 1467, 1379, 1060, 823, 765; ESI-MS *m/z* 371.7 (M^+).

Trioctyl(methyl-d_3)ammonium acetate

^{1}H NMR (300 MHz, $CDCl_3$): δ_{ppm} 3.44 (m, 6H), 1.96 (s, 3H), 1.64 (m, 6H), 1.35 – 1.27 (m, 30 H), 0.88 (t, J = 6.3 Hz, 9H); IR (cm^{-1}, neat): 3497 (b), 2925, 2855, 2261, 1467, 1378, 1056, 765; ESI-MS *m/z* 371.7 (M^+).

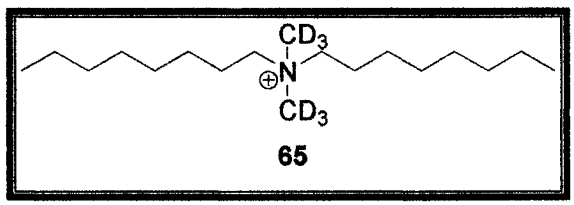

65

Dioctyldi(methyl-d_3)ammonium iodide

To freshly distilled dioctylamine (0.50 mL, 1.66 mmol, 1 eq.) in acetonitrile (6 mL) were added potassium carbonate (0.3313 g, 2.4 mmol, 1.5 eq.) and methyl-d_3 iodide (0.25 mL, 4.0 mmol, 2.5 eq.). The mixture was stirred at room temperature overnight then ether (5

mL) was added and the solution was filtered. The filtrate was concentrated under reduced pressure and the product (0.6627g, 99%), a thick pale yellow liquid, was used crude.

^{1}H NMR (300 MHz, $CDCl_3$): δ_{ppm} 3.54 (m, 4H), 1.73 (m, 4H), 1.37 – 1.27 (m, 20H), 0.88 (t, J = 7.2 Hz, 6H); ^{13}C NMR (300 MHz, $CDCl_3$): δ_{ppm} 63.5 (CH_2), 31.6 (CH_2), 29.1 (CH_2), 29.0 (CH_2), 26.2 (CH_2), 22.7 (CH_2), 22.5 (CH_2), 14.0 (CH_3); IR (cm^{-1}, neat): 3459 (b), 2924, 2855, 2670, 2260, 2074, 1615, 1467, 1377, 1144, 1106, 1062, 812, 723; ESI-MS *m/z* 276.5 (M^+).

Dioctyldi(methyl-d_3)ammonium hydroxide

^{1}H NMR (300 MHz, $CDCl_3$): δ_{ppm} 3.48 (m, 4H), 1.88 (s, 3H), 1.68 (m, 4H), 1.35 – 1.26 (m, 20H), 0.87 (t, J = 5.4 Hz, 6H); IR (cm^{-1}, neat): 3393 (b), 2926, 2856, 2671, 2271, 2126, 2078, 1651, 1466, 1379, 1285, 1142, 1067, 880, 828, 723; ESI-MS *m/z* 276.5 (M^+).

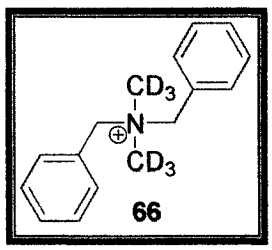

66

Dibenzyldi(methyl-d_3) ammonium iodide

To an oven-dried flask equipped with a magnetic stirbar was added dibenzylamine (50 µL, 0.26 mmol, 1 eq.) and potassium carbonate (0.0722 g, 0.52 mmol, 2 eq.). The system was flushed with nitrogen and acetonitrile (1 mL) followed iodomethane-d_3 (50 µL, 0.11 mmol, 2.5 eq.) were added. The mixture was stirred at room temperature 2h then diluted

with dichloromethane (3 mL) and filtered. The solvent was removed under reduced pressure affording the product (92.6 mg, 99% y.) as a yellow solid.

^{1}H NMR (300 MHz, $CDCl_3$): δ_{ppm} 7.64 (d, J = 3.3 Hz, 4H), 7.36 (m, 6H), 5.07 (s, 4H); ^{13}C NMR (300 MHz, $CDCl_3$): δ_{ppm} 133.3 (CH), 130.8 (C4), 129.2 (CH), 126.9 (CH), 67.1 (CH2); IR (cm^{-1}, neat): 3468 (b), 3031, 2946, 2428, 2263, 2074, 1497, 1457, 1350, 1214, 1099, 1050, 739; mp = 190.5 - 192.0; ESI-MS *m/z* 232.2 (M^+).

Dibenzyldi(methyl-d_3) ammonium hydroxide

^{1}H NMR (300 MHz, $CDCl_3$): δ_{ppm} 7.65 (m, 4H), 7.43 – 7.33 (m, 6H), 5.09 (s, 4H); IR (cm^{-1}, neat): 3382 (b), 3061, 3036, 2988, 2957, 2270, 2077, 1632, 1457, 1294, 1214, 1099, 749; mp = 188.3 – 189.8; ESI-MS *m/z* 232.2 (M^+).

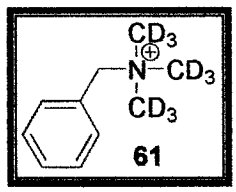

61

Benzyltri(methyl-d_3)ammonium iodide

Freshly distilled benzylamine (50 µL, 0.46 mmol, 1 eq.) and potassium carbonate (0.1580 g, 1.145 mmol, 2.5 eq.) were placed in a round-bottom flask which was then flushed with nitrogen. The mixture was suspended in acetonitrile (2 mL) and iodomethane-d_3 (90 µL, 1.42 mmol, 3.1 eq.) was added. After vigorously stirring overnight at room temperature, the reaction was diluted with dichloromethane (4 mL) and filtered. The solvent was removed under reduced pressure and pumped, affording the product (0.1259 g, 96%) as a yellow solid.

^{1}H NMR (300 MHz, $CDCl_3$): δ_{ppm} 7.68 (m, 2H), 7.47 (m, 3H), 5.06 (s, 2H); ^{13}C NMR (300 MHz, $CDCl_3$): δ_{ppm} 133.0 (CH), 130.9 (C_4), 129.3 (CH), 127.1 (CH), 68.5 (CH_2); IR

(cm^{-1}, neat): 3450 (b), 3035, 2969, 2250, 1458, 1148, 745; mp = 177.8 – 180.9; ESI-MS *m/z* 159.2 (M^+).

Benzyltri(methyl-d_3)ammonium hydroxide

^1H NMR (300 MHz, $CDCl_3$): 7.67 (d, J = 3.0 Hz, 2H), 7.47 (m, 3H), 5.06 (s, 2H); IR (cm^{-1}, neat): 3398 (b), 3066, 2989, 2265, 2078, 1634, 1458, 1148, 1062, 754; mp = 158.5 – 156.3; ESI-MS *m/z* 159.2 (M^+).

4 Kinetic Study of C-H Hydrogen Bonds in Phase-Transfer Catalysis

4.1 Introduction

Since experimental evidence of the existence of C-H hydrogen bonds in solution was achieved, we wondered how much these hydrogen bonds might impact actual phase-transfer catalyzed reactions. A classical means of evaluating the importance of specific hydrogen atoms in chemical reactions is via isotope effects. Kinetic, equilibrium and solvent isotope effects all yield important information about reaction processes, rates and hydrogen bonding.

Kinetic isotope effects are said to occur when an isotopically-labeled bond is broken or formed or is adjacent to a bond that is broken/formed in or before the rate-determining step of a reaction. The isotopic labeling affects the overall rate constant of the reaction and the rate difference can be used to obtain mechanistic information. Solvent isotope effects are used to probe interactions between a substrate and the solvent during the rate-determining step of a reaction. The rate is measured separately in the fully hydrogenated solvent (usually water or methanol) and the fully or partially deuterated solvent. Deuterium labeling in this case affects both the potential solvent deprotonation rate and/or the extent of hydrogen bonding to the solvent at the transition state.[115]

Similarly, equilibrium isotope effects are the result of a change in equilibrium constant upon isotopic substitution. The term is applied to experiments where isotopic enrichment

of one product occurs preferentially to another as well as experiments where the association constant of a complex is affected by noncovalent interactions with isotopically labeled atoms (for example in enzyme-substrate complexes). Deuterium substitution reduces the stabilization provided by hydrogen bonding and thus reduces the binding energy between the two molecules. This is precisely what we expected to observe if we were to label the α-carbons of phase-transfer catalysts with deuterium. The binding of counterions should be affected since deuterium is known to normally form weaker H-bonds than hydrogen.

The actual impact of deuterium substitution of the catalyst on reaction rate will most likely depend on the mechanism and the rate constant of each step of the reaction. It is difficult to predict whether the deuterated catalysts will lead to a faster or slower reaction rate.

To study this potential isotope effect, we chose a reaction that was previously used in a comparative evaluation of different phase-transfer catalysts:[116] the allylbenzene isomerization shown in Scheme 11. We felt this was a wise choice because the reaction was already well known, simple and intrinsically rate-limiting, meaning that the rate is directly dependant on the rate of substrate deprotonation, not on the rate of reaction of the anion generated with a third compound. If the rate limiting step of a reaction is the alkylation instead, the rate expression is no longer directly linked to the rate of deprotonation and it becomes more complicated to estimate the impact that the phase-transfer catalyzed deprotonation will have on the overall reaction rate.

Scheme 12: Phase-Transfer Catalyzed Isomerization of Allylbenzene

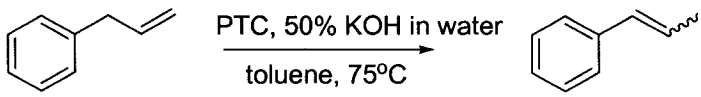

68 **69**

The catalyst was also chosen to optimize anion interaction with the deuterated sections. Since counterions interact simultaneously with three branches,[34,35,37,39] we chose catalysts with at least two deuterated methyl groups. Ideally, it would have been to our advantage to use TMA-d_{12} or alkyltri(methyl-d_3)ammonium catalysts but these are not soluble enough in the organic phase to get reasonable reaction rates. We therefore compromised and decided to use dioctyldi(methyl-d_3)ammonium.

4.2 Results of our Kinetic Studies

With all phase-transfer catalyzed reactions, the surface contact between both phases has a dramatic impact on the rate. For that reason, the size and shape of the reaction vessel, the volume of the reaction mixture, the type and size of the stirbar as well as the stirring rate must be very tightly controlled. All of our reactions were done under nitrogen, in 10 mL round-bottom flasks with freshly distilled solvents and 1.3 x 0.3 cm stirbars. The mixture was heated in an oil bath equipped with a digital temperature controller and the flask immersed up to the bottom of neck, with no more than two flasks per bath so that they could be centred as much as possible. Whenever possible, the reactions catalyzed by the hydrogenated and deuterated catalysts were carried out simultaneously.

The reactions were performed as described by the authors,[116] albeit on a smaller scale. Although the aliquots taken were small, there is a possibility that the minute changes in the organic phase volume might have sped up the reaction as it progressed. We performed our reactions in 3 mL of preheated toluene, with 40 μL of 1,3-dimethoxybenzene as a standard. The allylbenzene and catalyst were added followed by the aqueous potassium hydroxide. Subsequent addition of base was marked as t_0.

With the iodide catalyst, the reaction was heated to 75°C with 10 % mol catalyst loading. Under those conditions, the reaction was relatively slow, being only about 15% done after four hours. Our first trials appeared very successful as we observed a very pronounced isotope effect. The reaction with the hydrogenated catalyst was about 40% faster than with the deuterated catalyst and, using the same batches of catalysts these results were quite reproducible (see Figure 23). Unfortunately, when we tried to repeat them with new, fresh batches of catalysts, we found that once again, within the same catalyst batch we were getting reproducible results (see Figure 24) but the isotope effect was diminished and the rate of the deuterated catalyst runs were not comparable to the ones we had previously measured (see Figure 25).

Figure 23: Kinetics of Phase-Transfer Catalyzed Allylbenzene Isomerization with our First Batch of Dioctyldimethylammonium Iodide.

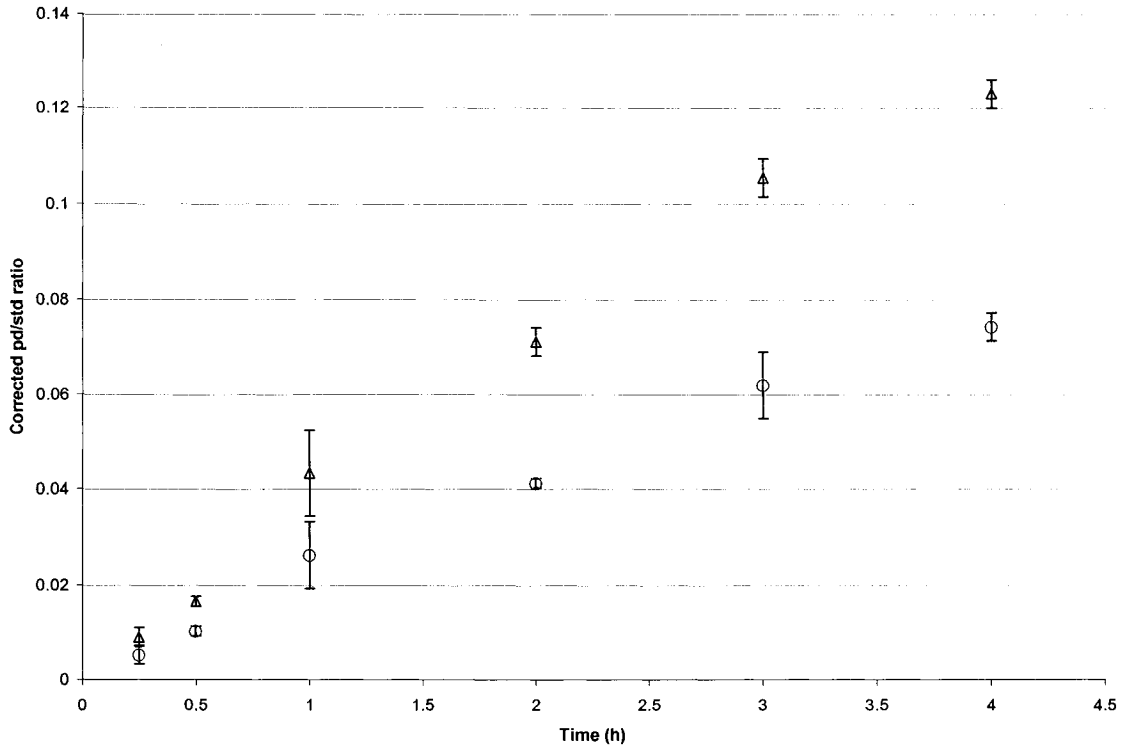

Note: blue triangle = catalyzed by $Oct_2Me_2N^+I^-$; red circle = catalyzed by $Oct_2(Me\text{-}d_3)_2N^+I^-$. pd = product; std = standard.

Figure 24: Kinetics of Phase-Transfer Catalyzed Allylbenzene Isomerization with our Second Batch of Dioctyldimethylammonium Iodide.

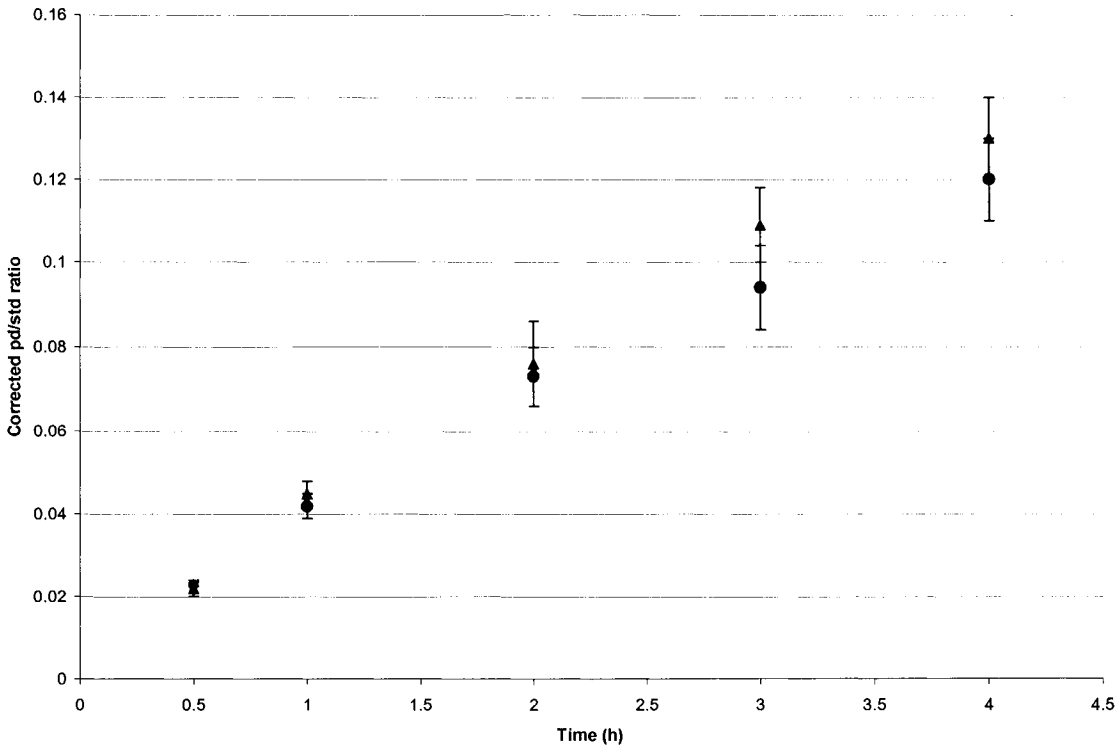

Note: blue triangle = catalyzed by $Oct_2Me_2N^+I^-$; red circle = catalyzed by $Oct_2(Me\text{-}d_3)_2N^+I^-$. pd = product; std = standard.

Figure 25: Comparative Kinetics of Phase-Transfer Catalyzed Allylbenzene Isomerization with our First and Second Batches of Dioctyldimethylammonium Iodide.

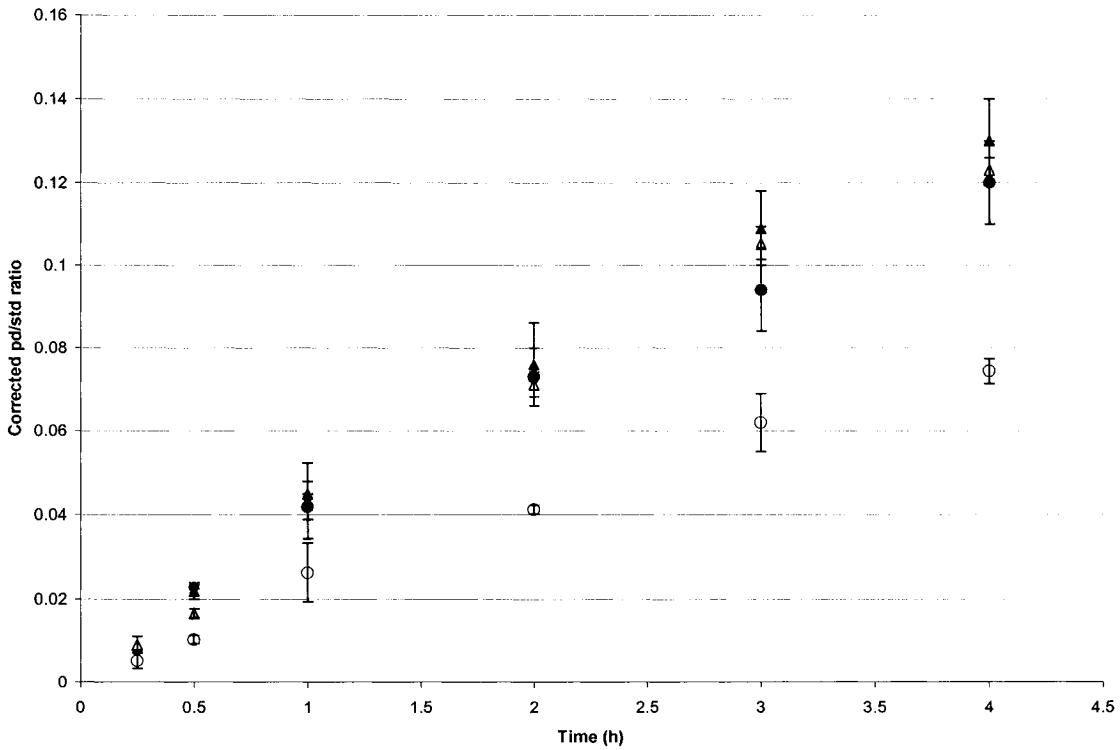

Note: empty blue triangle = catalyzed by $Oct_2Me_2N^+I^-$, first batch; full blue triangle = catalyzed by $Oct_2Me_2N^+I^-$, second batch; empty red circle = catalyzed by $Oct_2(Me\text{-}d_3)_2N^+I^-$, first batch; full red circle = catalyzed by $Oct_2(Me\text{-}d_3)_2N^+I^-$, second batch.
pd = product; std = standard.

Since we were having problems using iodide as a counterion, we decided to try doing the reactions with dioctyldimethylammonium chloride instead. This time the reactions were much faster, being 15% done within two hours. The isotope effect completely disappeared and moreover, reproducibility was still an issue. Our more reliable trials are included in Figure 26. (Some trials were excluded because in the process of optimization, a few parameters such as flask size, temperature and stirring rate, were modified to see their impact on reaction rate) We were also surprised to notice that with chloride as a counterion, the reaction still turned orange then red within a few minutes of the catalyst addition. With iodide this could have been due to the production of iodine but with chloride it seemed somewhat strange. This observation prompted us to try and degas our solvent before making the catalyst stock solution and before using it in our reactions. From then on, the freshly distilled toluene was degassed for at least 10 minutes with nitrogen prior to use. Although this did not affect the colour change, it dramatically sped up the reactions and in order to be able to accurately measure the rate, we had to drop the catalyst loading to 5 mol%. Degassing our solutions finally allowed us to get the reproducibility we wanted but in the end, we were not able to observe an isotope effect (see Figure 27).

Figure 26: Kinetics of Phase-Transfer Catalyzed Allylbenzene Isomerization with Dioctyldimethylammonium Chloride.

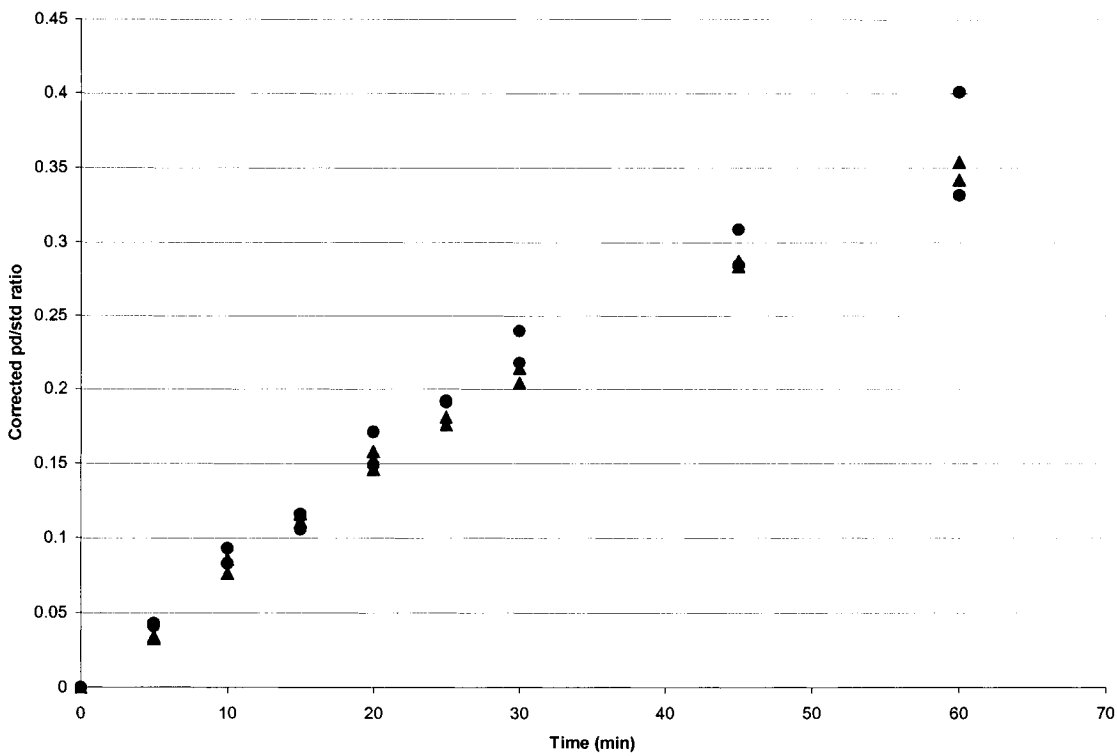

Note: blue triangle = catalyzed by $Oct_2Me_2N^+Cl^-$; red circle = catalyzed by $Oct_2(Me\text{-}d_3)_2N^+Cl^-$. pd = product; std = standard.

Figure 27: Kinetics of Phase-Transfer Catalyzed Allylbenzene Isomerization with Dioctyldimethylammonium Chloride and Degassed Solvent.

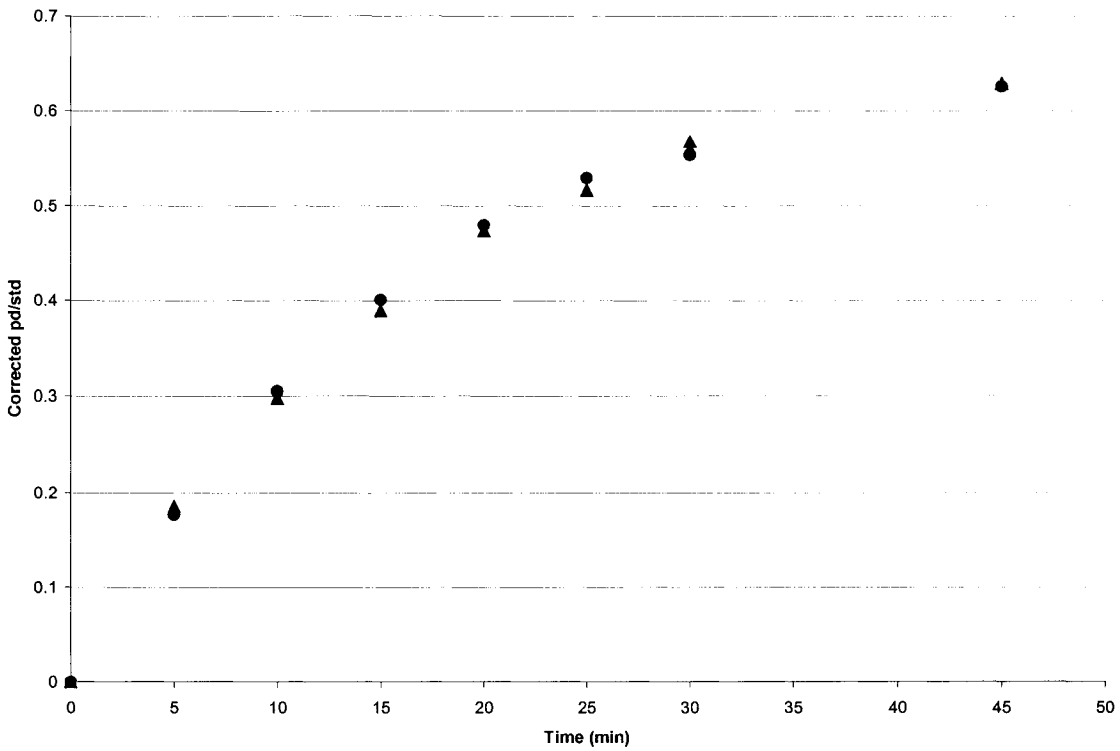

Note: blue triangle = catalyzed by $Oct_2Me_2N^+Cl^-$; red circle = catalyzed by $Oct_2(Me\text{-}d_3)_2N^+Cl^-$. pd = product; std = standard.

So after months of trials and optimization, we had to admit that there was in fact no isotope effect observable in this reaction.

4.3 Conclusions

What is unfortunate about this project is that it leaves us with no clear answer regarding isotope effects in phase-transfer catalyzed reactions. The reader may recall from our introduction that hydration even by a single water molecule severely reduces hydrogen bonding.[50] At the time this research was performed we were not aware of those results. Had we known about it, we probably would have chosen a different reaction to study. Even now, there is regrettably no simple solution to this problem. Most alkaline bases used in phase-transfer reactions are hydrated so C-H hydrogen bonds may not be of critical importance in these processes after all. Nonetheless, it would be interesting to see if neutral phase-transfer reactions are affected by isotopic substitution at all, particularly reactions with anhydrous potassium fluoride.

Finally, although no isotope effect was observed under the conditions we chose, it does not mean that hydrogen bonding does not play any role in phase-transfer catalysis. We have never encountered experimental studies of isotope effect with blue-shifted hydrogen bonds. They may simply not behave in the expected manner or it is also possible that phase-transfer reactions are too finicky to properly measure the subtle rate changes they may cause.

4.4 Experimental

For the catalyst synthesis and ion exchange procedure, please refer to the Experimental information for Chapter 3.

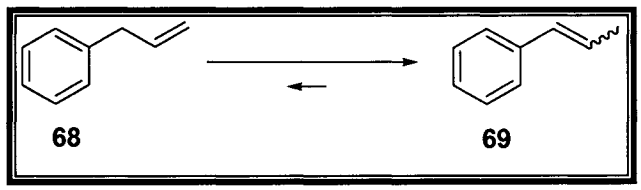

Allylbenzene Isomerization to *cis*- and *trans*-propenylbenzene:

Optimized Procedure

Freshly distilled toluene was degassed for 10 to 20 minutes with nitrogen then 3 mL were transferred to a flame-dried 10 mL round-bottom flask equipped with a 1.3 cm x 0.3 cm x 0.3 cm stirbar under nitrogen atmosphere. The solvent was heated to 75°C for 10 min and the stirring rate was set to 1000 rpm. 1,3-Dimethoxybenzene was added as a standard (40 μL, 0.305 mmol, 0.48 eq.) followed by 85 μL (0.641 mmol, 1 eq.) of allylbenzene. An aliquot was taken before the addition of the catalyst (190 μL, 0.032 mmol, 0.05 eq.). (Stock solutions of our catalyst were prepared at 0.167 M concentration.) Immediately after, 1 mL of 50 % wt KOH was added and the timer was started. All aliquots were 10 μL samples and they were immediately filtered through a small cotton pad straight into GC autosample bottles with HPLC grade hexanes. The reactions were followed by GCMS analysis.

References

[1] Starks, C.; Liotta, C.; Halpern, M. *Phase-Transfer Catalysis: Fundamentals, Applications and Industrial Perspectives*, Chapman & Hall, New York, **1994**.

[2] (a) Starks, C. M. *J. Am. Chem. Soc.* **1971**, *93*, 195.; (b) Starks, C. M.; Liotta, C. *Phase Transfer Catalysis. Principles and Technique,* N.Y.: Acad Press, 1978.

[3] (a) Makosza, M. *Pure Appl. Chem.* **1975**, *43*, 439.; (b) Makosza, M. *Usp. Khim.* **1977**, *46*, 2174.; (c) Makosza, M.; Fedorynski, M. *Adv. Catal.* **1987**, *35*, 375.

[4] (a) Brändström, A. *Adv. Phys. Org. Chem.* **1977**, *15*, 267.; (b) Brändström, A. *Pure Appl. Chem.* **1982**, *54*, 1769.

[5] Goldberg, Y. *Phase-Transfer Catalysis. Selected Problems and Application* Gordon and Breach Science Publishers, Singapore, 1992.

[6] Gordon, J.E.; Kutina, R.E. *J. Am Chem. Soc.* **1977**, *99*, 3903.

[7] (a) Landini, D.; Maia, A.; Montanari, F. *J. Chem. Soc., Chem. Commun.* **1977**, 112.; (b) Landini, D.; Maia, A.; Montanari, F. *J. Am. Chem. Soc.* **1978**, *100*, 2796.

[8] Trifonov, A.Z.; Nikolova, B.M.; Kuzmanova, R.B.; Ivanov, C. *Z. Phys. Chem. (Leipzig)*, **1983**, *264*, 664.

[9] (a) Dehmlow, E.V; Dehmlow, S.S. *Phase Transfer Catalysis*, 2nd Ed, Weinheim: Verlag Chemie, **1983**.; (b) Dehmlow, E.V. *Angew. Chem. Int. Ed.* **1977**, *16*, 493.

[10] Taylor, R.; Kennard, O. *Acc. Chem. Res.* **1984**, *17*, 320.

[11] Murray-Rust, P.; Glusker, J. P. *J. Am. Chem. Soc.* **1984**, *106*, 1018.

[12] (a) Sutor, D. J. *Nature*, **1962**, *165*, 68; (b) Sutor, D. J. *J. Chem. Soc.* **1963**, 1105.

[13] Donohue, J. *Structural Chemistry and Molecular Biology,* Rich, A, Davidson, N., Eds; W. H. Freeman: San Francisco, **1968**; pp 459 – 463.

[14] Green, R. D. *Hydrogen Bonding by C – H groups*, Wiley Interscience: New York, **1974**.

[15] Ts'O, P. O. P.; Kondo, N. S.; Schweizer, M. P.; Hollis, D. P. *Biochemistry*, **1969**, 8, 997.

[16] Harmon, K. M.; Gennick, I.; Madeira, S. L. *J. Phys. Chem.* **1974**, *78*, 2585.

[17] Kollman, P.; McKelvey, J.; Johansson, A.; Rothenberg, S. *J. Am. Chem. Soc.* **1975**, *97*, 955.

[18] Umeyama, H.; Morokuma, K. *J. Am. Chem. Soc.* **1977**, *99*, 1316.

[19] Vishveshwara, S. *Chem. Phys. Lett.* **1978**, *59*, 26.

[20] Gay, R.; Vanderkooi, G. *J. Chem. Phys.* **1981**, *75*, 2281.

[21] Taylor, R.; Kennard, O. *J. Am. Chem. Soc.* **1982**, *104*, 5063.

[22] Allen, F.H.; Bellard, S.; Brice, M.D.; Cartwright, B.A.; Doubleday, A.; Higgs, H.; Hummelink, T.; Hummelink-Peters, B.G.; Kennard, O.; Motherwell, W.D.S.; Rodgers, J.R.; Watson, D.G. *Acta Crystallogr. B* **1979**, *35*, 2331.

[23] Jiang, L.; Lai, L. *J. Biol. Chem.* **2002**, *277*, 37732.

[24] Baures, P.W.; Beatty, A.M.; Dhanasekaran, M.; Helfrich, B.A. *J. Am. Chem. Soc.* **2002**, *124*, 11315.

[25] Scheiner, S. *J. Phys. Chem. B* **2005**, *109*, 16132.

[26] Chamberlain, A.K.; Bowie, J.U. *J. Mol. Bio.* **2002**, *322*, 497.

[27] Mandel-Gutfreund Yael, H.M.; Jernigan, R.L.; Zhurkin, V.B. *J. Mol. Biol.* **1998**, *277*, 1129.

[28] Musah, R.A.; Jensen, G.M.; Rosenfeld, R.J.; McRee, D.E.; Goodin, D.B.; Bunte, S.W. *J. Am. Chem. Soc.* **1997**, *119*, 9083.

[29] Reetz, M. T.; Hutte, S.; Goddard, R. *J. Am. Chem. Soc.* **1993**, *115*, 9339.

[30] Ohshima, T.; Shibuguchi, T.; Fukuta, Y.; Shibasaki, M. *Tetrahedron,* **2004**, *60*, 7749.

[31] (a) Reetz, M. T.; Hütte, S.; Goddard, R.; *Z. Naturforsch., G: Chem. Sci.* **1995**, *50*, 415.; (b) Reetz, M. T.; Hütte, S.; Goddard, R. *J. Phys. Org. Chem.* **1995**, *8*, 231.; (c) Reetz, M. T.; Hütte, S.; Goddard, R.; Minet, U. *J. Chem. Soc., Chem. Commun.* **1995**, 275. (d) Reetz, M. T.; Hütte, S.; Goddard, R.; Robyr, C. *Chem. – Eur. J.* **1996**, *2*, 382.; (e) Reetz, M. T.; Hütte, S.; Herzog, H. M.; Goddard, R. *Macromol Symp* **1996**, *107*, 209.; (f) Reetz, M. T.; Hütte, S.; Goddard, R. *J. Prakt. Chem.* **1999**, *341*, 297.; (g) Reetz, M. T.; Hütte, S.; Goddard, R. *Eur. J. Org. Chem.* **1999**, 2475.; (h) Goddard, R.; Hütte, S.; Reetz, M. T. *Acta Crystallogr., Sect. C: Cryst. Sruct. Commun.* **2000**, *56*, 878.; (i) Goddard, R.; Herzog, H. M.; Reetz, M. T. *Tetrahedron*, **2002**, *58*, 7847.; (j) Reetz, M.T.; Knauf, T.; Minet, U.; Bingel, C. *Angew. Chem. Int. Ed.* **1988,** *27*, 1373.

[32] Harder, S. *Chem. – Eur. J.* **1999**, *5*, 1852.

[33] Steiner, T. *J Chem. Soc. Perkin Trans. 2*, **1995**, 1315.

[34] Koller, J.; Grdadolnik, J.; Hadži, D. *J. Mol. Struct. (Theochem),* **1992**, *259*, 199.

[35] Cannizzaro, C.E.; Houk, K.N. *J. Am. Chem. Soc.* **2002,** *124*, 7163.

[36] Mo, H.; Pochapsky, T.C. *Prog. Nucl. Mag. Res. Spect.* **1997**, *30*, 1.

[37] Harmon, K.M.; Madeira, S.L. *J. Mol. Struct.* **2001**, *560*, 179.

[38] Harmon, K.M.; Drum, D.K.; Nikolla, E. *J. Mol. Struct.* **2002**, *616*, 181.

[39] van Mourik, T.; van Duijneveldt, F.B. *J. Mol. Struct. (Theochem)* **1995**, *341*, 63.

[40] Davies, A.S.; George, W.O.; Howard, S.T. *Phys. Chem. Chem. Phys.*, **2003**, *5*, 4533.

[41] Weston, R.E. *J. Mol. Struct.* **1986**, *147*, 1.

[42] Novak, A. *Struct. Bonding*, **1974**, *18*, 177.

[43] Rozenberg, M.A.; Locwensehuss, A.; Marcus, Y. *Phys. Chem. Chem. Phys.* **2000**, *2*, 2699.

[44] Christe, K.O.; Wilson, W.W.; Wilson, R.D.; Bau, R.; Feng, J.-A. *J. Am. Chem. Soc.* **1990**, *112*, 7619.

[45] Eckert, J.; Sewell, T.D.; Kress, J.D.; Kober, E.M.; Wang, L.L.; Olah, G. *J. Phys. Chem. A* **2004**, *108*, 11369.

[46] Deakyne, C.A.; Meot-Ner, M. *J. Am. Chem. Soc.* **1999**, *121*, 1546.

[47] Cashin, A.L., Petersson, E.J.; Lester, H.A.; Dougherty, D.A. *J. Am. Chem. Soc.* **2005**, *127*, 350.

[48] Scheiner, S.; Kar, T., Gu, Y. *J. Biol. Chem.* **2001**, *276*, 9832.

[49] Harmon, K.M.; De Santis, N.J.; Brandt, D.O. *J. Mol. Struct.* **1992**, *265*, 47.

[50] Harmon, K.M.; Gennick, I. *Inorg Chem.* **1975**, *14*, 1840.

[51] Turner, J.Z.; Soper, A.K.; Finney, J.L. *J. Chem. Phys.* **1995**, *102*, 5438.

[52] Kabisch, G.; Möbius, G. *Spectrochim. Acta A*, **1982**, *38*, 1189.

[53] Berg, R.W. *Spectrochim. Acta A*, **1978**, *34*, 655.

[54] Von der Ohe, W. *J Chem. Phys.* **1975**, *62*, 3933.

[55] Gennick, I.; Harmon, K.M.; Potvin, M.M. *Inorg. Chem.* **1977**, *16*, 2033.

[56] Heyns, A.M.; de Beer, W.H.J. *Spectrochim. Acta A*, **1983**, *39*, 601.

[57] (a) de Beer, W.H.J.; Heyns, A.M.; Richter, P.W.; Clark, J.B. *J. Solid State Chem.* **1981**, *36*, 181. (b) de Beer, W.H.J.; Heyns, A.M. *Spectrochim. Acta A*, **1981**, *37*, 1099.

[58] Berg, R.W. *J Chem. Phys.* **1978,** *69*, 1325.

[59] Berg, R.W.; Poulsen, F.W.; Bjerrum, N.J. *J. Chem. Phys.*, **1977**, *67*, 1829.

[60] Berg, R.W. *J. Chem. Phys.* **1979**, *71*, 29713

531.

[61] Ratcliffe, C.I.; Waddington, T.C. *J. Chem. Soc. Faraday Trans. 2*, **1976**, 1935.

[62] M. Stammler *J. Inorg. Nuclear Chem.* **1967**, *29*, 2203.

[63] Andrew, E.R.; Canepa, P.C. *J. Mag. Res.* **1972**, *7*, 429.

[64] Chang, S.-S.; Westrum, E.F. *J. Chem. Phys.* **1962**, *36*, 2420.

[65] Albert, S.; Gutowsky, H.S.; Ripmeester, J.A. *J. Chem. Phys.* **1972**, *56*, 3672.

[66] Pal, M.; Raghuvanshi, G.S.; Bist, H.D. *Chem. Phys. Lett.* **1982**, *92*, 85.

[67] Pal, M.; Agarwal, A.; Khanderwal, P.D.; Bist, H.D. *J. Mol. Struct.* **1984**, *112*, 309.

[68] Joesten, M.D, Schaad, L.J. *Hydrogen Bonding* ,M. Dekker, New York, **1974**.

[69] (a) Meot-Ner, M. *J. Am. Chem. Soc.* **1983**, *105*, 4912.; (b) Meot-Ner, M.; Deakyne, C.A. *J. Am. Chem. Soc.* **1985**, *107*, 469.; (d) Meot-Ner, M. *Chem. Rev.* **2005**, *105*, 213.

[70] Reuben, B.G.; Iraqi, M.; Lifshitz, C. *J. Phys. Chem.* **1991**, *95*, 9713.

[71] Blades, A.T.; Klassen, J.S.; Kebarle, P. *J. Am. Chem. Soc.* **1996**, *118*, 12437.

[72] (a) Dollling, U.-H., Davis, P., Grabowski, E.J.J. *J. Am. Chem. Soc.* **1984**, *106*, 446.; (b) Hughes, D.L., Dolling, U.-H., Ryan, K. M., Shoenewaldt, E.F., Grabowski, E.J.J. *J. Org Chem.* **1987**, *52*, 4745.; (c) O'Donnell, M.J. Asymmetric Phase-Transfer Reactions. In

Catalytic Asymmetric Synthesis. 2nd ed., Ojima, I. Ed.; Verlag Chemie: New York **2000**.; (d) Shioiri, T., Chiral Phase-Transfer Catalysts. *In Handbook of Phase-Transfer Catalysis*; Sasson, Y., Neumann, R.; Eds.; Blackie: London **1997**.

[73] Preliminary communication: (a) Ooi, T., Kameda, M., Maruoka, K. *J. Am. Chem. Soc.* **1999**, *121*, 6519.; see also (b) Ooi, T., Kameda, M., Maruoka, K. *J. Am. Chem. Soc.* **2003**, *125*, 5139.; (c) Ooi, T.; Uematsu, Y.; Kameda, M.; Maruoka, K. *Angew. Chem. Int. Ed.* **2002**, *41*, 1551.

[74] Shibuguchi, T.; Fukuta, Y.; Akachi, Y.; Sekine, A.; Ohshima, T.; Shibasaki, M. *Tet. Lett.* **2002**, *43*, 9539.

[75] Corey, E.J.; Xu, F.; Noe, M.C. *J. Am. Chem. Soc.* **1997**, *119*, 12414.

[76] (a)Kita, T.; Georgieva, A.; Hashimoto, Y.; Nakata, T.; Nagasawa, K. *Angew. Chem. Int. Ed.* **2002**, *41*, 2832.; (b) Arai, S.; Tsuji, R.; Nishida, A. *Tet. Lett.* **2002**, *43*, 9535.; (c) Kowtoniuk, W.E.; Rueffer, M.E.; MacFarland, D.K. *Tetrahedron: Asymmetry* **2004**, *15*, 151.; (d) Kumar, S.; Sobhia, M.E.; Ramachandran, U. *Tetrahedron: Asymmetry* **2005**, *16*, 2599.; (e) Kumar, S.; Ramachandran, U.; *Tetrahedron* **2005**, *61*, 4141.

[77] Kretcher, V.R.P., Seubert, J., Schmitt, D., Use, G., Kohl, N. *Chemiker-Zeitung*, **1988,** *112*, 85.

[78] Ooi, T.; Uematsu, Y.; Maruoka, K, *J. Org. Chem.* **2003**, *68*, 4576.

[79] Ohta, T.; Ito, M.; Inagaki, K,; Takaya, H. *Tetrahedron Lett.* **1993**, *34*, 1615.

[80] Beak, P., Brown, R. A.; *J. Org. Chem.* **1982**, *47*, 34.

[81] Clark, R. D., Jahangir, *J. Org. Chem.* **1989**, *54*, 1174.

[82] Still, W.C.; Kahn, M; Mitra, A. *J. Org. Chem.* **1989**, *54*, 5667.

[83] Pena, D., Perez, D., Guition, E., Castedo, L. *J. Org. Chem.*, **2000**, *65*, 6944.

[84] Weberd, B., Czugler, M. *J. Am. Chem. Soc.* **1984**, *106*, 3297.

[85] (a) Mendelsohn, R.; Koch, C. *Biochim. Biophys. Acta*, **1980**, *598*, 260.; (b) Dluhy, R.A.; Mendelsohn, R.; Casal, H.L.; Mantsch, H.H. *Biochemistry*, **1983**, *22*, 1170.

[86] Brauner, J.W.; Dugan, C.; Mendelsohn, R. *J. Am. Chem. Soc.* **2000**, *122*, 677.

[87] Silverstein, R.M.; Webster, F.X. *Spectrometric Identification of Organic Compounds*, 6th Ed., John Wiley & Sons, Inc. New York, USA, **1998**.

[88] Becker, J.; Becher, F.; Hucke, O.; Labahn, A.; Koslowski, T. *J. Phys. Chem. B* **2003**, *107*, 12878.

[89] Grajcar, L.; Baron, M.H.; Becouran, S.; Czernecki, S.; Valery, J.M.; Reiss, C. *Spect. Acta A* **1999**, *55*, 2231.

[90] Arbely, E.; Arkin, I. *J. Am. Chem. Soc.* **2004**, *126*, 5362.

[91] Bowie, J.U. *Nature*, **2005**, *438*, 581.

[92] Ohshima, T.; Shibugushi, T.; Fukuta, Y.; Shibasaki, M. *Tetrahedron* **2004**, *60*, 7743.

[93] Bar, R.; Sasson, Y.; Blum, J. *Reactive Polymers,* **1983**, *1*, 315.

[94] Buděšinský, M.; Fiedler, P.; Arnold, Z. *Synthesis*, **1989**, 858.

[95] Bodeskul, I.E.; Tsymbal, I.F.; Ryltsev, E.V.; Latajka, Z.; Barnes, A.J. *J. Mol. Struct.* **1997**, *436*, 167.

[96] (a) Hobza, P.; Špirko, V.; Selzle, H.L.; Schlag, E.W. *J. Phys. Chem. A* **1998**, *102*, 2501. (b) Hobza, P.; Špirko, V.; Havlas, Z.; Buchold, K.; Reimann, B.; Barth, H.-D.; Brutschy, B. *Chem. Phys. Lett.* **1999**, *299*, 180.

[97] Hobza, P.; Havlas, Z. *Chem. Phys. Lett.* **1999**, *303*, 447.

[98] Hobza, P.; Havlas, Z. *Chem. Rev.* **2000**, *100*, 4253.

[99] Reimann, B.; Buchhold, K.; Vaupel, S.; Brutschy, B.; Havlas, Z.; Špirko, V.; Hobza, P. *J. Phys. Chem. A* **2001**, *105*, 5560.

[100] Van der Veken, B.J.; Herrebout, W.A.; Szotak, R.; Shchepkin, D.M.; Havlas, Z.; Hobza, P. *J. Am. Chem. Soc.* **2001**, *123*, 12290.

[101] Scheiner, S.; Kar, T. J. *Phys. Chem. A* **2002**, *106*, 1784.

[102] (a) Gu, Y.; Kar, T.; Scheiner, S. *J. Am. Chem. Soc.* **1999**, *121*, 9411. (b) Gu, Y.; Kar, T.; Scheiner, S. *J. Mol. Struct. (Theochem)*, **2000**, *500*, 441.

[103] Fidanza, N.G.; Suvire, F.D.; Sosa, G.L.; Lobayan, R.M., Enriz, R.D.; Peruchena, N.M. *J. Mol. Struct. (Theochem),* **2001**, *543*, 185.

[104] Kryachko, E.S.; Zeegers-Huyskens, T. *J. Phys. Chem. A,* **2001**, *105*, 7118.

[105] Marques, M.P.M.; da Costa, A.M.A.; Ribeiro-Claro, P.J.A. *J. Phys. Chem. A* **2001**, *105*, 5292.

[106] Zierkiewicz, W.; Jurečka, P.; Hobza, P. *ChemPhysChem* **2005**, *6*, 609.

[107] Wang, X.; Zhou, G.; Tian, A.; Wong, N.-B. *J. Mol. Struct. (Theochem)* **2005**, *718*, 1.

[108] McDowell, S.A.C.; Buckingham, A.D. *J. Am. Chem. Soc.* **2005**, *127*, 15515.

[109] Masunov, A.; Dannenberg, J.J. *J. Phys. Chem. A* **2001**, *105*, 4737.

[110] Qian, W.; Krimm, S. *J. Phys. Chem. A* **2002**, *106*, 6628.

[111] Fang, Y.; Fan, J.-M.; Liu, L.; Li, X.-S.; Gau, Q.-X. *Chem. Lett.* **2002**, 116.

[112] (a) Hermansson, K. *J. Phys. Chem. A* **2002**, *106*, 4695; (b) Pejov, L.; Hermansson, K. *J. Chem. Phys.* **2003**, *119*, 313.

[113] Alabugin, I.V.; Manoharan, M.; Peabody, S.; Weinhold, F. *J. Am. Chem. Soc.* **2003**, *125*, 5973.

[114] Wang, J.-T.; Feng, Y.; Liu, L; Li, X.-S.; Gau, Q.-X. *Chem. Lett.* **2003**, 746.

[115] Coetzee, J.F.; Ritchie, C.D. *Solute-Solvent Interactions*, Marcel Dekker Ed., New York, **1969**.

[116] Halpern, M.; Sasson, Y.; Rabinovitz, M. *J. Org. Chem.* **1983**, *48*, 1022.

Appendix

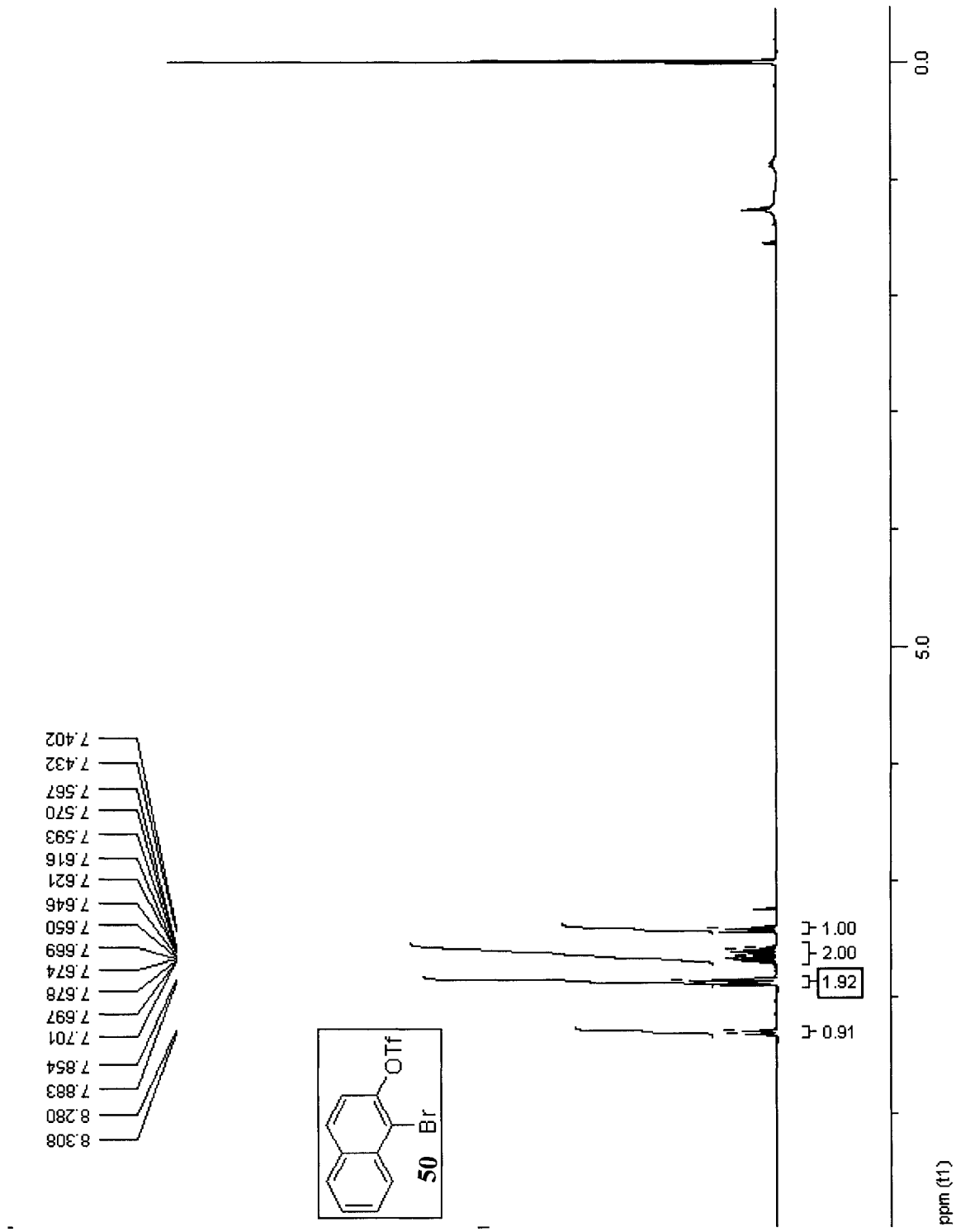
8.308
8.280
7.883
7.854
7.701
7.697
7.678
7.674
7.669
7.650
7.646
7.621
7.616
7.593
7.570
7.567
7.432
7.402
OTf
Br
50
1.00
2.00
1.92
0.91
0.0
5.0
ppm (t1)

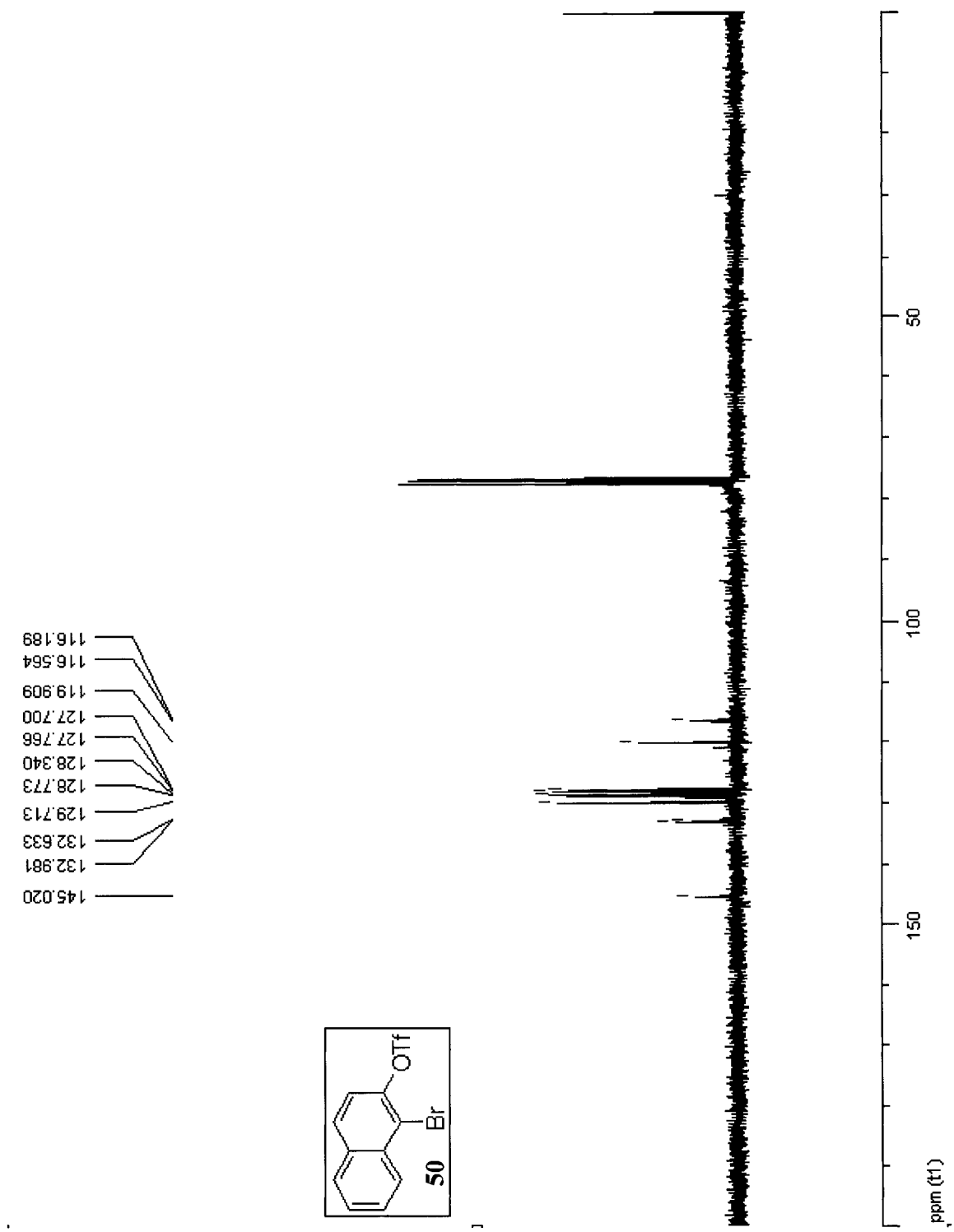
OTf
Br
50
145.020
132.981
132.633
129.713
128.773
128.340
127.766
127.700
119.909
116.564
116.189
150
100
50
ppm (t1)

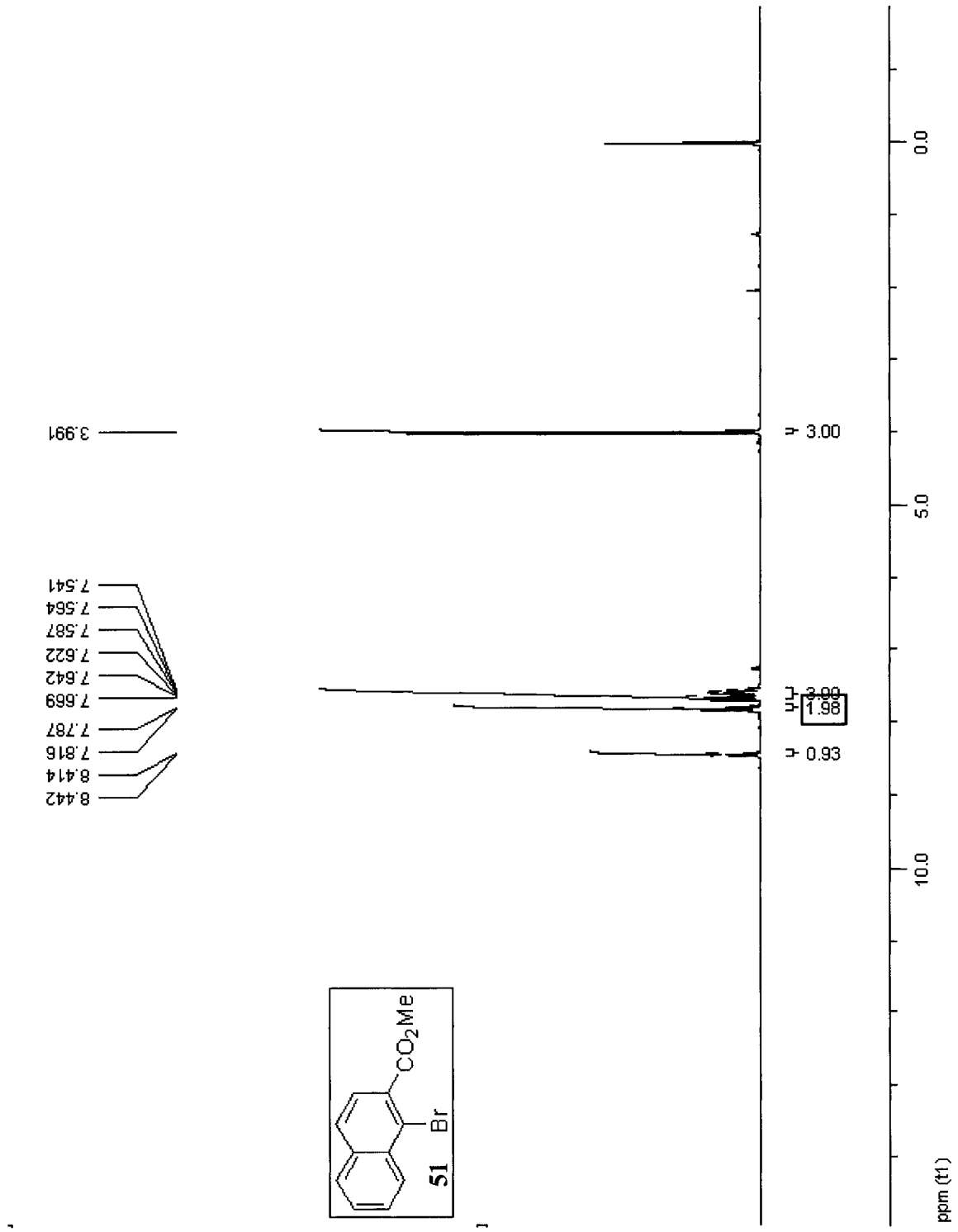
3.991
7.541
7.564
7.587
7.622
7.642
7.669
7.787
7.816
8.414
8.442
3.00
1.98
0.93
0.0
5.0
10.0
ppm (t1)
CO2Me
Br
51

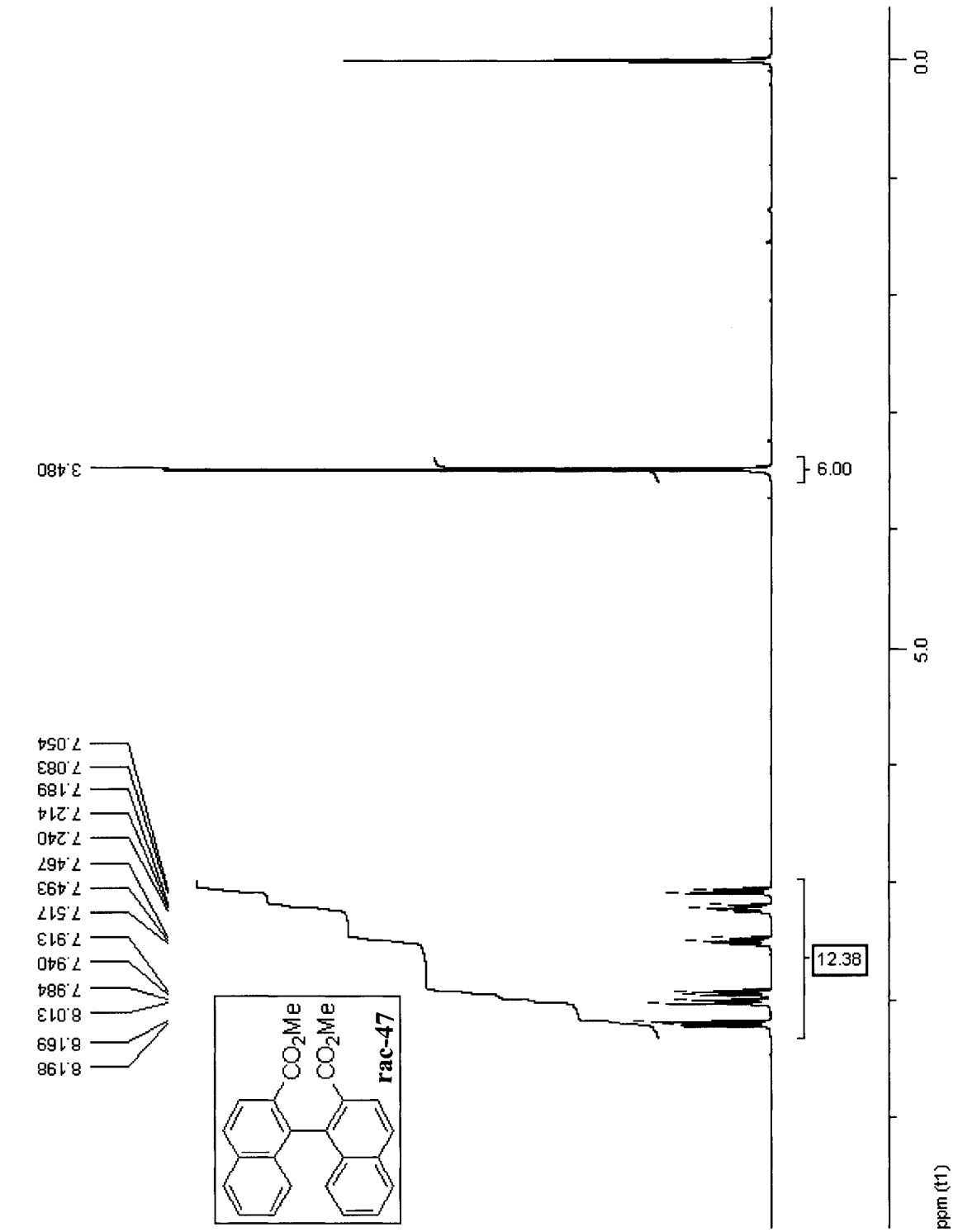
3.480
6.00
12.38
8.198
8.169
8.013
7.984
7.940
7.913
7.517
7.493
7.467
7.240
7.214
7.189
7.083
7.054
CO2Me
CO2Me
rac-47
0.0
5.0
ppm (t1)

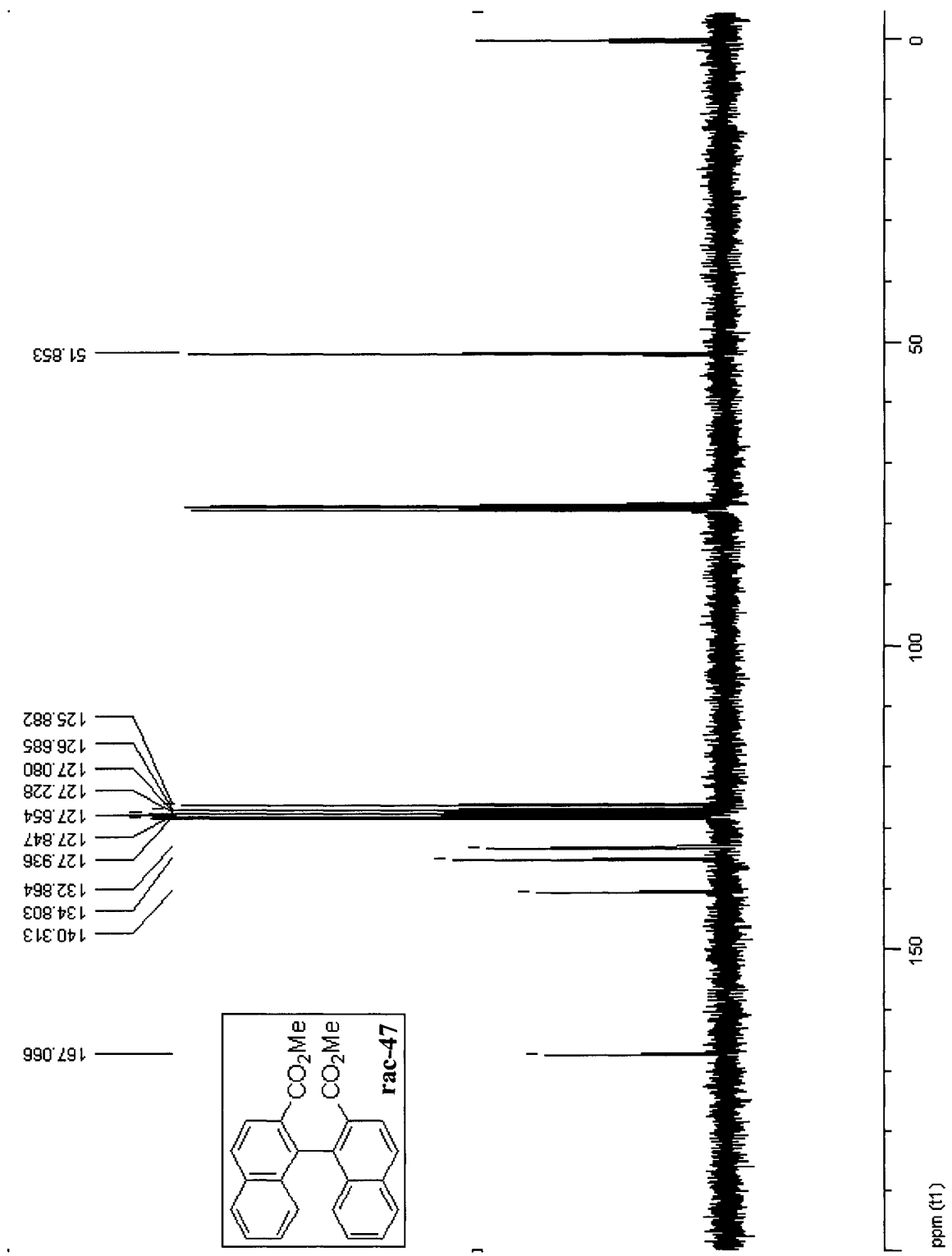
51.853
125.882
126.685
127.080
127.228
127.654
127.847
127.936
132.864
134.803
140.313
167.066
CO_2Me
CO_2Me
rac-47
0
50
100
150
ppm (t1)

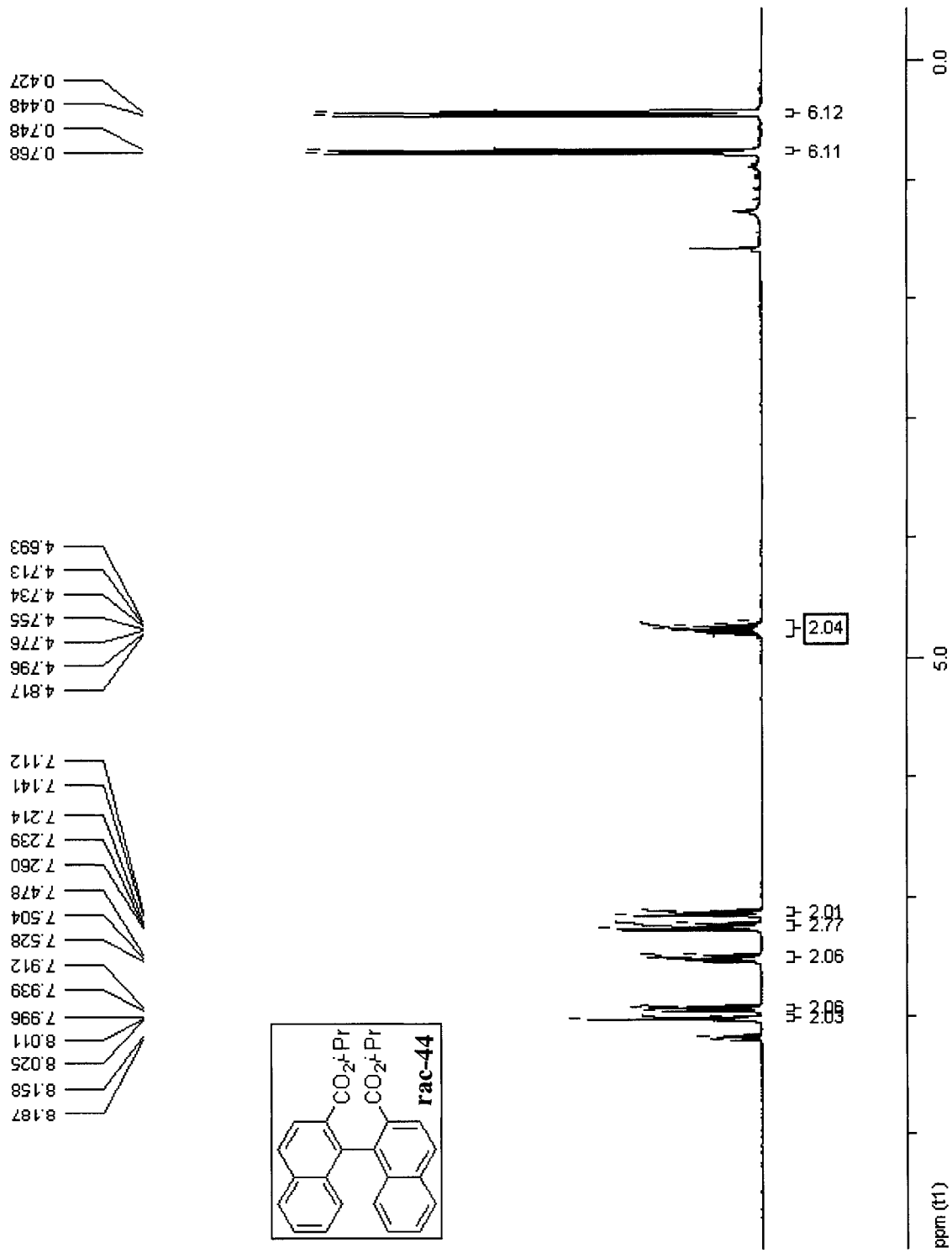
0.427
0.448
0.748
0.768
4.693
4.713
4.734
4.755
4.776
4.796
4.817
7.112
7.141
7.214
7.239
7.260
7.478
7.504
7.528
7.912
7.939
7.996
8.011
8.025
8.158
8.187
6.12
6.11
2.04
2.01
2.77
2.06
2.06
2.03
rac-44
CO2i-Pr
CO2i-Pr
0.0
5.0
ppm (t1)

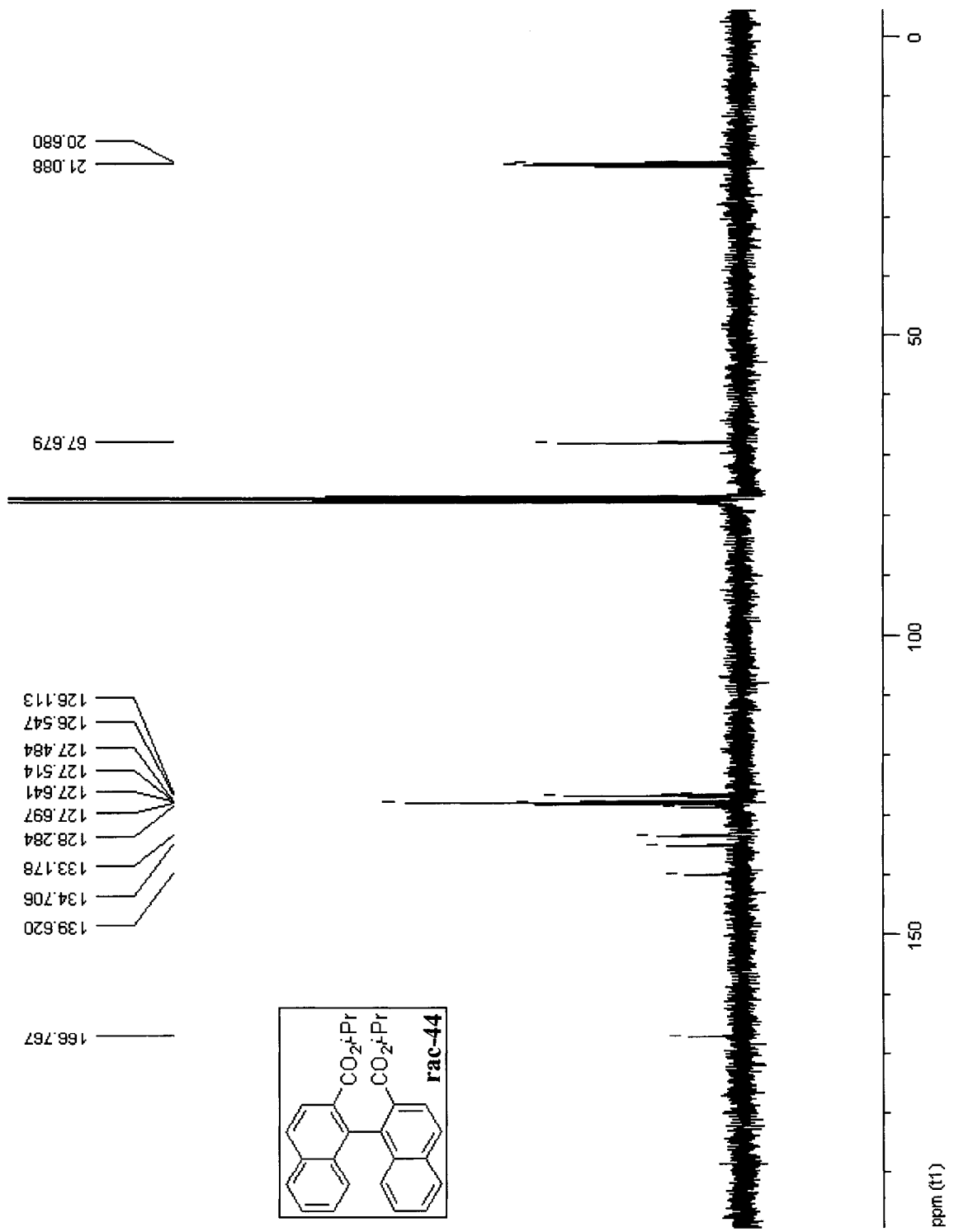
20.680
21.088
67.679
126.113
126.547
127.484
127.514
127.641
127.697
128.284
133.178
134.706
139.620
166.767
CO_2-i-Pr
CO_2-i-Pr
rac-44
0
50
100
150
ppm (t1)

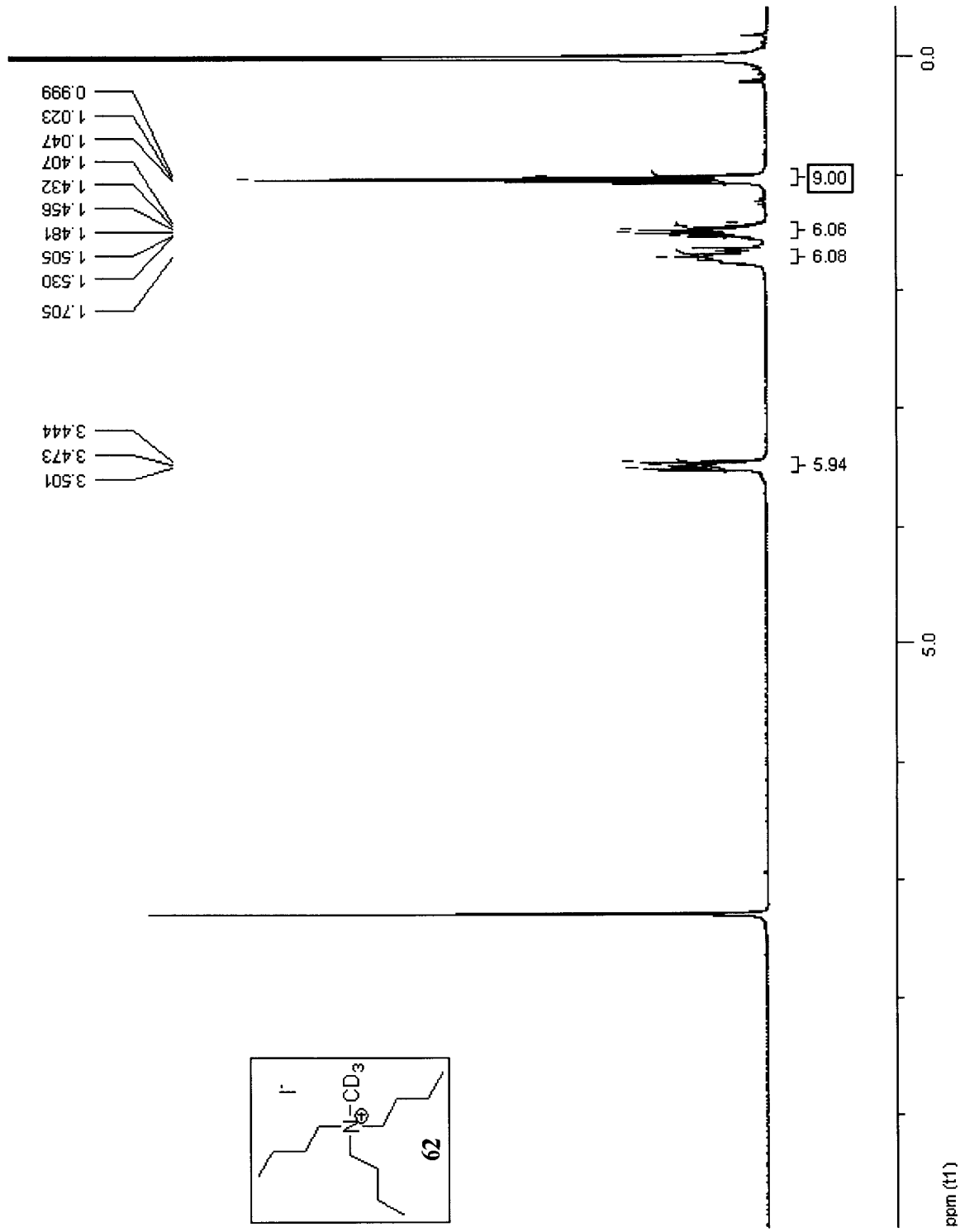
0.999
1.023
1.047
1.407
1.432
1.456
1.481
1.505
1.530
1.705
3.444
3.473
3.501
9.00
6.06
6.08
5.94
0.0
5.0
ppm (f1)
62

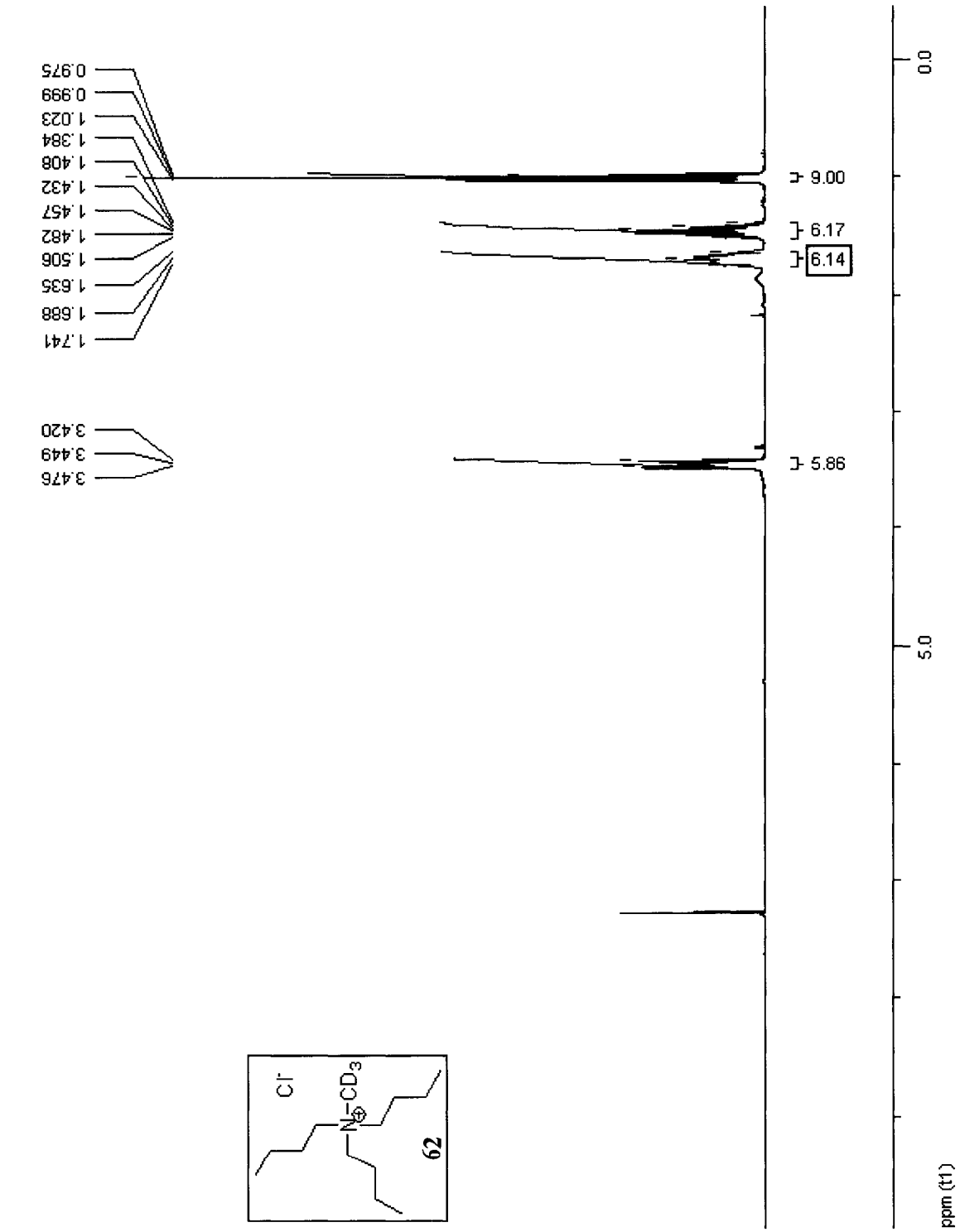
0.975
0.999
1.023
1.384
1.408
1.432
1.457
1.482
1.506
1.635
1.688
1.741
3.420
3.449
3.476
9.00
6.17
6.14
5.86
0.0
5.0
ppm (t1)
Cl⁻
N⊕–CD3
62

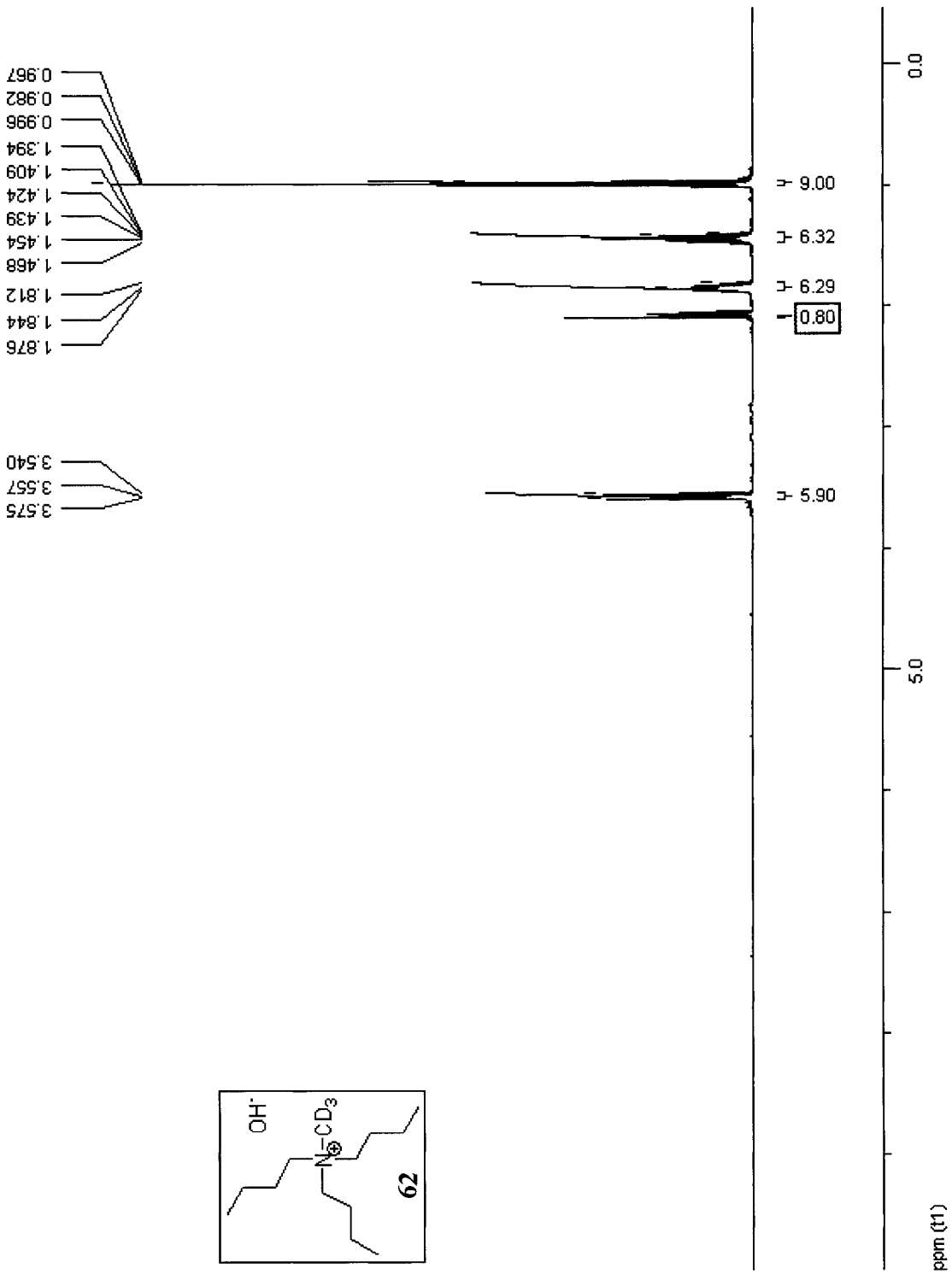
0.967
0.982
0.996
1.394
1.409
1.424
1.439
1.454
1.468
1.812
1.844
1.876
3.540
3.557
3.575
9.00
6.32
6.29
0.80
5.90
0.0
5.0
ppm (t1)
OH⁻
CD3
62

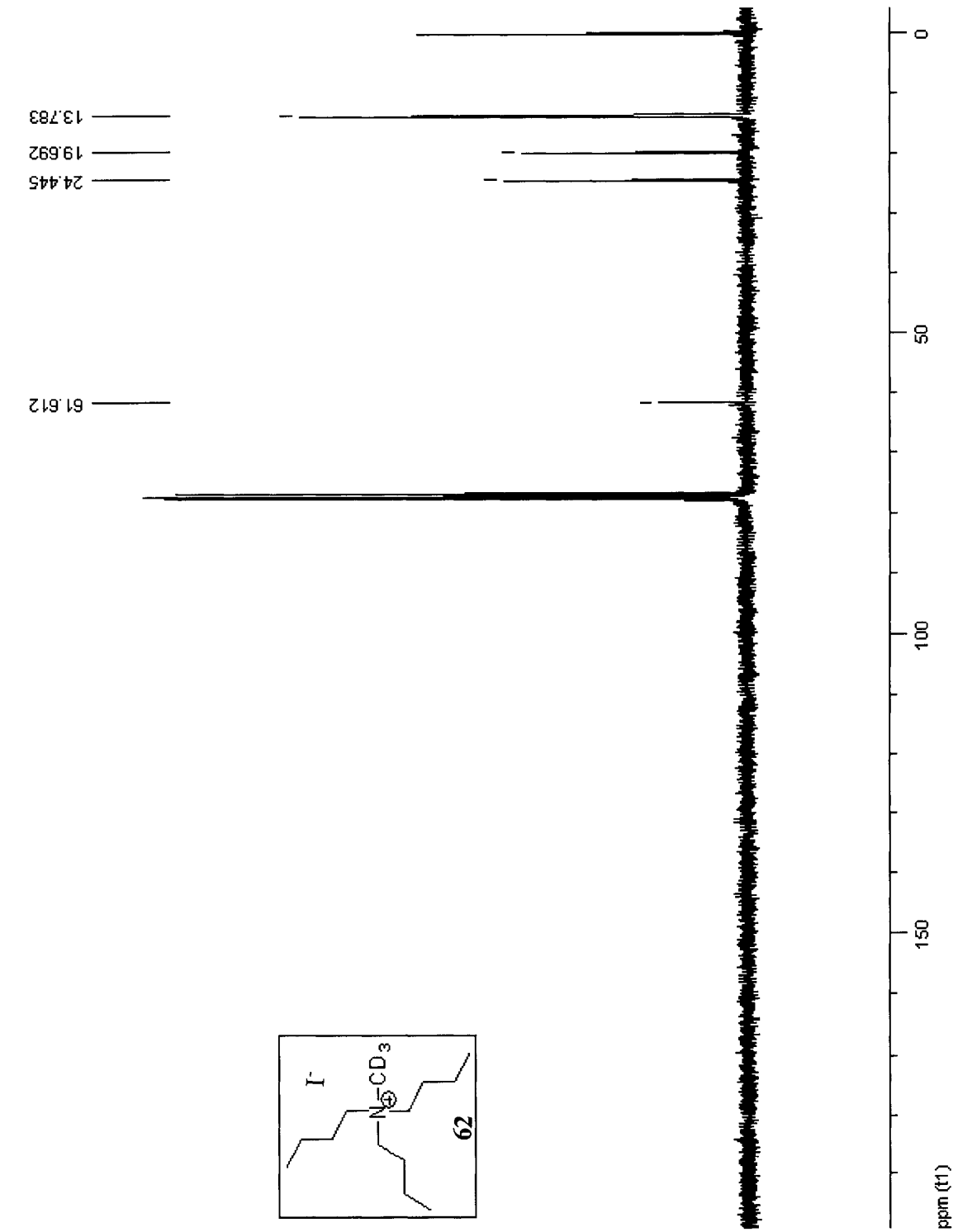
13.783
19.692
24.445
61.612
62
I-
CD_3
0
50
100
150
ppm (t1)

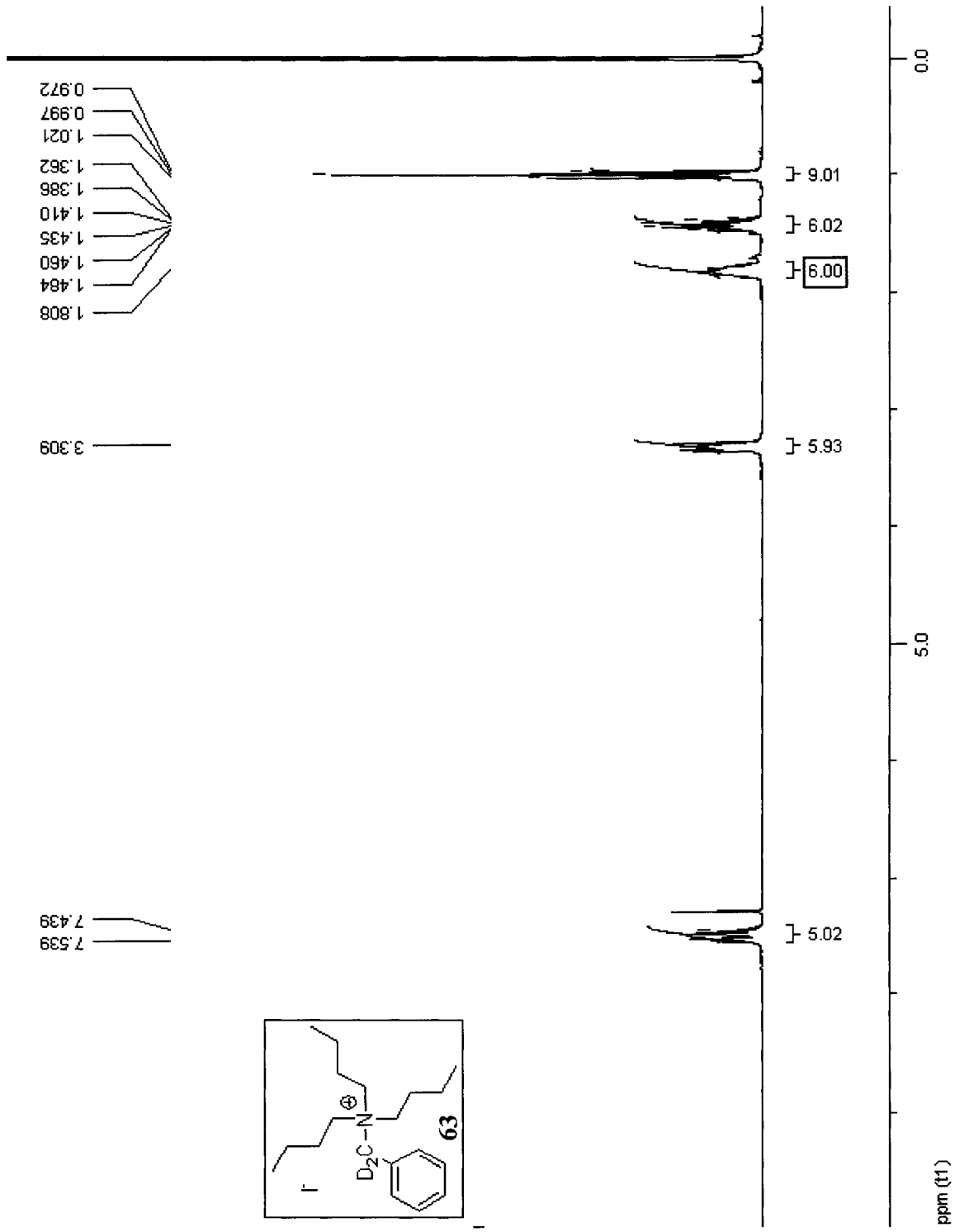
0.972
0.997
1.021
1.362
1.386
1.410
1.435
1.460
1.484
1.808
3.309
7.439
7.539
9.01
6.02
6.00
5.93
5.02
0.0
5.0
ppm (t1)
63

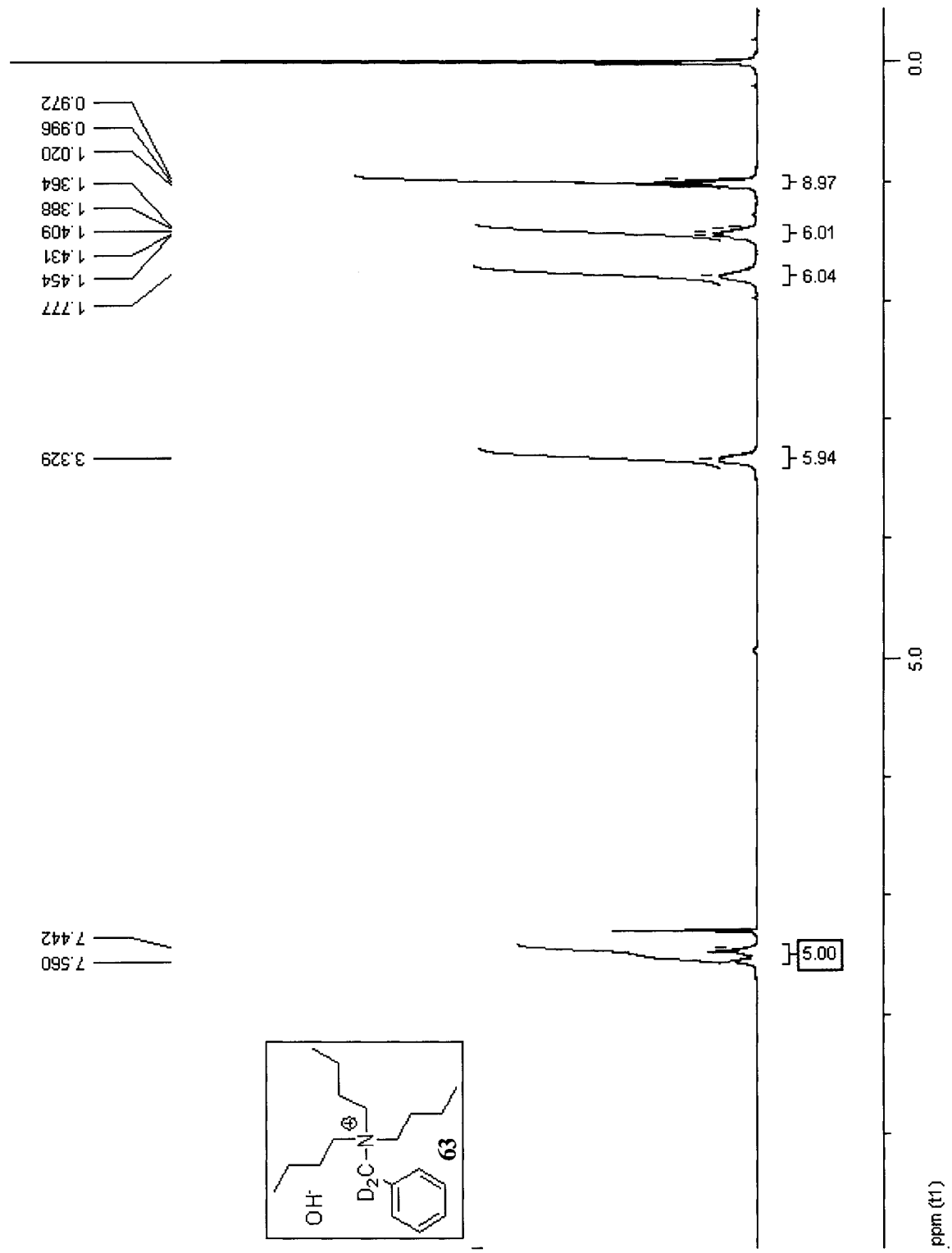
0.972
0.996
1.020
1.364
1.388
1.409
1.431
1.454
1.777
3.329
7.442
7.560
8.97
6.01
6.04
5.94
5.00
0.0
5.0
ppm (t1)
OH⁻
D2C–N⊕
63

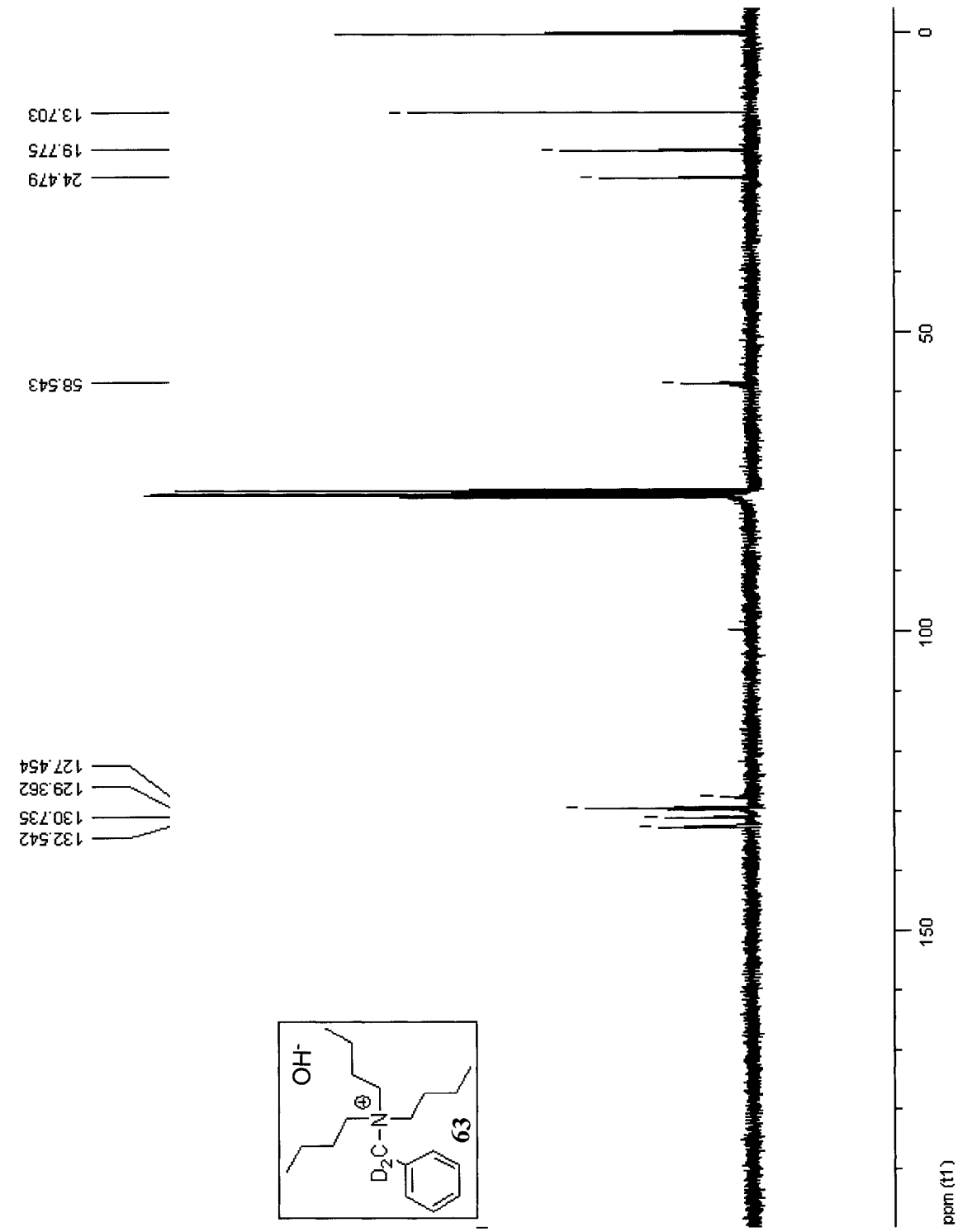
13.703
19.775
24.479
58.543
127.454
129.362
130.735
132.542
OH-
63
D2C
N
0
50
100
150
ppm (t1)

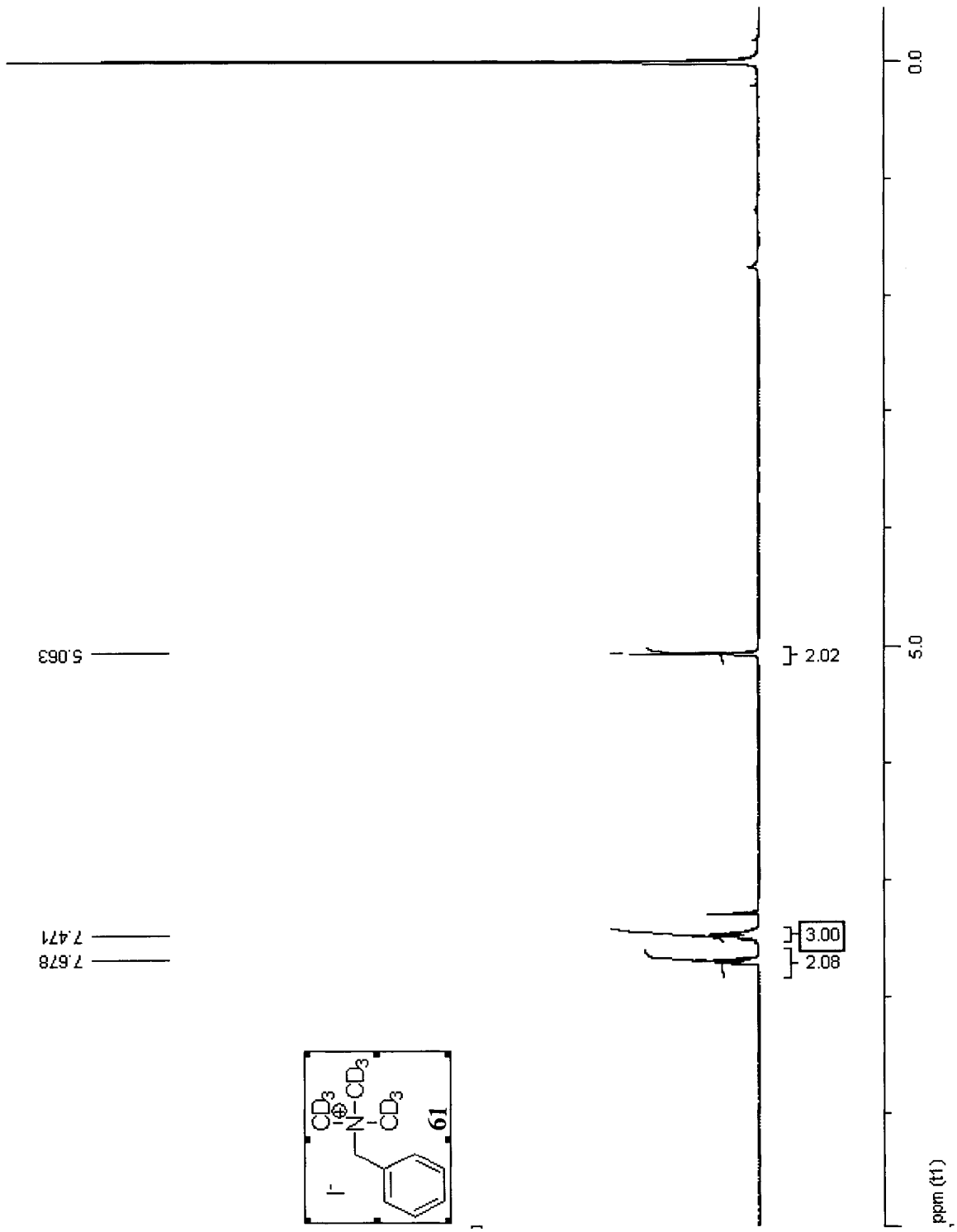
5.063
7.678
7.471
2.02
3.00
2.08
0.0
5.0
ppm (t1)
61

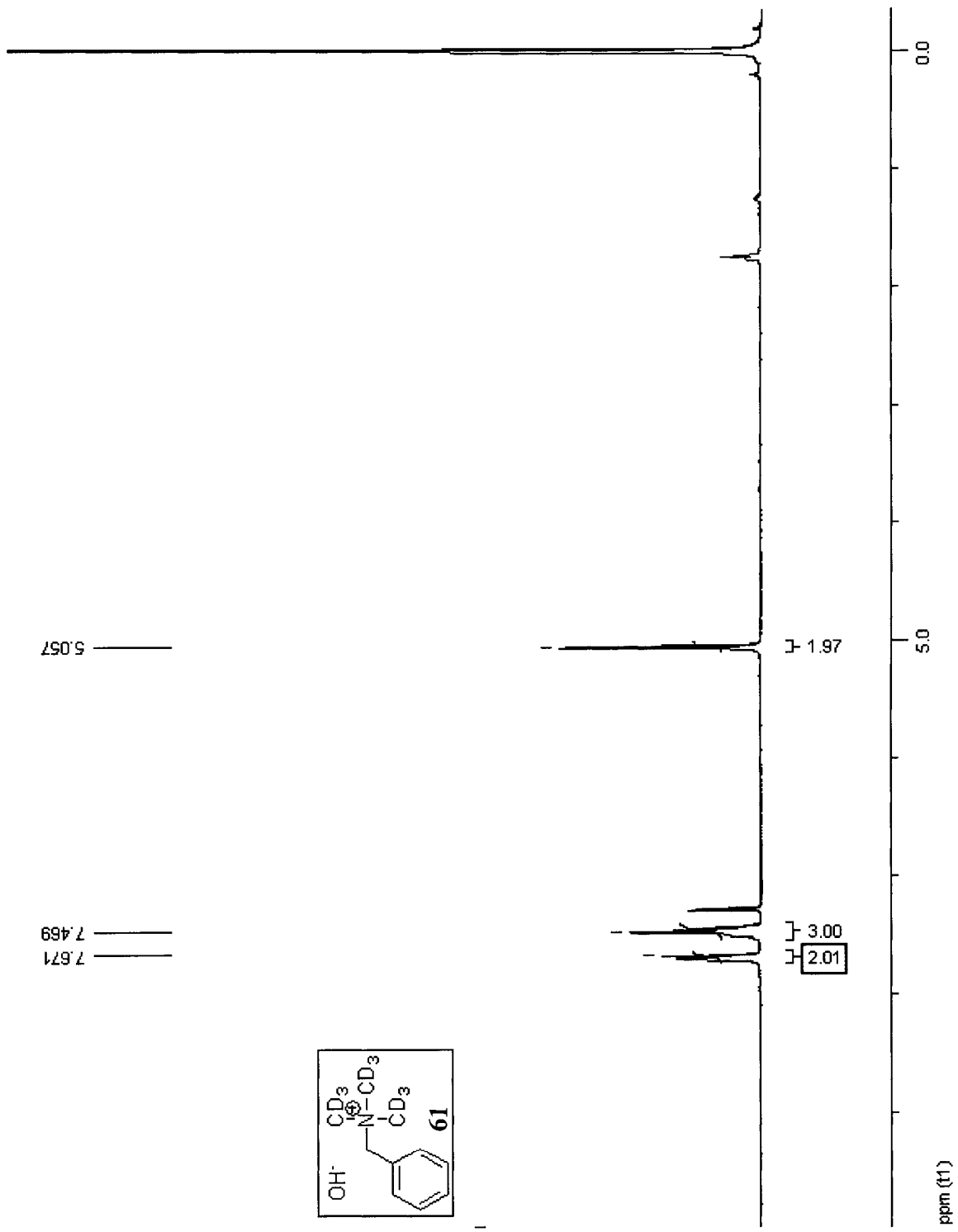
5.057
7.469
7.671
1.97
3.00
2.01
0.0
5.0
ppm (t1)
OH-
CD3
N
CD3
CD3
19

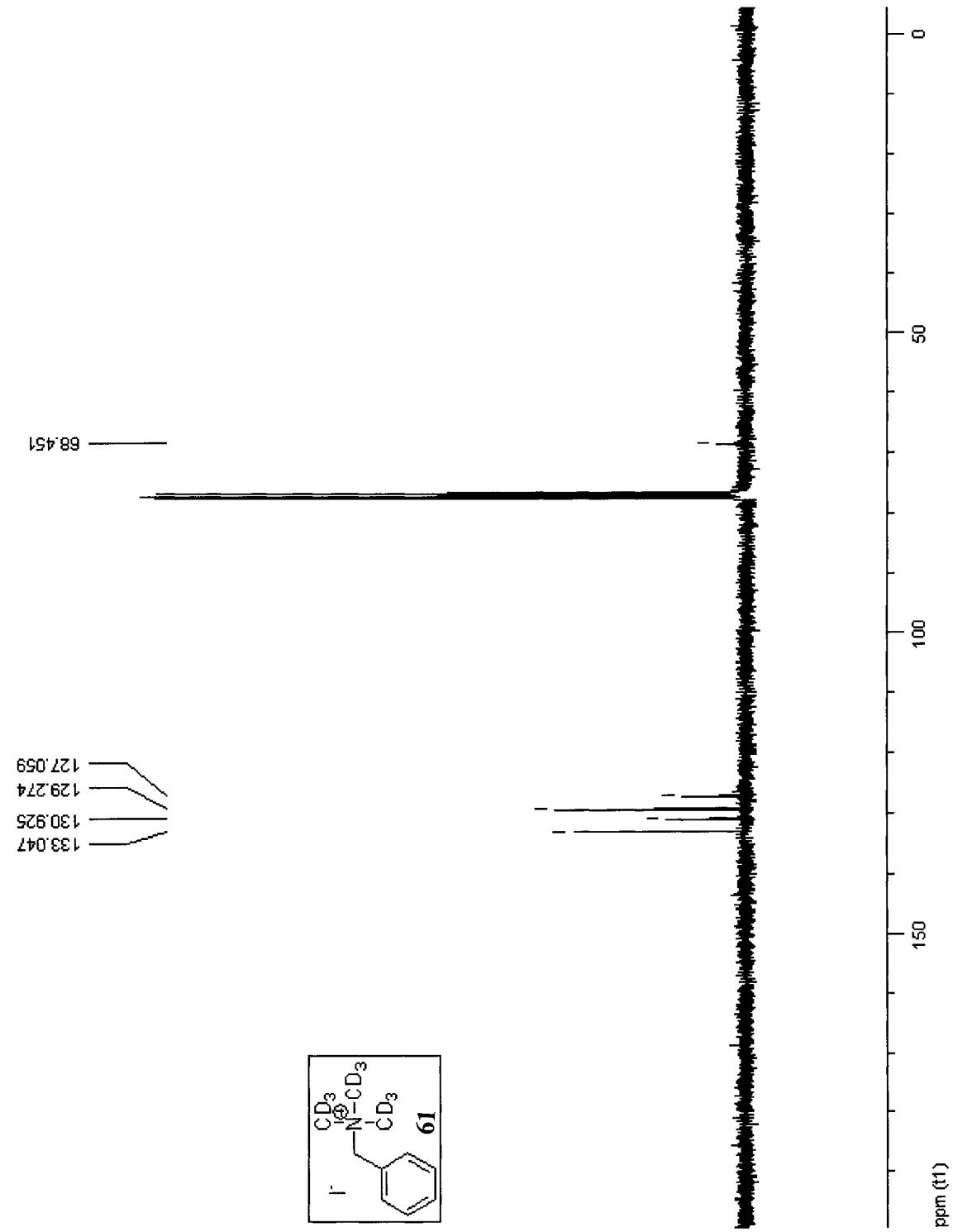
68.451
127.059
129.274
130.925
133.047
61
ppm (t1)
0
50
100
150

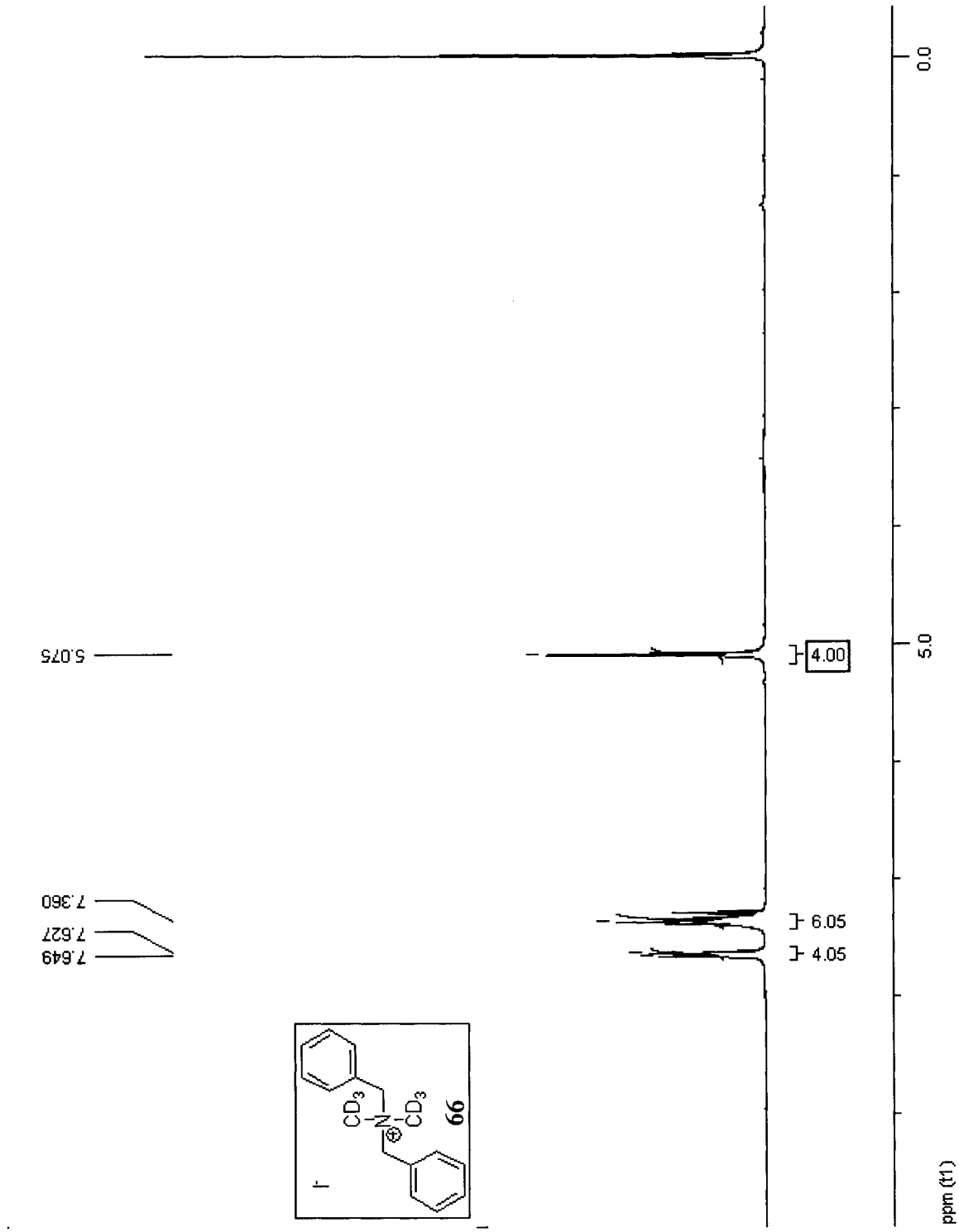
0.0
5.0
ppm (t1)
4.00
6.05
4.05
5.075
7.360
7.627
7.649
99
CD_3
CD_3

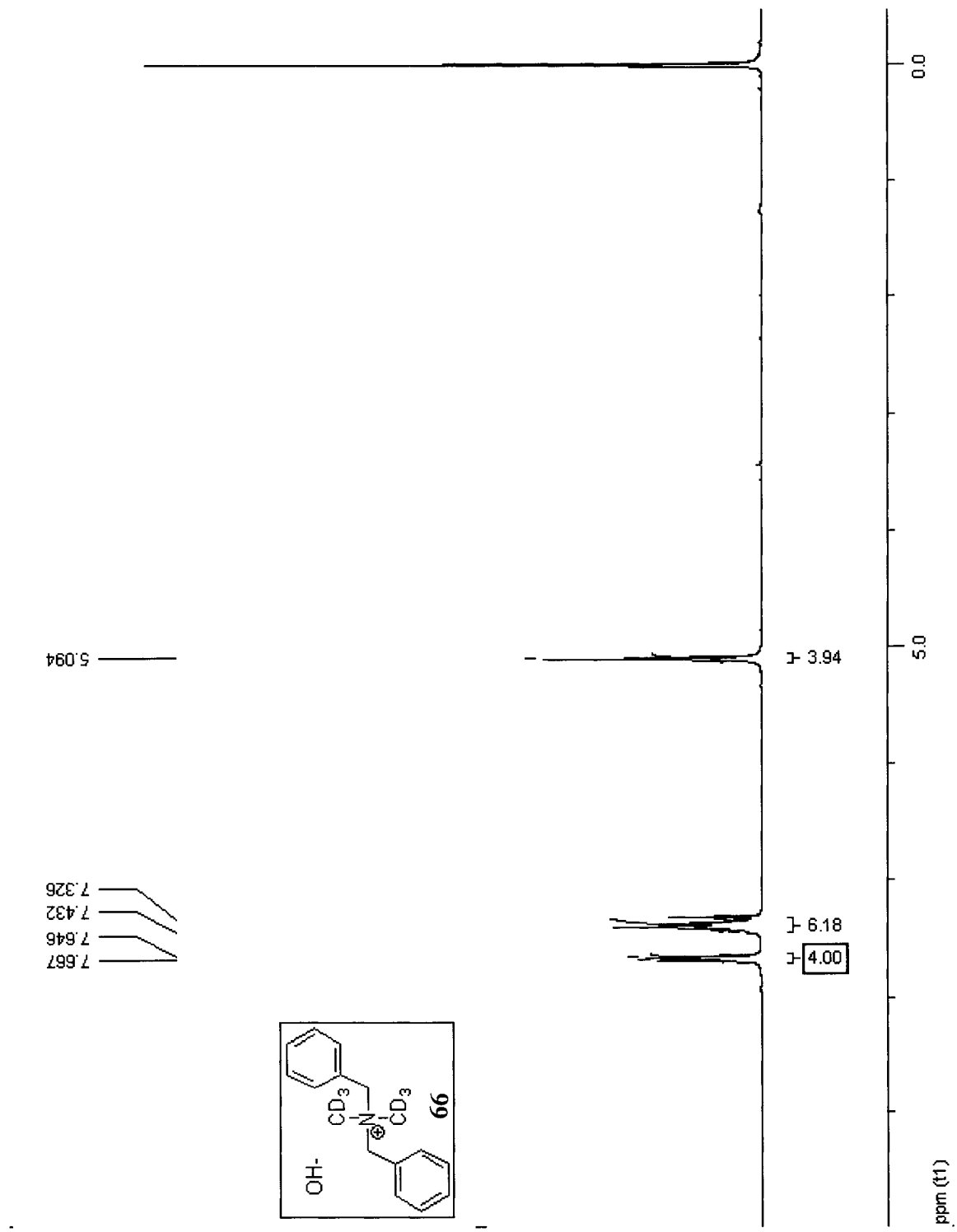
5.094
7.326
7.432
7.646
7.667
3.94
6.18
4.00
0.0
5.0
ppm (t1)
OH-
CD_3
CD_3
99

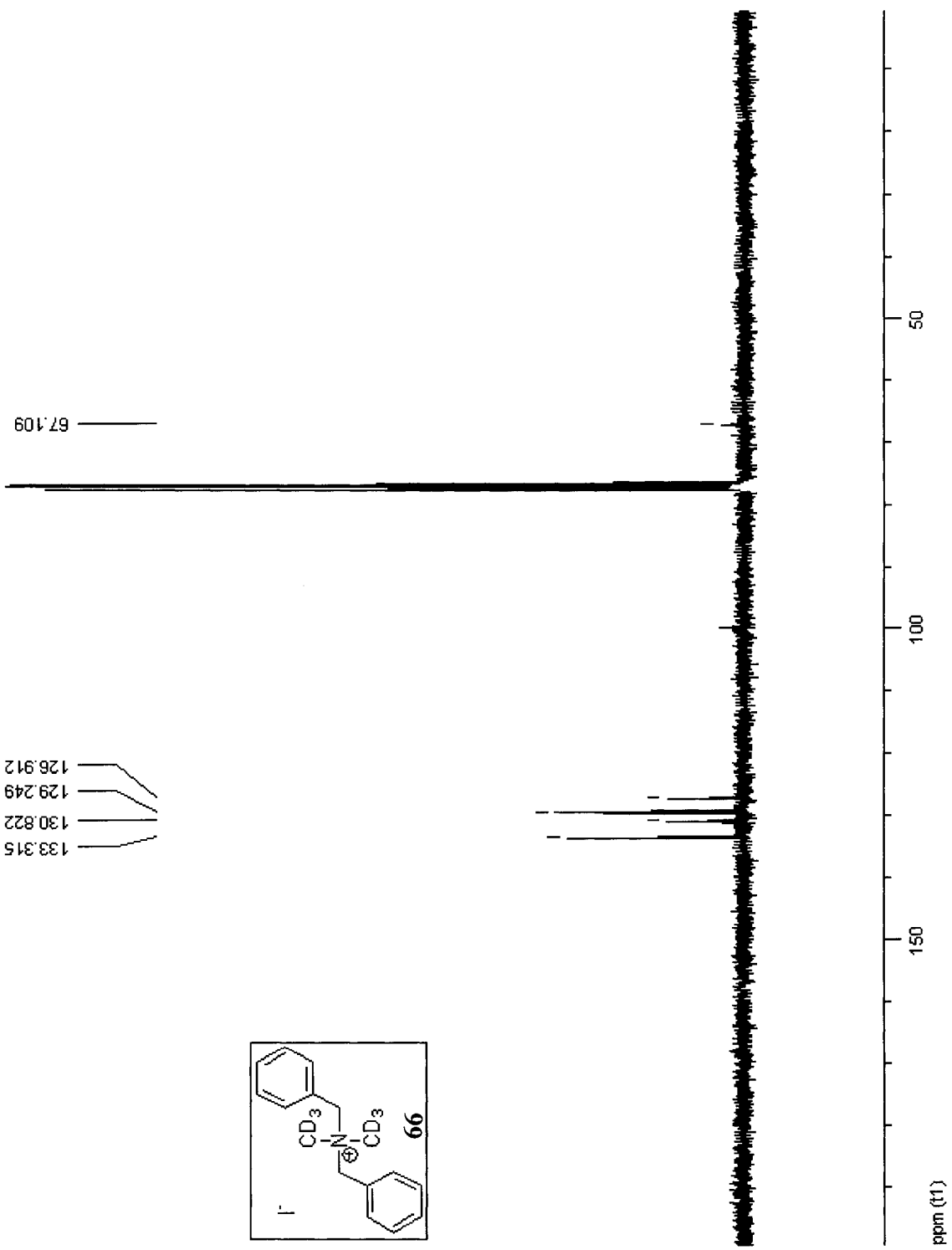
67.109
126.912
129.249
130.822
133.315
I⁻
CD3
N⊕
CD3
66
50
100
150
ppm (t1)

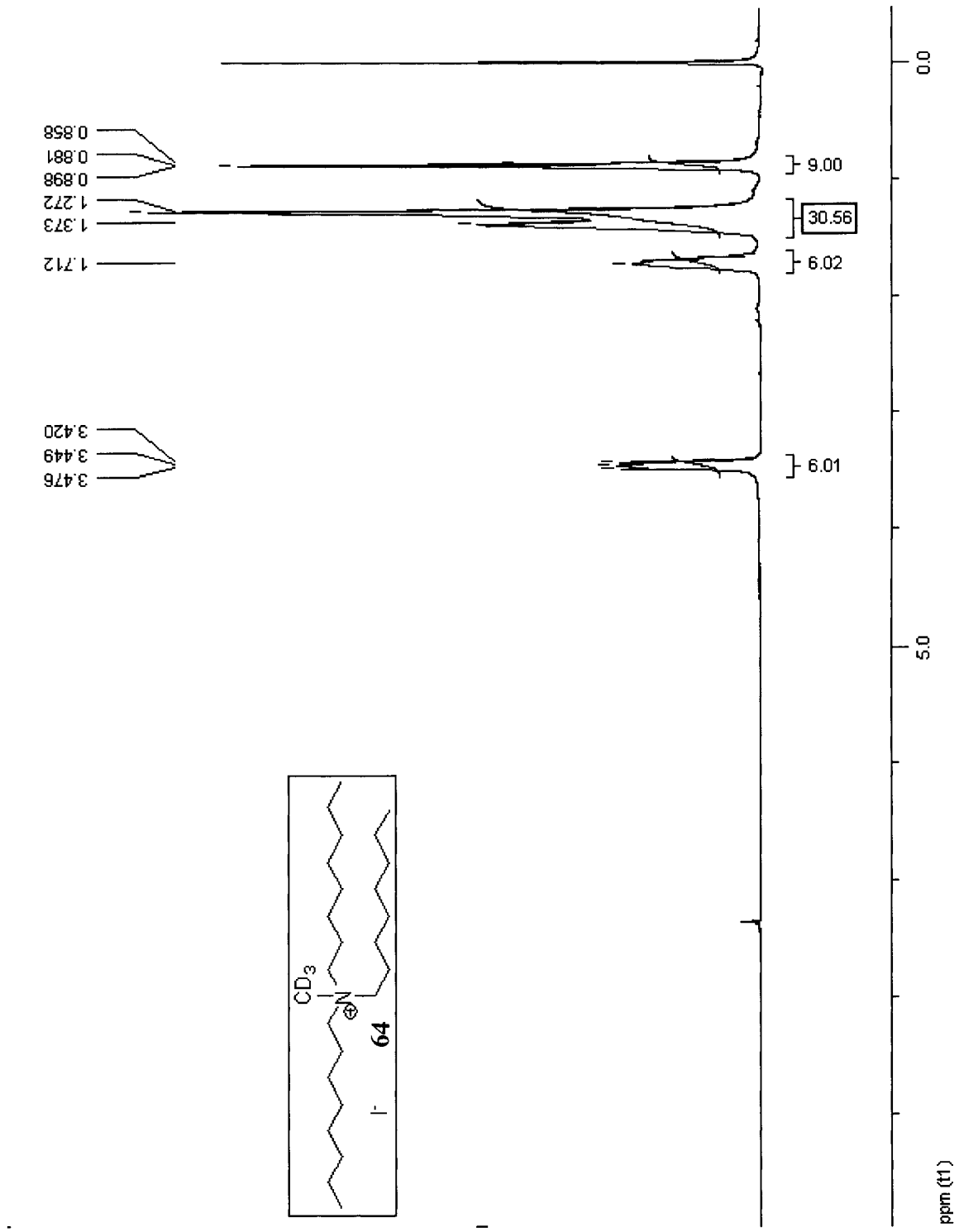
0.858
0.881
0.898
1.272
1.373
1.712
3.420
3.449
3.476
9.00
30.56
6.02
6.01
0.0
5.0
ppm (t1)
CD_3
$N^{\oplus}$
I^-
64

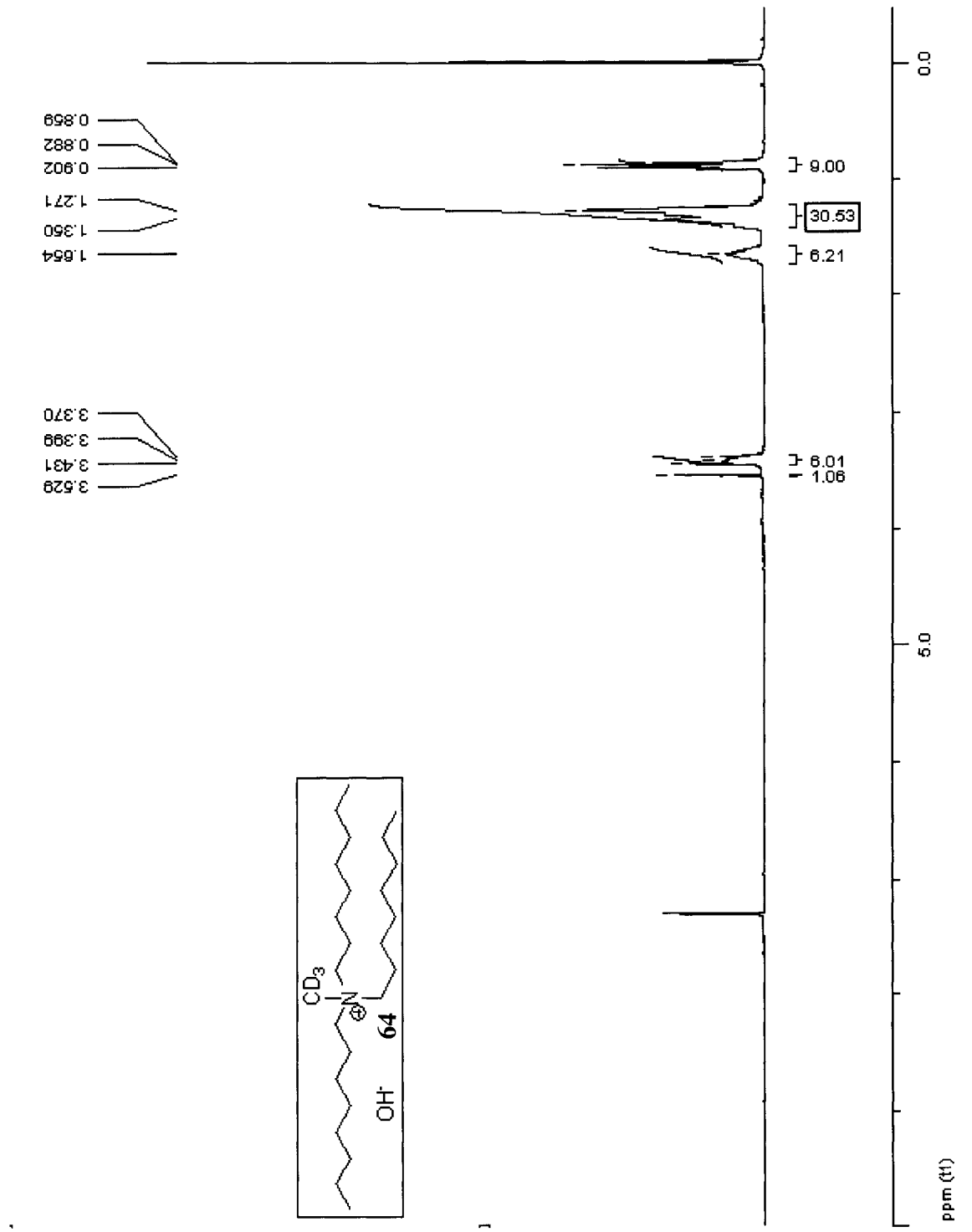
0.869
0.882
0.902
1.271
1.360
1.654
3.370
3.399
3.431
3.529
9.00
30.53
6.21
6.01
1.06
0.0
5.0
ppm (t1)
CD3
N
OH-
64

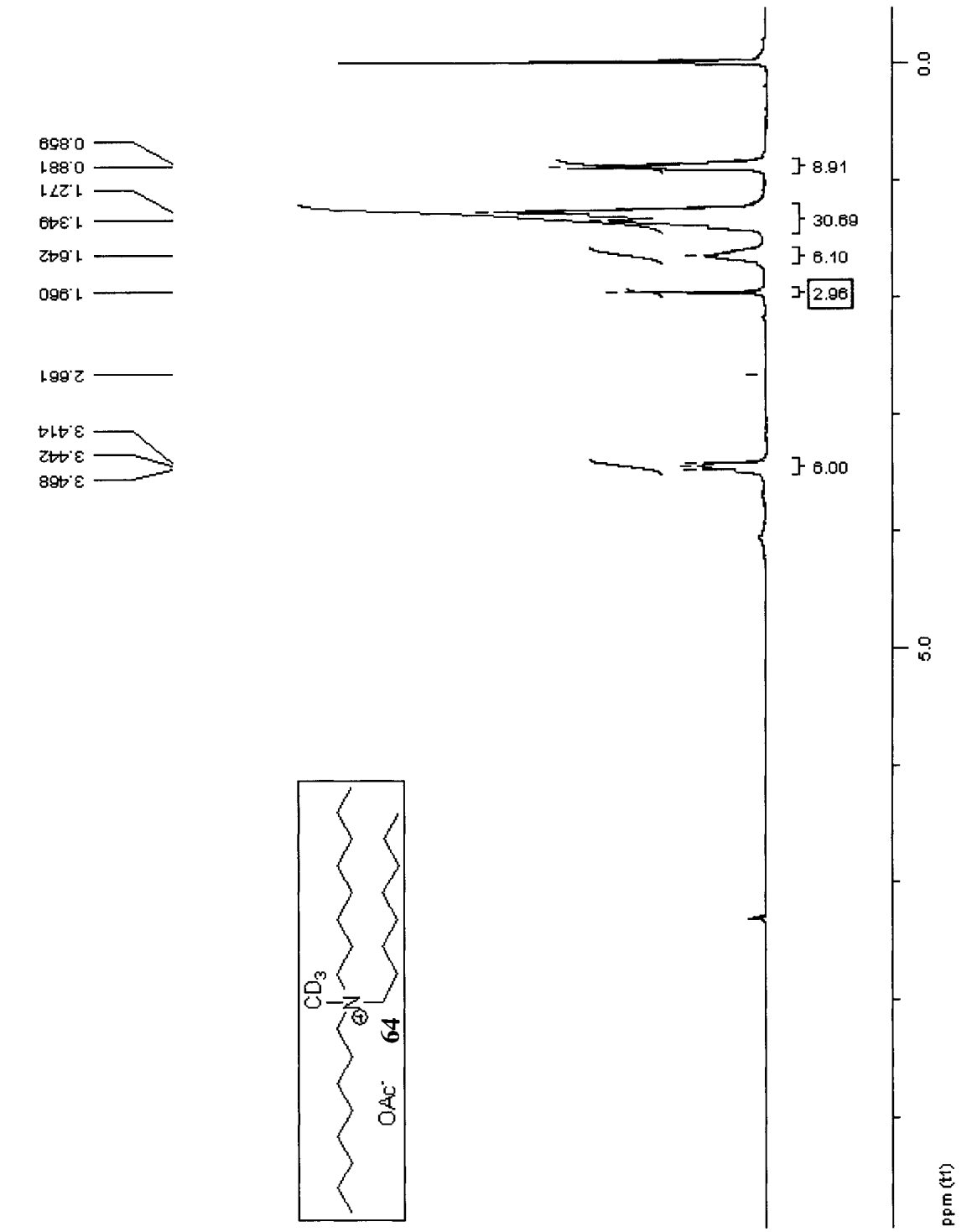
0.859
0.881
1.271
1.349
1.642
1.960
2.661
3.414
3.442
3.468
8.91
30.69
6.10
2.96
6.00
0.0
5.0
ppm (f1)
CD3
N
OAc
64

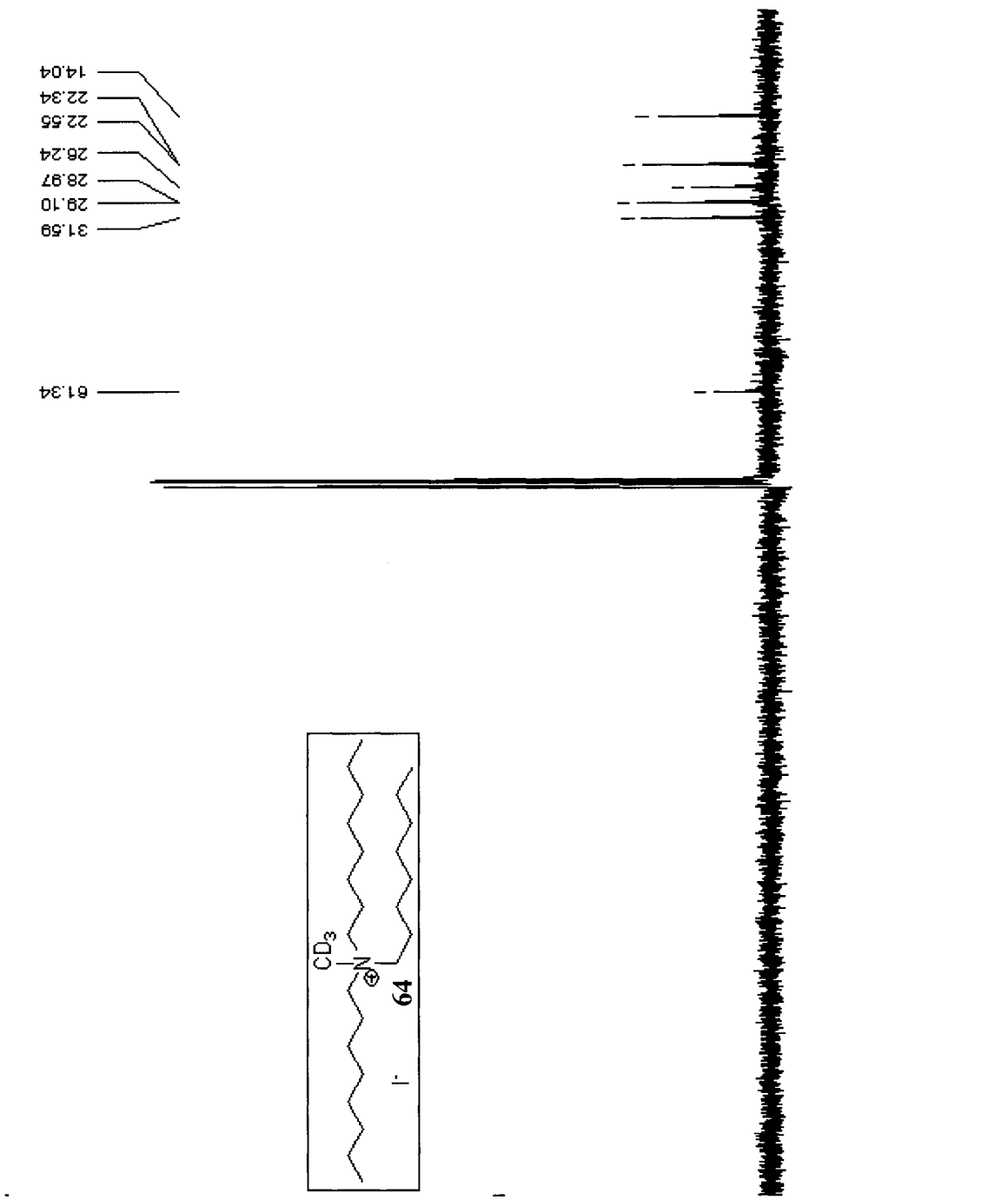
14.04
22.34
22.55
26.24
28.97
29.10
31.59
61.34
CD3
N
64

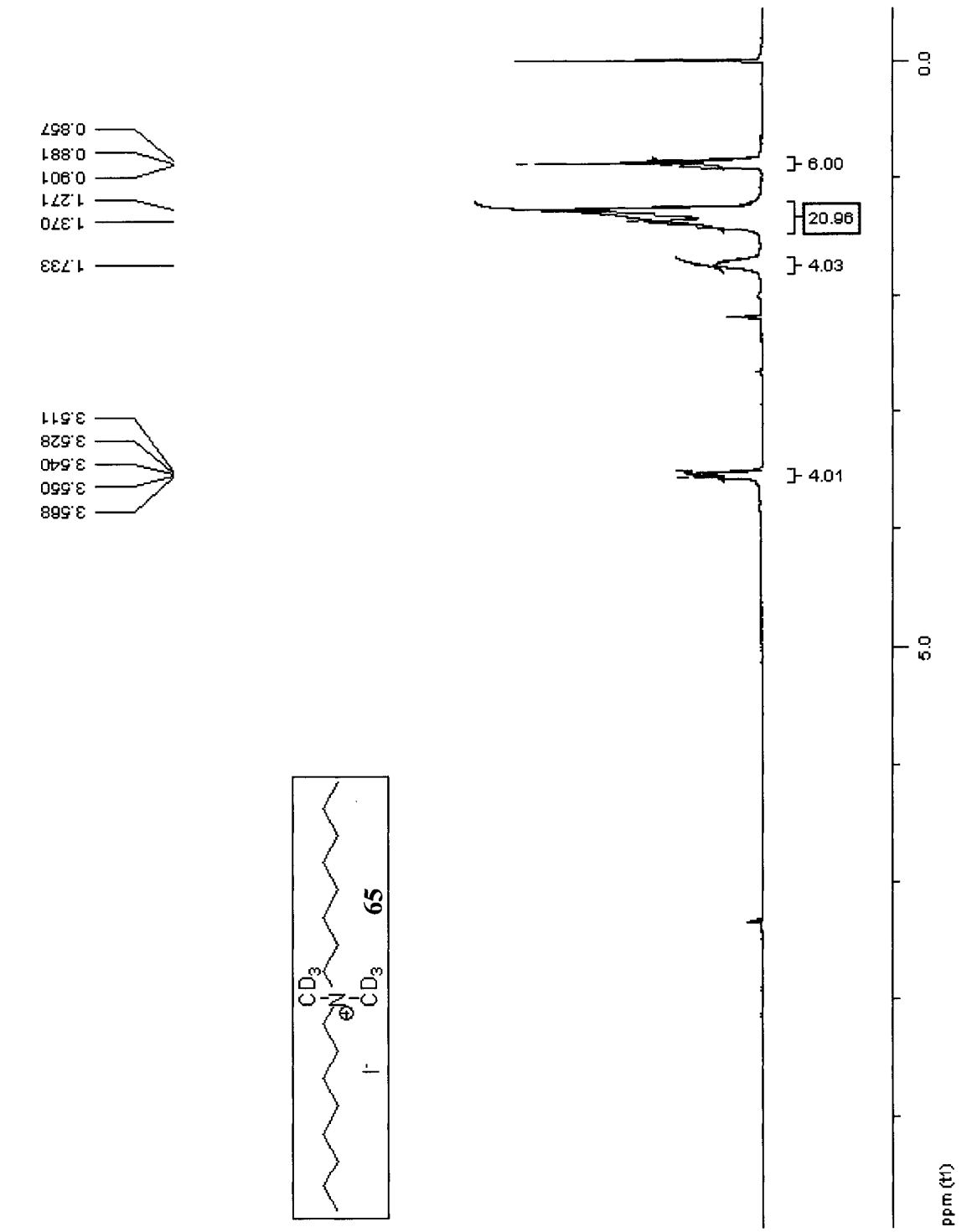
0.857
0.881
0.901
1.271
1.370
1.733
3.511
3.528
3.540
3.550
3.568
6.00
20.96
4.03
4.01
0.0
5.0
ppm (t1)
65

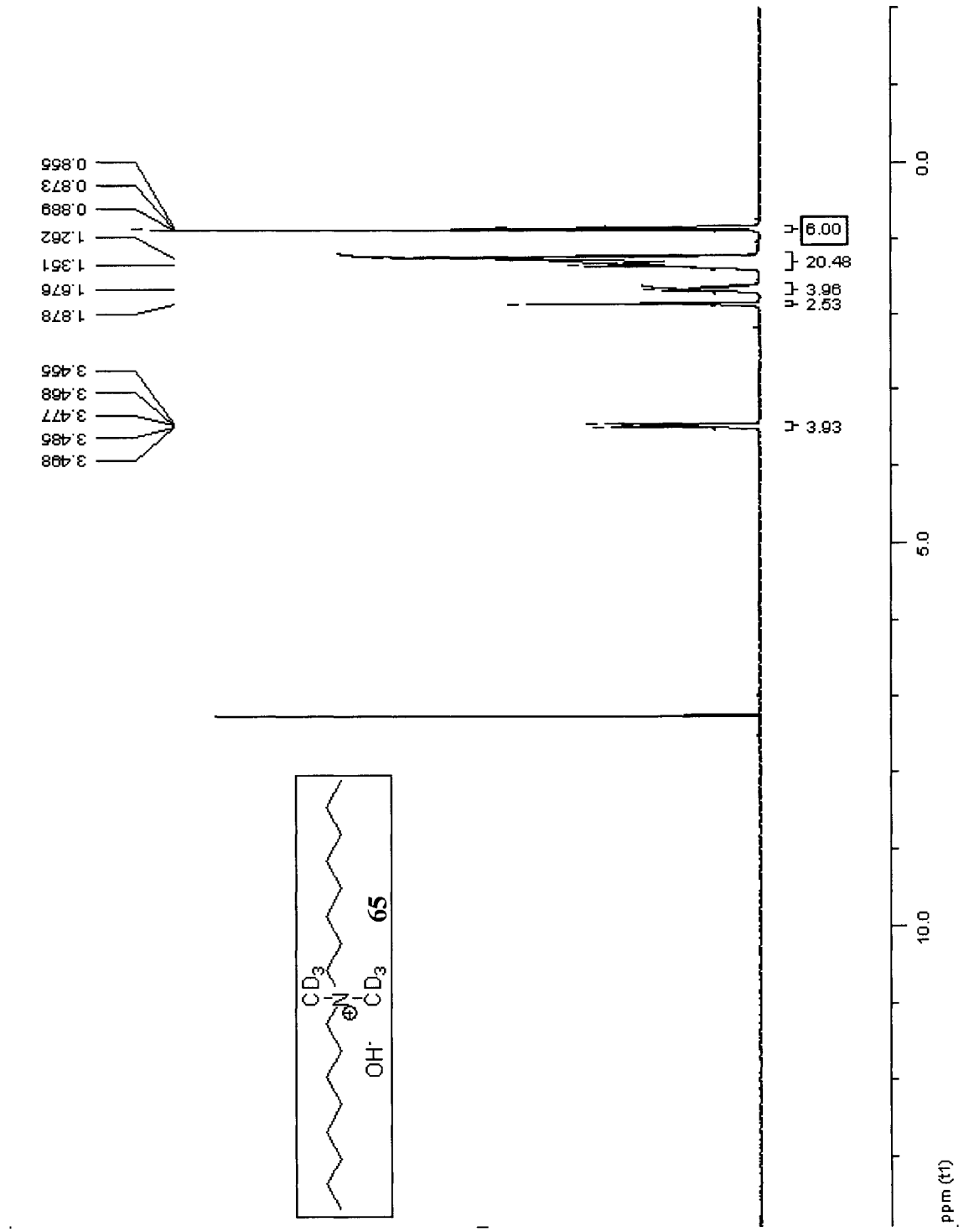
0.855
0.873
0.889
1.262
1.351
1.676
1.878
3.465
3.468
3.477
3.485
3.498
6.00
20.48
3.96
2.53
3.93
0.0
5.0
10.0
ppm (t1)
CD3
N
OH
CD3
65

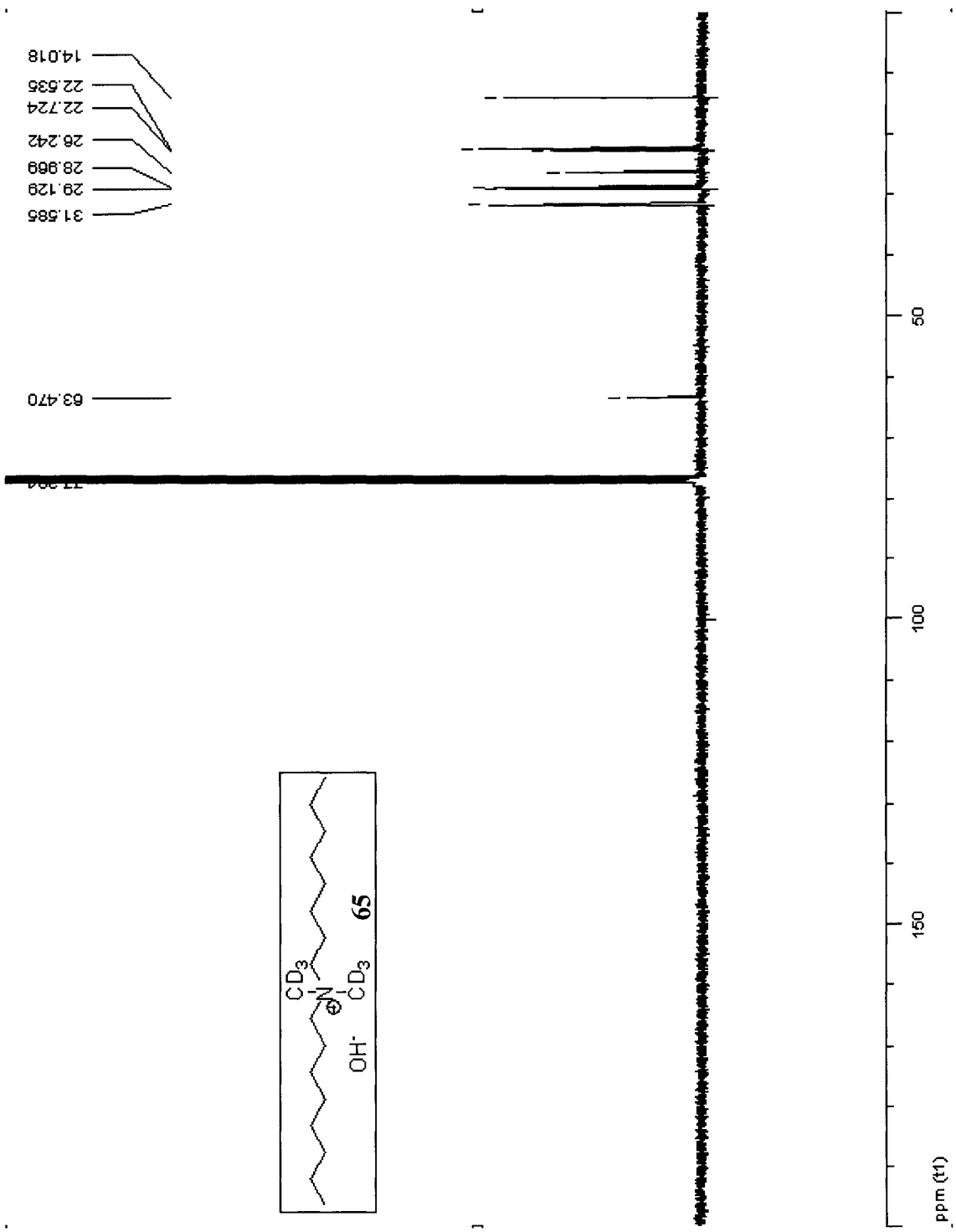
14.018
22.535
22.724
26.242
28.969
29.129
31.586
63.470
77.264
CD3
N
CD3
OH-
65
150
100
50
ppm (t1)